VOL. 465 NO. 1 MARCH 10, 1989

30th Rocky Mountain Conf. (IC and SFC), Denver, CO, July 31–August 5, 1988, and 12th Int. Symp. on Column LC, Washington, DC, June 19–24, 1988 (late papers

RNAL OF

HROMATOGRAPHY

NATIONAL JOURNAL ON CHROMATOGRAPHY, ELECTROPHORESIS AND RELATED METHODS

SYMPOSIUM VOLUMES

ELSEVIER

Denver City, 1859

0021-9673/89/$03.50

Printed in The Netherlands

SYMPOSIUM ISSUE

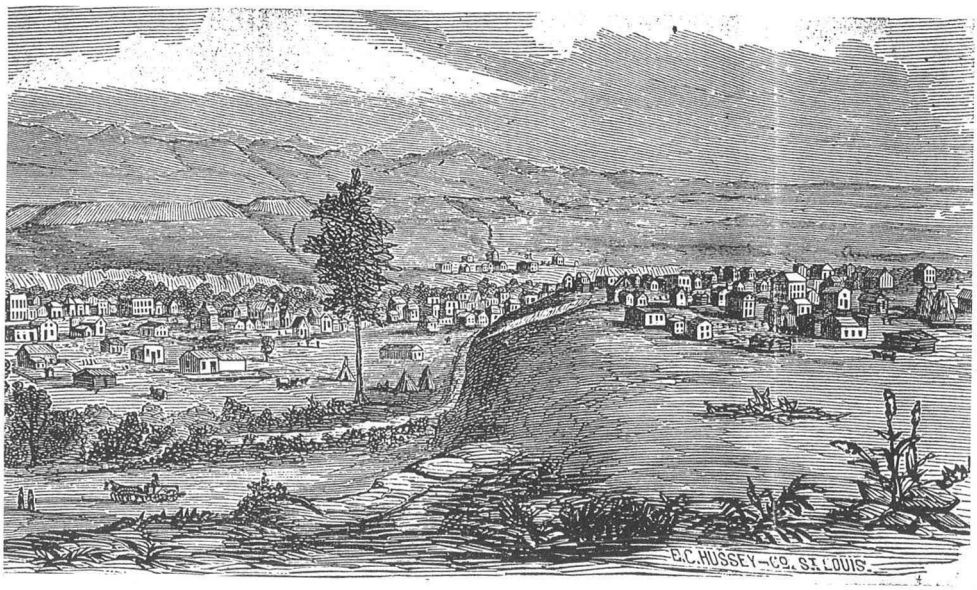

30TH ROCKY MOUNTAIN CONFERENCE

ION CHROMATOGRAPHY and SUPERCRITICAL FLUID CHROMATOGRAPHY Symposia

Denver, CO (U.S.A.), July 31–August 5, 1988

SYMPOSIUM VOLUMES

CONTENTS

30TH ROCKY MOUNTAIN CONFERENCE (ION CHROMATOGRAPHY AND SUPER CRITICAL FLUID CHROMATOGRAPHY SYMPOSIA), DENVER, CO, JULY 31–AUGUST 5, 1988

R. T. Talasek, Determination of fluoride in semiconductor process chemicals by ion chromatography with ion-selective electrodes 1

A. C. Rosselli, D. S. Boyer and R. K. Houck, Reproducibility of packed-column supercritical-fluid chromatography with helium head-pressure carbon dioxide 11

M. Bohm, F. Umland and B. Wenclawiak, Splitting control and solvent effects in supercritical-fluid chromatography with fused-silica capillary columns 17

W. T. Foreman, C. L. Shellum, J. W. Birks and R. E. Sievers, Supercritical fluid chromatography with sulfur chemiluminescence detection 23

JOURNAL OF CHROMATOGRAPHY

Scope. The *Journal of Chromatography* publishes papers on all aspects of chromatography, electrophoresis and related methods. Contributions consist mainly of research papers dealing with chromatographic theory, instrumental development and their applications. The section *Biomedical Applications*, which is under separate editorship, deals with the following aspects: developments in and applications of chromatographic and electrophoretic techniques related to clinical diagnosis or alterations during medical treatment; screening and profiling of body fluids or tissues with special reference to metabolic disorders; results from basic medical research with direct consequences in clinical practice; drug level monitoring and pharmacokinetic studies; clinical toxicology; analytical studies in occupational medicine.

Submission of Papers. Papers in English, French and German may be submitted, in three copies. Manuscripts should be submitted to: The Editor of *Journal of Chromatography*, P.O. Box 681, 1000 AR Amsterdam, The Netherlands, or to: The Editor of *Journal of Chromatography, Biomedical Applications*, P.O. Box 681, 1000 AR Amsterdam, The Netherlands. Review articles are invited or proposed by letter to the Editors. An outline of the proposed review should first be forwarded to the Editors for preliminary discussion prior to preparation. Submission of an article is understood to imply that the article is original and unpublished and is not being considered for publication elsewhere. For copyright regulations, see below.

Subscription Orders. Subscription orders should be sent to: Elsevier Science Publishers B.V., P.O. Box 211, 1000 AE Amsterdam, The Netherlands, Tel. 5803 911, Telex 18582 ESPA NL. The *Journal of Chromatography* and the *Biomedical Applications* section can be subscribed to separately.

Publication. The *Journal of Chromatography* (incl. *Biomedical Applications*) has 37 volumes in 1989. The subscription prices for 1989 are:

J. Chromatogr. + *Biomed. Appl.* (Vols. 461–497):
Dfl. 6475.00 plus Dfl. 999.00 (p.p.h.) (total *ca.* US$ 3933.75)

J. Chromatogr. only (Vols. 461–486):
Dfl. 5200.00 plus Dfl. 702.00 (p.p.h.) (total *ca.* US$ 3106.25)

Biomed. Appl. only (Vols. 487–497):
Dfl. 2200.00 plus Dfl. 297.00 (p.p.h.) (total *ca.* US$ 1314.25).

Our p.p.h. (postage, package and handling) charge includes surface delivery of all issues, except to subscribers in Argentina, Australia, Brasil, Canada, China, Hong Kong, India, Israel, Malaysia, Mexico, New Zealand, Pakistan, Singapore, South Africa, South Korea, Taiwan, Thailand and the U.S.A. who receive all issues by air delivery (S.A.L. — Surface Air Lifted) at no extra cost. For Japan, air delivery requires 50% additional charge; for all other countries airmail and S.A.L. charges are available upon request. Back volumes of the *Journal of Chromatography* (Vols. 1–460)are available at Dfl. 230.00 (plus postage). Claims for missing issues will be honoured, free of charge, within three months after publication of the issue. Customers in the U.S.A. and Canada wishing information on this and other Elsevier journals, please contact Journal Information Center, Elsevier Science Publishing Co. Inc., 655 Avenue of the Americas, New York, NY 10010. Tel. (212) 989-5800.

Abstracts/Contents Lists published in Analytical Abstracts, ASCA, Biochemical Abstracts, Biological Abstracts, Chemical Abstracts, Chemical Titles, Chromatography Abstracts, Current Contents/Physical, Chemical & Earth Sciences, Current Contents/Life Sciences, Deep-Sea Research/Part B: Oceanographic Literature Review, Excerpta Medica, Index Medicus, Mass Spectrometry Bulletin, PASCAL-CNRS, Referativnyi Zhurnal and Science Citation Index.

See inside back cover for Publication Schedule, Information for Authors and information on Advertisements.

0021-9673/89/$03.50

Printed in The Netherlands

VOL. 465, NO. 1 JOURNAL OF CHROMATOGRAPHY MARCH 1, 1989

CONTENTS

(*Abstracts/Contents Lists published in Analytical Abstracts, ASCA, Biochemical Abstracts, Biological Abstracts, Chemical Abstract, Chemical Titles, Chromatography Abstracts, Current Contents/Physical, Chemical & Earth Sciences, Current Contents/Life Sciences, Deep Sea Research/Part B: Oceanographic Literature Review, Excerpta Medica, Index Medicus, Mass Spectrometry Bulletin, PASCAL-CNRS, Referativnyi Zhurnal and Science Citation Index*)

30TH ROCKY MOUNTAIN CONFERENCE (ION CHROMATOGRAPHY AND SUPERCRITICAL FLUID CHROMATOGRAPHY SYMPOSIA), DENVER, CO, JULY 31–AUGUST 5, 1988

Determination of fluoride in semiconductor process chemicals by ion chromatography with ion-selective electrodes
by R. T. Talasek (Dallas, TX, U.S.A.) 1

Reproducibility of packed-column supercritical-fluid chromatography with helium head-pressure carbon dioxide
by A. C. Rosselli, D. S. Boyer and R. K. Houck (Pittsburgh, PA, U.S.A.) 11

Splitting control and solvent effects in supercritical-fluid chromatography with fused-silica capillary columns
by M. Bohm, F. Umland and B. Wenclawiak (Münster, F.R.G.) 17

Supercritical fluid chromatography with sulfur chemiluminescence detection
by W. T. Foreman, C. L. Shellum, J. W. Birks and R. E. Sievers (Boulder, CO, U.S.A.) . 23

TWELFTH INTERNATIONAL SYMPOSIUM ON COLUMN LIQUID CHROMATOGRAPHY, WASHINGTON, DC, JUNE 19–24, 1988 (LATE PAPERS)

Packing technology, column bed structure and chromatographic performance of 1–2-μm non-porous silicas in high-performance liquid chromatography
by H. Giesche, K. K. Unger, U. Esser, B. Eray and U. Trüdinger (Mainz, F.R.G.) and J. N. Kinkel (Darmstadt, F.R.G) 39

Artificial intelligence techniques for peak homogeneity validation in liquid chromatography
by T. P. Bridge and M. H. Williams (Edinburgh, U.K.) and A. F. Fell (Bradford, U.K.) . 59

Polarographic detection of non-ionic surfactants analyzed by reversed-phase partition chromatography
by P. L. Desbène, B. Desmazieres, J. J. Basselier and A. Desbène-Monvernay (Paris, France) 69

High-performance liquid chromatographic determination of mitoxantrone in plasma utilizing non-bonded silica gel for solid-phase isolation to reduce adsorptive losses on glass during sample preparation
by K. T. Lin, G. E. Rivard and J.-M. Leclerc (Montreal, Canada) 75

Derivatization and high-performance liquid chromatographic determination of urinary glycolic acid
by M. Petrarulo, S. Pellegrino, O. Bianco, M. Marangella, F. Linari and E. Mentasti (Turin, Italy) 87

High-performance liquid chromatographic evaluation of PCF 39, a new immunomodulator agent
by A. Marzo, N. Monti, M. Ripamonti and G. Cardace (Como, Italy) and E. Arrigoni Martelli (Rome, Italy) 95

Protein A, hydroxyapatite and diethylaminoethyl: evaluation of three procedures for the preparative purification of monoclonal antibodies by high-performance liquid chromatography
by C. Poiesi, A. Tamanini, S. Ghielmi and A. Albertini (Brescia, Italy) 101

Full automation of catecholamine metabolite determination by column switching and high-performance liquid chromatography
by G. Grossi, A. Bargossi, R. Battistoni, A. Lippi and G. Sprovieri (Bologna, Italy) . . . 113

ADVANCED SCIENTIFIC COMPUTING IN BASIC: with applications in chemistry, biology and pharmacology

P. VALKÓ, *Eötvös Loránd University, Budapest, Hungary, and*
S. VAJDA, *Mount Sinai School of Medicine, New York, NY, USA*

Data Handling in Science and Technology Volume 4

Advanced Scientific Computing in BASIC gives a practical introduction to numerical methods and presents BASIC subroutines for real-life computations in the areas of chemistry, biology, and pharmacology. The choice of BASIC as the programming language is motivated by its simplicity, its availability on all personal computers and by its power in data acquisition. While most of the scientific packages currently available in BASIC date back to the period of limited memory and speed, the subroutines presented here can handle a broad range of realistic problems with the power and sophistication needed by professionals and with simple, step-by-step instructions for students and beginners.

The book shows how to extract useful information from measurements via modelling, simulation, and statistical data evaluations. Efficient, robust numerical methods have been chosen to solve related problems in numerical algebra, nonlinear equations and optimization, parameter estimation, signal processing, and differential equations. For each class of routines an introduction to the relevant theory and techniques is given, so that the reader will recognise and use the appropriate method for solving his or her particular problem. Simple examples illustrate the use and applicability of each method.

Contents: 1. Computational linear algebra. 2. Nonlinear equations and extremum problems. 3. Parameter estimation. 4. Signal processing. 5. Dynamical models. Subject index.

1989 xvii + 322 pages; US$ 92.75 / Dfl. 190.00
ISBN 0-444-87270-1
5.25" Diskette: US$ 53.75 / Dfl. 110.00
ISBN 0-444-87271-X

ELSEVIER SCIENCE PUBLISHERS

P.O. Box 211, 1000 AE Amsterdam, The Netherlands
P.O. Box 882, Madison Square Station, New York, NY 10159, USA

Analytical Artifacts

GC, MS, HPLC, TLC and PC

by **B.S. MIDDLEDITCH,** *Dept. of Biochemical and Biophysical Sciences, University of Houston, Houston, TX, USA*

(Journal of Chromatography Library, 44)

This encyclopaedic catalogue of the pitfalls and problems that all analysts encounter in their work is destined to spend more time on the analyst's workbench than on a library shelf. The author has dedicated the book to "the innumerable scientists who made mistakes, used impure chemicals and solvents, suffered the consequences of unanticipated side-reactions, and were otherwise exposed to mayhem yet were too embarrassed to publish their findings".

Traditionally, the mass spectroscopist or gas chromatographer learnt his trade by participating in a 4-6 year apprenticeship as graduate student and post-doctoral researcher. Generally, no formal training was provided on the things that go wrong, but this information was accumulated by sharing in the experiences of colleagues. Nowadays, many novice scientists simply purchase a computerized instrument, plug it in, and use it. Much time can be wasted in studying and resolving problems due to artifacts and there is also a strong possibility that artifacts will not be recognized as such. For example, most analysts realize that they should use glass rather than plastic containers; but few of them would anticipate the possibility of plasticizer residues on glassware washed using detergent from a plastic bottle.

This book is an easy-to-use compendium of problems encountered when using various commonly used analytical techniques. Emphasis is on impurities, by-products, contaminants and other artifacts. A separate entry is provided for each artifact. For specific chemicals, this entry provides the common name, mass spectrum, gas chromatographic data, CAS name and registry number, synonyms and a narrative discussion. More than 1100 entries are included. Mass spectral data are indexed in a 6-peak index (molecular ion, base peak, second peak, third peak) and there are also formula, author and subject indexes. An extensive bibliography contains complete literature citations.

The book is designed to be *used*. It will not only allow experienced analysts to profit from the mistakes of others, but it will also be invaluable to other scientists who use analytical instruments in their work.

1989 xxiv + 1028 pages
US$ 241.50 / Dfl. 495.00
ISBN 0-444-87158-6

ELSEVIER SCIENCE PUBLISHERS

P.O. Box 211, 1000 AE Amsterdam, The Netherlands
P.O. Box 882, Madison Square Station, New York, NY 10159, USA

NATURAL PRODUCTS ISOLATION

Separation Methods for Antimicrobials, Antivirals and Enzyme Inhibitors

edited by **GERALD H. WAGMAN** *and* **RAYMOND COOPER,**
Schering-Plough Research, Bloomfield, NJ, USA

(Journal of Chromatography Library, 43)

This new book encompasses, in great detail, the most recent progress made in the isolation and separation of natural products. Written by experts in their respective fields, it covers antibiotics, marine and plant-derived substances, enzyme inhibitors and interferons. The book has extensive isolation schemes, tables, figures and chemical structures. In many instances a short summary of the producing organism, brief chemical description and structure and biological activity of the compounds is presented. Detailed information of extraction, separation and purification techniques follow. Each chapter has an extensive bibliography and, where applicable, an appendix showing sources of materials and equipment. A detailed index to the subject matter is also provided.

The book thus offers the reader: up-to-date reviews (including 1988) of specific topics in the natural products field not to be found elsewhere; information on new chromatographic methods and techniques described in sufficient detail to be utilized by investigators in this area of research; and extensive references to enable the serious researcher to pursue particular information. It will appeal to pharmaceutical and natural products researchers and is a valuable acquisition for university chemistry and biochemistry departments.

Contents: Countercurrent chromatography *(J.B. McAlpine, J.E. Hochlowski)*. HPLC detection methods for microbial products from fermentation broth *(R. Mierzwa et al.)*. Affinity and purification of glycopeptide antibiotics *(R.D. Sitrin, G.F. Wasserman)*. Nikkomycins and polyoxins *(H.-P. Fiedler)*. Saframycins and isoquinolines *(T. Arai)*. New cephalosporins *(S. Harada)*. Monocyclic β-lactam antibiotics *(W.L. Parker)*. Isolation of carbapenems *(K.E. Wilson)*. Avermectins and related compounds *(T. Miller, V.P. Gullo)*. Bioactive compounds from marine organisms and cultivated blue-green algae *(J.S. Mynderse et al.)*. The interferons *(S. Pestka)*. Enzyme inhibitors produced by microorganisms *(H. Umezawa)*. Alkaloidal glycosidase inhibitors from plants *(L.E. Fellows, G.W.J. Fleet)*. Chemical communication and control of development *(C.E. Smith, J.D. Orr, D.G. Lynn)*. Subject Index.

1989 xii + 618 pages
US$ 150.00 / Dfl. 285.00
ISBN 0-444- 87147-0

ELSEVIER SCIENCE PUBLISHERS

P.O. Box 211, 1000 AE Amsterdam, The Netherlands
P.O. Box 882, Madison Square Station, New York, NY 10159, USA

JOURNAL OF CHROMATOGRAPHY

VOL. 465 (1989)

JOURNAL *of* CHROMATOGRAPHY

INTERNATIONAL JOURNAL ON CHROMATOGRAPHY,
ELECTROPHORESIS AND RELATED METHODS

ELSEVIER
AMSTERDAM — OXFORD — NEW YORK — TOKYO

J. Chromatogr., Vol. 465 (1989)

Journal of Chromatography, 465 (1989) 1–10
Elsevier Science Publishers B.V., Amsterdam — Printed in The Netherlands

CHROMSYMP. 1526

DETERMINATION OF FLUORIDE IN SEMICONDUCTOR PROCESS CHEMICALS BY ION CHROMATOGRAPHY WITH ION-SELECTIVE ELECTRODES

R.T. TALASEK
Texas Instruments, Inc., P. O. Box 655012, M/S 46, Dallas, TX 75265 (U.S.A.)

SUMMARY

A method for the analysis of fluoride by ion chromatography with ion-selective electrode detection is described. This method provides uninterfered detection and quantitation of fluoride in ppb concentrations. Direct application to the analysis of samples significant to the semiconductor industry is described.

INTRODUCTION

The analyses of anions in deionized water, water extracts for determination of surface contamination, and process chemicals[1] has become increasingly important to the semiconductor industry as device geometries continue to shrink. The rapid development of ion chromatography in the past few years has played a significant role in these analyses. One anion that is critical in these determinations is fluoride. In acid solution, fluoride becomes an etchant for silicon dioxide, which comprises a significant portion of any silicon-based integrated circuit. With the additional presence of nitrate ions, etching of silicon may also take place. While controlled etching processes are necessary in integrated circuit manufacturing, etching of materials at inappropriate steps in the manufacturing process is disastrous.

The direct determination of fluoride by suppressed-conductivity ion chromatography is problematic. In standard isocratic ion chromatography, fluoride is poorly retained on the exchange material, due to its high pK_a value and small size. This causes fluoride to be eluted in the void volume ("water dip") along with a number of other weak acids anions (*e.g.*, formate, acetate), which makes positive peak identification difficult due to closely matching retention times. Quantitation is also problematic due to the variable magnitude of the negative water dip, and detection limits suffer for similar reasons. Various approaches have been suggested to remedy this problem. For example, gradient ion chromatography[2] can adequately separate fluoride from the water dip and organic anions. However, analysis times for the common anions of interest (F^-, Cl^-, NO_2^-, NO_3^-, Br^-, SO_4^{2-}, PO_4^{3-}) are relatively long and typically are limited to ppm level detection. Ion-exclusion chromatography[3] is also capable of this type separation, but all strong acid anions are co-eluted in the void volume. Ion-selective electrodes, used in stand-alone analysis[4], potentiometric titra-

0021-9673/89/$03.50

tions[5], or flow-injection analysis (FIA)[6] may begin to approach reasonable detection limits, but are obviously limited to the fluoride ion determination. The combination of ion-selective electrode detection in series with suppressed-conductivity ion chromatography offers a potential combination that may be useful for simultaneous determination of fluoride and other inorganic anions in the ppb[a] concentration range in relatively short analysis time. The use of the ion-selective electrode in combination with ion chromatography has been explored in the past for determination of both cations and anions[7]. At least one example[8] of fluoride analysis by ion chromatography ion-selective electrode has been reported in rainwater analysis. The absolute detection limit was 1.25 ng of fluoride, and an eluent modified to increase total ionic strength was used. Taking advantage of the development of the anion micromembrane suppressor and the availability of a combination fluoride ion-selective electrode reference electrodes, an improved method is presented which requires no eluent modification.

EXPERIMENTAL

Chromatography was performed on a Dionex (Sunnyvale, CA, U.S.A.) Model 2120i ion chromatograph with conductivity detection. The separator column was a Dionex AS4 anion separator with an AG4 guard column. The eluent was 2.8 m*M* $NaHCO_3$–2.2 m*M* Na_2CO_3 at a flow-rate of 1 ml min^{-1} and the anion micromembrane suppressor regenerant was 12.5 m*M* sulfuric acid. A 50 μl sample loop was used for sample injection. Detection was performed with an Orion (Cambridge, MA, U.S.A.) solid state combination fluoride electrode placed in a flow cell subsequent to the conductivity cell in the eluent stream. The custom flow cell was constructed from an epoxy body with an approximate cell volume of 100 μl, and was situated outside the chromatograph. Although the dead volume was dramatically increased by this cell position, it provided easy access to the cell and electrode. Flow within the cell was parallel to the electrode surface. Electrode potential was measured with an Orion Model 940 pH–ion-selective electrode meter operated in the absolute potential mode. Signal processing for each detector was performed with a Spectra-Physics (San Jose, CA, U.S.A.) SP4270 integrator.

RESULTS AND DISCUSSION

Fig. 1A and B shows typical chromatograms of an anion mixture, detected by conductivity and fluoride ion-selective electrode, respectively. Note that at a concentration of 1 ppm, fluoride is detectable by conductivity. However, as this concentration is reduced, detection becomes unreliable due to the inconsistency of the depth of the negative water dip. However, detection of fluoride at 0.1 ppm by ion-selective electrode (Fig. 1B) is quite reproducible, since little or no baseline deflection due to the water dip is present in ion-selective electrode detection. Precision measured at 50 ppb was 2% relative standard deviation (R.S.D.) and drift over 8 h was less than 1%. Although the phosphate present in the standard does produce a detectable ion-selective electrode peak, it is separated from the fluoride peak and causes no difficulties in

[a] Throughout this article the American billion (10^9) is meant.

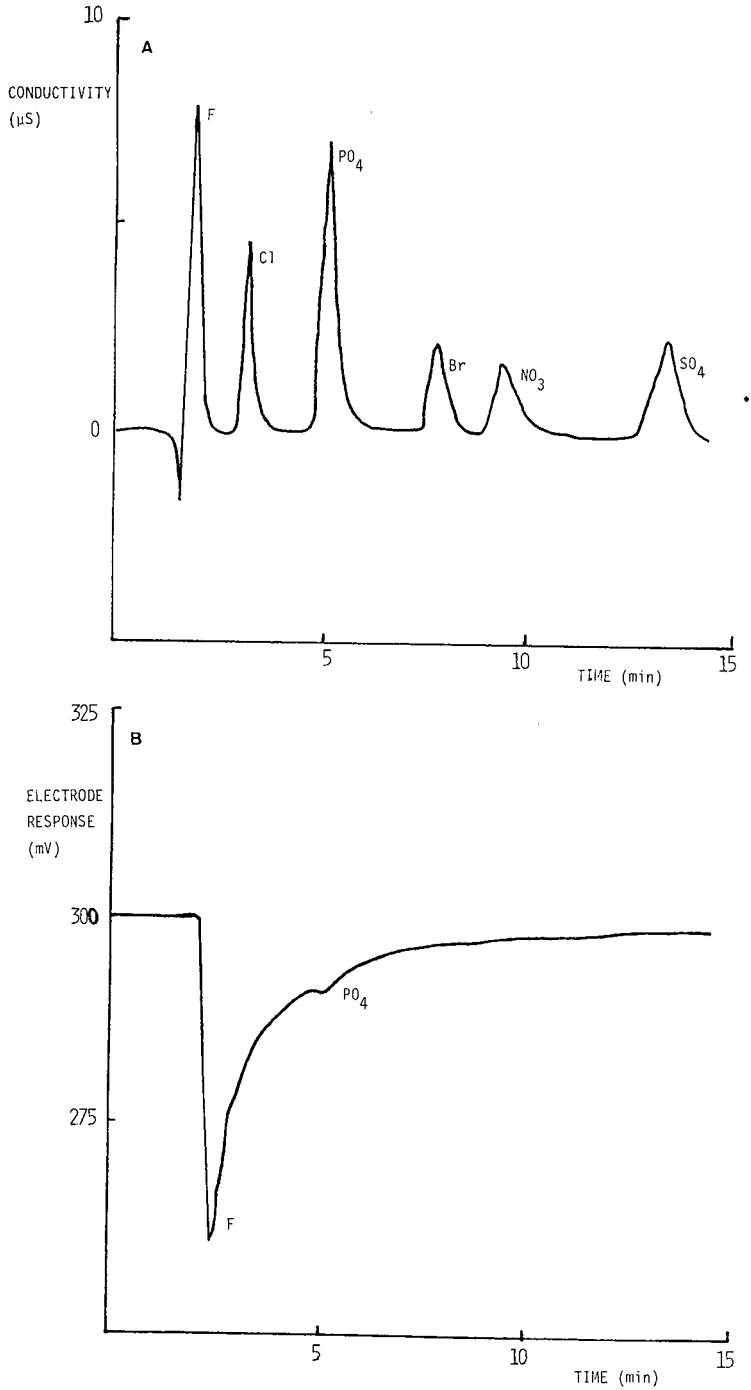

Fig. 1. Chromatograms of a mixed anion standard containing 1 ppm fluoride and chloride, and 2.5 ppm phosphate, bromide, nitrate and sulfate. (A) Conductivity detection. (B) Ion-selective electrode detection after ten-fold dilution.

quantitation by peak height until the concentration is sufficient to prevent chromatographic resolution. Similar problems occur with other anions at higher concentrations. These interferences are likely due to substantial changes in total ionic strength rather than to any specific ionic interference, since no modification to the eluent was made to maintain ionic strength.

One problem with the chromatogram obtained with the ion-selective electrode is the poor peak shape. Initially is was thought that the asymmetry was due to the substantial dead volume of the conductivity cell, ion-selective electrode cell, and transfer lines. To some extent, this must be a contributing factor, but when a chloride ion-selective electrode is substituted in the same system, a symmetrical peak is obtained at similar concentrations of chloride. (Chloride ion-selective electrode detection suffers from poor detection limits and almost unlimited interferences, and will not be discussed further). Therefore, the asymmetry must be due to slow recovery by the fluoride ion-selective electrode. However, quantitation with the fluoride ion-selective electrode is unaffected, as is shown by the linear relationship of peak height *vs.* fluoride concentration with a slope of 0.4 mV ppb^{-1}. Linear response is obtained to a concentration of 5 ppb (0.25 ng absolute detection with the 50-μl sample loop). Between 1 and 5 ppb, the normal negative peak changes polarity and is positive at a concentration of 1 ppb. This change in polarity is not well understood, but could be due either to the change in ionic strength in the water dip, or non-Nernstian behavior of the electrode. The latter is supported by the manufacturer's claim of non-Nernstian behavior in approximately the correct concentration range. Although the improved detection limits are significant, perhaps a more important aspect of this method is the ability to quantitate fluoride specifically in the presence of chromatographic interferences. Fig. 2A and B illustrates the ability of the fluoride ion-selective electrode to distinguish fluoride in the presence of substantial quantities of formate and acetate, which are eluted nearly at the same retention time as fluoride. This ability has proven itself useful in a number of samples with substantial significance to the semiconductor industry.

One sample which comes to mind is the analysis of water extracts. Water extraction of finished devices, piece parts, wafers, and almost any solid object used in semiconductor processing has evolved into perhaps the most effective method available for determining levels of anionic surface contamination. However, a significant number of these samples have substantial levels of short-chain organic acids which may interfere with the determination of trace levels of fluoride. Fig. 3 illustrates the effectiveness of this technique in the specific determination of fluoride contamination. Previously, the large peak present in the water dip may have been attributed to fluoride.

Another significant analysis is the determination of anions in 30% hydrogen peroxide, which is used as an etchant and as part of several different cleaning solutions. Since 30% hydrogen peroxide and a number of the mixed cleaning solutions (piranha, RCA [$HCl:H_2O_2:H_2O$] clean, etc.) are acidic, trace levels of fluoride could cause significant process problems. Before analyzing this solution by ion chromatography, the hydrogen peroxide is decomposed with platinum to protect the column resin. However, residual unidentified peaks in the water dip associated with hydrogen peroxide still remain after decomposition (Fig. 4A). Ion-selective electrode detection correctly identifies only a small fraction of this peak as fluoride (Fig. 4B).

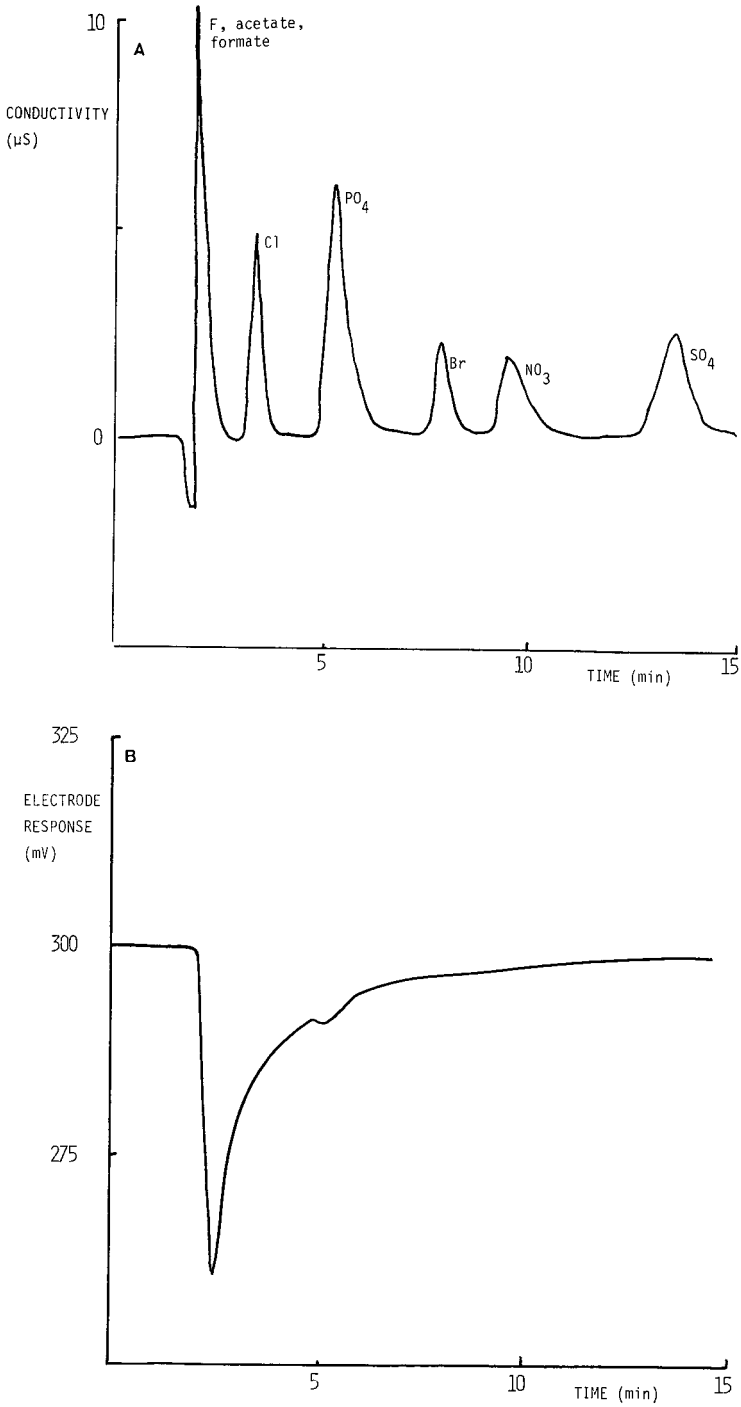

Fig. 2. Chromatograms of mixture in Fig. 1 with 10 ppm formate and acetate added. (A) Conductivity detection. (B) Ion-selective electrode detection.

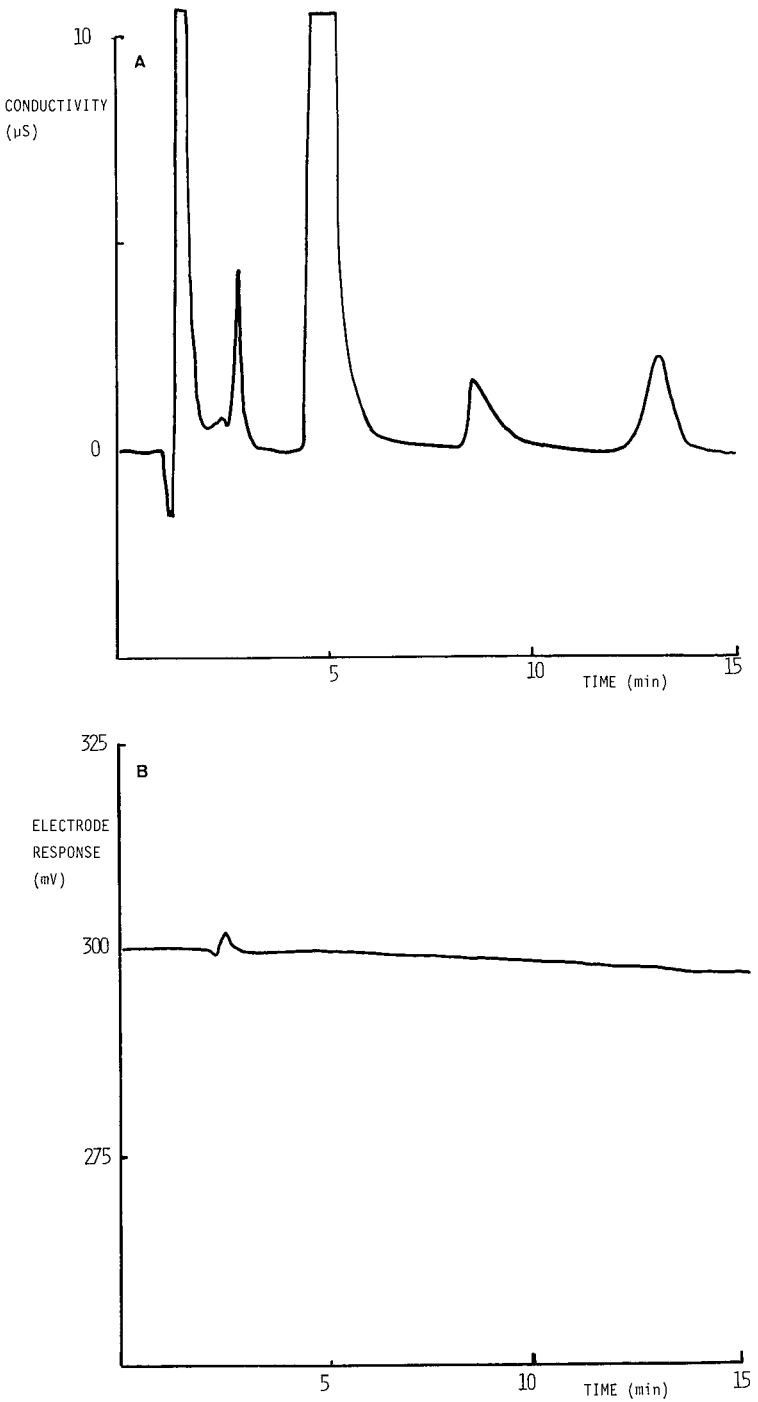

Fig. 3. Chromatograms of a water extract of encapsulation material, used in integrated circuit manufacture. (A) Conductivity detection. (B) Ion-selective electrode detection.

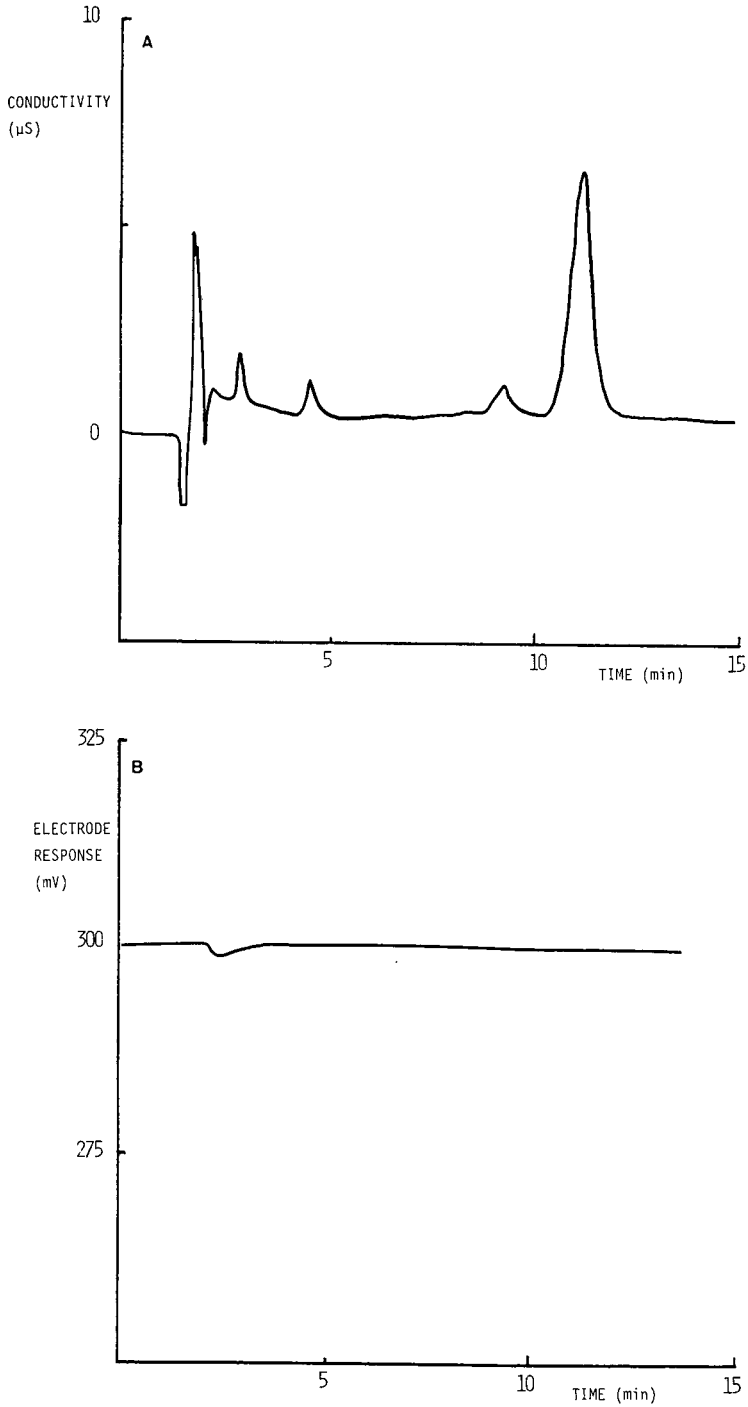

Fig. 4. Chromatograms of 30% hydrogen peroxide decomposed with platinum. (A) Conductivity detection. (B) Ion-selective electrode detection.

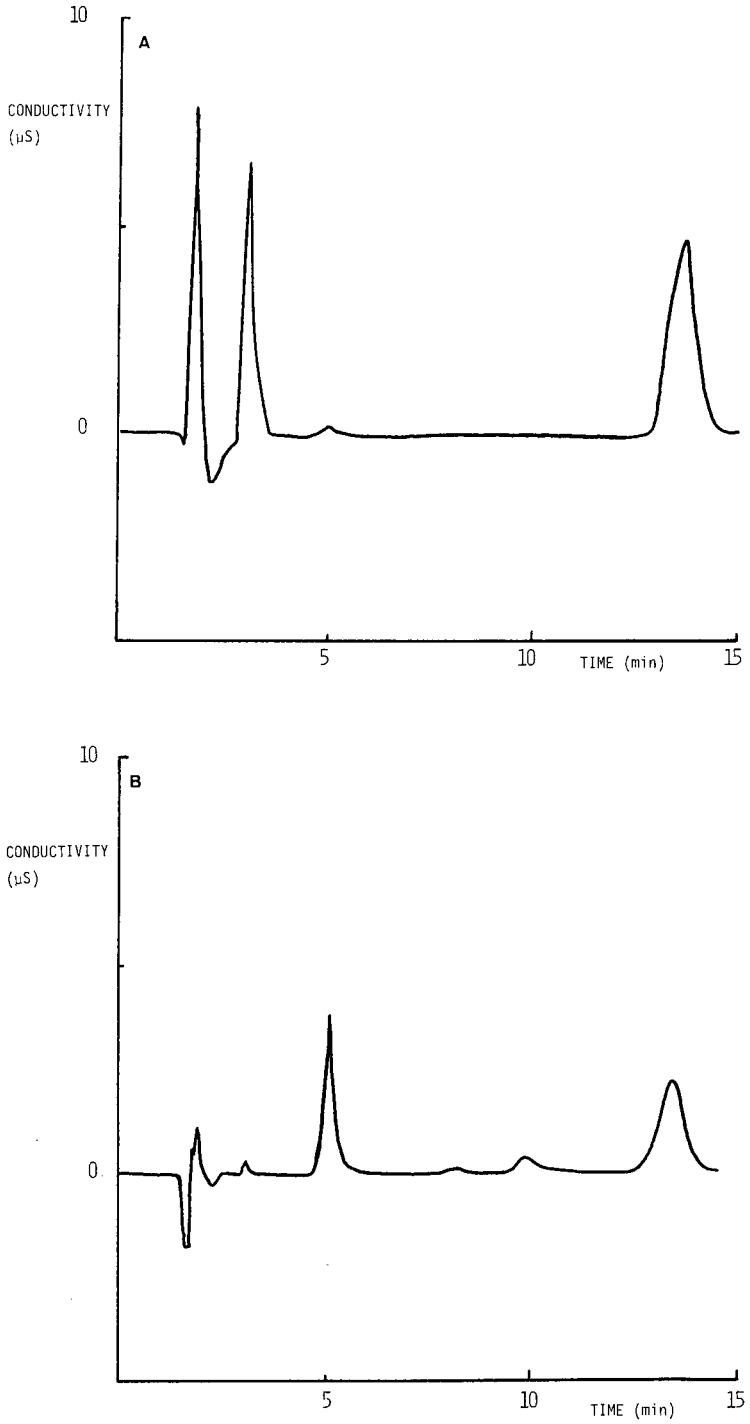
10
A
CONDUCTIVITY
(μS)
0
5
10
TIME (min)
15
10
B
CONDUCTIVITY
(μS)
0
5
10
TIME (min)
15

Fig. 5.

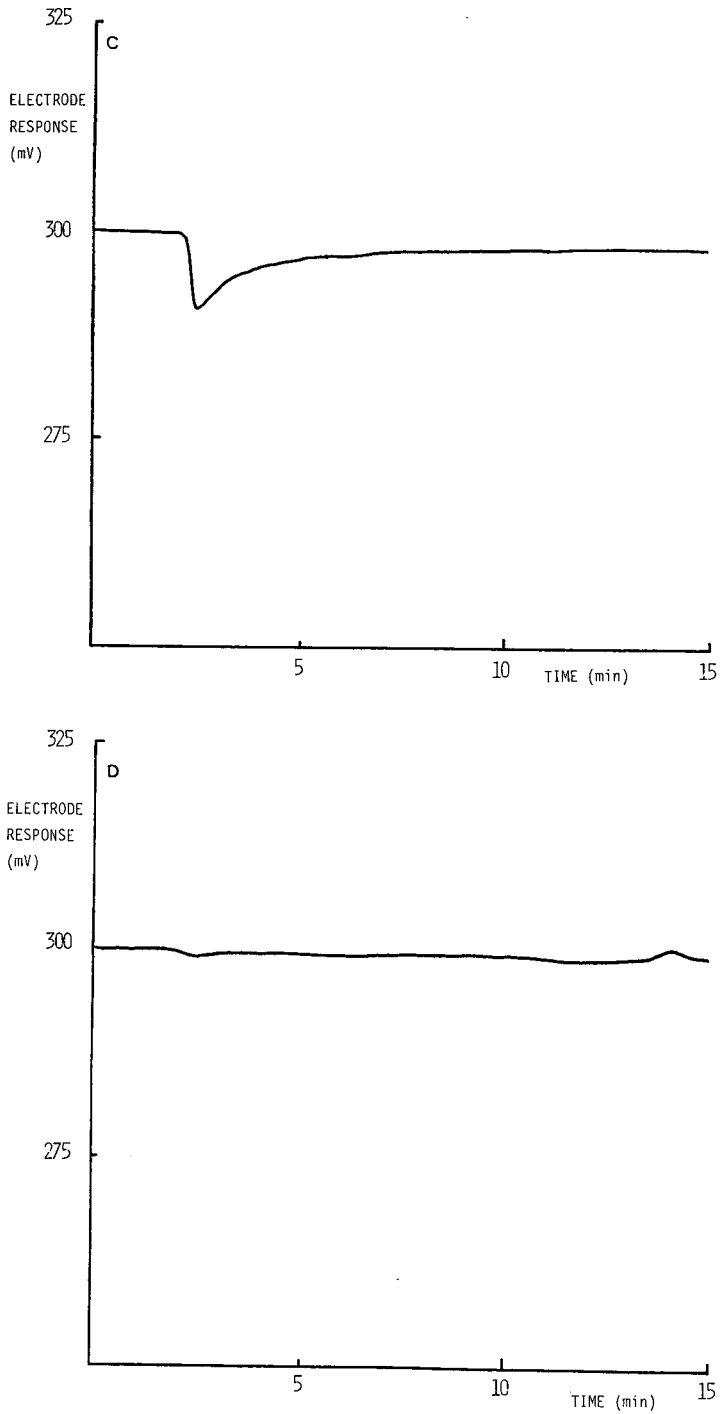

Fig. 5. Chromatograms of two silica polishing slurries, diluted 100-fold. (A,B) Conductivity detection. (C,D) Ion-selective electrode detection of samples in 5A and B, respectively.

The final illustration of fluoride ion-selective electrode detection is the analysis of anionic impurities in silica polishing slurries used for polishing silicon wafers prior to processing. Fluoride impurities in these materials could cause inconsistency in particle size by dissolution, as well as potential fluoride contamination of the wafers. Fig. 5A–D illustrates the analysis of two slurry samples by ion chromatography with simultaneous suppressed condictivity and ion-selective electrode detection. Conductivity detection alone would indicate substantial levels of fluoride contamination in both samples, but ion-selective electrode analysis demonstrates that only one of them contains an appreciable concentration of fluoride.

CONCLUSION

It has been demonstrated that the fluoride ion-selective electrode can perform as an effective additional detector in chromatography without interfering with the established suppressed-conductivity detection. Definitive identification and quantitation of fluoride are significant applications of ion chromatography in the semiconductor industry. An improvement in detection limits of *ca.* five times over previously reported analysis by this method has also been demonstrated.

REFERENCES

1 J. Weiss, in E. L. Johnson (Editor), *Handbook of Ion Chromatography*, Dionex, Sunnyvale, CA, 1986, pp. 202–205.
2 R. D. Rocklin and C. Pohl, paper presented at the *37th Pittsburg Conference on Analytical Chemistry and Applied Spectroscopy, Atlantic City, NJ, March 10–14, 1986*, Abstract 447.
3 P. E. Buell and J. E. Girard, in J. G. Tarter (Editor), *Ion Chromatography*, Marcel Dekker, New York, 1986, pp. 183–186.
4 E. Kissa, *Anal. Chem.*, 55 (1983) 1445–1448.
5 J. J. Ligane, *Anal. Chem.*, 39 (1967) 881.
6 W. L. Chek, R. W. Cattrall and I. C. Hamilton, *Anal. Chim. Acta.*, 177 (1985) 235.
7 P. K. Dasgupta, in J. G. Tarter (Editor), *Ion Chromatography*, Marcel Dekker. New York 1986, pp. 242–245.
8 J. Slanina, F. P. Bakker, P. A. C. Jongejan, L. V. Lamoen and J. J. Mols, *Anal. Chim. Acta.*, 130 (1981) 1–8.

Journal of Chromatography, 465 (1989) 11–15
Elsevier Science Publishers B.V., Amsterdam — Printed in The Netherlands

CHROMSYMP. 1533

REPRODUCIBILITY OF PACKED-COLUMN SUPERCRITICAL-FLUID CHROMATOGRAPHY WITH HELIUM HEAD-PRESSURE CARBON DIOXIDE

A. C. ROSSELLI*, D. S. BOYER and R. K. HOUCK
Suprex Corporation, 125 William Pitt Way, Pittsburgh, PA 15238 (U.S.A.)

SUMMARY

Controversy still exists concerning the use of helium head-pressure carbon dioxide as a pump-filling technique in supercritical-fluid chromatography. Previously published work in this area has produced contradictory results, with some authors reporting good reproducibility with this technique, while others have reported very poor results. This paper attempts to clarify this situation by seeking to determine whether this discrepancy in reported results is due to some factor related to instrument hardware such as the type of injection system or pumping system used, or perhaps to some inherent property of the technology itself. Reproducibility data for a hydrocarbon series and for caffeine using helium head-pressure carbon dioxide and non-split injection is presented. A possible cause of previously reported poor reproducibility is suggested.

INTRODUCTION

The technique of supercritical-fluid chromatography (SFC) has made great strides since its early days. It has progressed from the early laboratory-built systems to the present fully integrated systems, designed specifically for SFC. However, this growth has not been without controversy. One of the more recent topics of discussion has been the use of carbon dioxide with a helium head-pressure for the filling of SFC pumps. This is of considerable consequence to many SFC users, since carbon dioxide with a head-pressure of 1200–1500 p.s.i.g. of helium permits quite complete filling of the pump with liquid without the inconvenience of resorting to external pump cooling. This is particularly desirable for users of the smaller-capacity (50 ml or less) uncooled pumps, who would probably find it difficult to obtain satisfactory operation without the use of helium head-pressure carbon dioxide. However, the use of such a technique must not degrade the precision of the SFC system.

A recent article by Porter *et al.*[1] reported very poor peak area reproducibility [*ca.* 22% relative standard deviation (R.S.D.)] and poor retention time reproducibility (*ca.* 4.3% R.S.D.) for an *n*-alkane series when using helium head-pressure carbon dioxide with capillary columns without pump cooling. The statement was also made in this article that the use of helium head-pressure carbon dioxide as a pump filling

0021-9673/89/$03.50

technique is unacceptable. A subsequent article by Schwartz *et al.*[2] presented much better data for capillary retention time reproducibility (*ca.* 0.1% R.S.D.) for a triglyceride mixture when helium head-pressure was used in an uncooled pump. They also obtained good peak area precision (*ca.* 1.2% R.S.D.), using packed columns to analyze a series of *n*-alkanes. This much better data was somewhat disconcerting because it was obtained with a pumping system that was different from that of Porter *et al.*[1], and from the one in our own laboratory. The concern was now expressed that perhaps the cause of the discrepancy was the pumping system. Work in our own laboratory[3] with helium head-pressure carbon dioxide generally tended to support the findings of Schwartz *et al.*[2], but we had heretofore not performed a direct comparison between the two pump-filling techniques with our single-syringe-pump instrument. Schwartz *et al.*[2] do present data obtained on a single-syringe-pump instrument similar to the one used by Porter *et al.*[1], but largely from unpublished sources. In an attempt to resolve this issue, we therefore set out to determine if the widely varying results obtained by Schwartz *et al.*[2] and Porter *et al.*[1] were due to the pumping systems employed or to some other factor, such as the injection system. To this end, we decided to effect a direct comparison between helium head-pressure carbon dioxide and normal pressure carbon dioxide (under its own vapor pressure) in a single-syringe-pump system similar to the one used by Porter *et al.*[1]. However, we elected to use a larger-capacity syringe pump (250 ml, or *ca.* 50% larger) than they did, so that a full day's uninterrupted operation with normal pressure carbon dioxide could be obtained without the cumbersome practice of pump cooling. In addition, we also decided to employ programming rates that would produce analysis times of 20 min or less, so as to approximate conditions that might actually exist in, for example, a quality control (QC) laboratory where large numbers of samples must be analyzed in a minimum amount of time. These rapid programming rates (*i.e.* 20 atm/min or greater) are also a more severe test of the pumping system in general than are lower rates. Packed columns were chosen for this work because of their robustness and ease of manipulation, coupled with their ability to provide good resolution at these high programming rates. It was found that the use of helium head-pressure carbon dioxide for pump filling in packed-column SFC utilizing a single uncooled syringe pump has a relatively small effect on retention time and area reproducibility.

EXPERIMENTAL

A Suprex (Pittsburgh, PA, U.S.A.) Model 200A supercritical-fluid chromatograph with a 250-ml capacity syringe pump was fitted with a Dynatech Precision (Baton Rouge, LA, U.S.A.) autosampler to permit unattended operation. This instrument is provided with a Valco (Houston, TX, U.S.A.) EC14W electronically actuated injector, containing a 1.0-μl internal sample loop. Upon actuation, the entire 1.0-μl sample is swept into the column. Two packed columns, both 10 cm × 1.0 mm I.D., were used for this work. The first column, wich was used to generate the hydrocarbon data, was an Alcoa (Pittsburgh, PA, U.S.A) Alcobond Alumina column packed with 5-μm particles. The second column was a Keystone Scientific (State College, PA, U.S.A) Deltabond Cyano column also packed with 5-μm particles and was used to generate the caffeine data. For the hydrocarbon data, the instrument was programmed from 150 atm to 400 atm at a rate of 20 atm/min with an initial hold of 8

min at 150 atm. Oven temperature was 150°C. For the caffeine data, the instrument was programmed from 175 atm to 350 atm at a rate of 40 atm/min. There was an initial hold at 175 atm for 8 min and a final hold at 350 atm of 2 min. The oven temperature was 100°C. The carbon dioxide, in cylinders with eductor tubes, was supplied both with and without *ca.* 1500 p.s.i.g. of helium head-pressure by Scott Speciality Gases (Plumbsteadville, PA, U.S.A.). For the experimental runs, the syringe pump was filled with carbon dioxide (either with or without helium head-pressure), the data were collected, then the pump was emptied, purged, and refilled with the other type of carbon dioxide. At no time was any external cooling applied to the pump. The hydrocarbon sample was prepared by dissolving each of the *n*-alkanes C_{21}, C_{24}, C_{26}, C_{28} and C_{31} (Aldrich, Milwaukee, WI, U.S.A.) in HPLC-grade chloroform at a concentration of 0.2 mg/ml. The caffeine sample was prepared by dissolving caffeine (Sigma, St. Louis, MO, U.S.A.) in chloroform at a level of 1.0 mg/ml.

RESULTS AND DISCUSSION

Experimental data used to generate the results presented in this paper passed student's *t*-test at the 99% confidence level. The raw peak area reproducibilities for 10 consecutive injections of an *n*-alkane mixture are summarized in Table I. The average % R.S.D. of the peak areas for the series with helium head-pressure is 2.82, while it is 2.06 without helium head-pressure, a difference of 0.76% R.S.D. These results are in sharp contrast to those of Porter *et al.*[1], who obtained an average difference in peak area reproducibility of 19.9% R.S.D. between helium head-pressure and normal pressure carbon dioxide for an *n*-alkane series. Schwartz *et al.*[2] obtained an average of 1.22% R.S.D. for an *n*-alkane series with helium head-pressure. They did not perform the experiment without helium head-pressure, so it was not possible to perform a comparison between the two types of carbon dioxide in their system. The difference between the two pump-filling techniques is even smaller in the case of retention time reproducibility, as indicated by Table II. The average retention time % R.S.D. for the series with helium head-pressure is 0.11 and it is 0.9 without helium head-pressure, for a difference of 0.02% R.S.D. Porter *et al.*[1] observed an average difference of 4.18% R.S.D. in retention time reproducibility for *n*-alkanes, while Schwartz *et al.*[2] obtained an average retention time precision of *ca.* 0.1% R.S.D. for a triglyceride series using helium head-pressure carbon dioxide.

This work was then repeated with caffeine, a more polar analyte. Caffeine was chosen as the analyte because it can sometimes produce a less-than-optimum peak

TABLE I

RAW AREA REPRODUCIBILITY FOR HYDROCARBONS

	% R.S.D.				
	C_{21}	C_{24}	C_{26}	C_{28}	C_{31}
With helium head-pressure	3.2	2.9	2.3	2.0	3.7
Without helium head-pressure	1.9	2.4	2.2	1.9	1.9

TABLE II

RETENTION TIME REPRODUCIBILITY FOR HYDROCARBONS

	% R.S.D.				
	C_{21}	C_{24}	C_{26}	C_{28}	C_{31}
With helium head-pressure	0.10	0.11	0.11	0.13	0.10
Without helium head-pressure	0.08	0.09	0.10	0.11	0.07

shape, even with well deactivated columns. A chromatogram of caffeine is shown in Fig. 1, where a slight tail can be seen on the caffeine peak which otherwise exhibits good peak shape. The programming rate was also increased to 40 atm/min to duplicate rapid analysis conditions. The results of these experiments are summarized in Table III. The difference in peak area % R.S.D. with and without helium head-pressure is 1.1, which can still be considered to be relatively small. From this data and the hydrocarbon data, it appears that the type of pumping system employed does not have a major effect on peak area and peak retention time reproducibility when using helium head-pressure carbon dioxide, in agreement with some of the unpublished

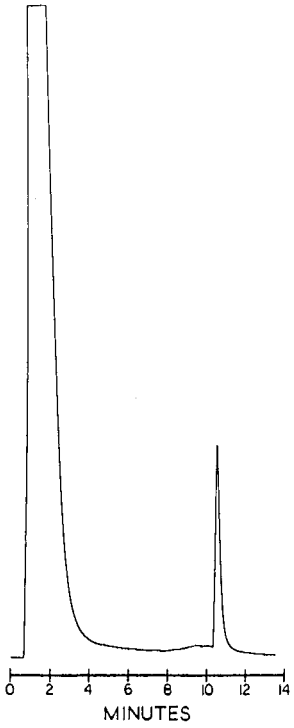

Fig. 1. Chromatogram illustrating the caffeine peak at a retention time of *ca.* 10.7 min.

TABLE III

REPRODUCIBILITY DATA FOR CAFFEINE

	Raw area (% R.S.D.)	*Retention time (% R.S.D.)*	*Average retention time*
With helium head-space	3.7	0.4	10.77
Without helium head-space	2.6	0.2	10.16

findings presented by Schwartz *et al.*[2]. The much poorer data reported by Porter *et al.*[1] (*ca.* 20% R.S.D.) may in fact be due to the injection system, as is suggested in their paper. These authors used timed-split (or moving) injection for their capillary work, while Schwartz *et al.*[2] used split injection for their capillary work and direct injection for the packed column work, as did we. Therefore, it seems that the timed-split injection system is the most likely source of poor reproducibility when using helium head-space carbon dioxide and that the use of this pump-filling technique has a relatively small effect on precision when used with injection systems other than timed-split injection. The possibility of a leak at the eductor tube as suggested by Schwartz *et al.*[2] does exist, but cannot be proved or disproved with the current set of data. It is interesting to note in Table III that a slight increase in retention time was observed when switching over to helium head-pressure, in agreement with a similar observation by Porter *et al.*[1]. This small increase may be due to a decrease in the solvating power of the mobile phase by the dissolution of helium in carbon dioxide.

In the case of both, our hydrocarbon data and caffeine data, it did not seem to make any difference whether the pump had just been filled with the helium head-pressure carbon dioxide or was near empty.

REFERENCES

1 N. L. Porter, B. E. Richter, D. J. Bornhop, D. W. Later and F. H. Beyerlein, *J. High Resolut. Chromatogr. Chromatogr. Commun.*, 10 (1987) 477.
2 H. E. Schwartz, P. J. Barthel and S. E. Moring, *J. High Resolut. Chromatogr. Chromatogr. Commun.*, 10 (1987) 668.
3 D. S. Boyer, Suprex Corporation, 1988, unpublished results.

Journal of Chromatography, 465 (1989) 17–21
Elsevier Science Publishers B.V., Amsterdam — Printed in The Netherlands

CHROM. 1512

SPLITTING CONTROL AND SOLVENT EFFECTS IN SUPERCRITICAL-FLUID CHROMATOGRAPHY WITH FUSED-SILICA CAPILLARY COLUMNS

M. BOHM, F. UMLAND and B. WENCLAWIAK[a,*]

Westfälische-Wilhelms-Universität Münster, Anorganisch-Chemisches Institut, Wilhelm-Klemm-Strasse 8, D-4400 Münster (F.R.G.)

SUMMARY

A computer-controlled splitting device was used to study splitting ratios from 1:3 to 1:500 in supercritical-fluid chromatography. At low to medium-high splitting ratios, a solvent effect, dependent on the solvent density, was observed. Chromatographic data obtained for two test mixtures (polynuclear aromatic hydrocarbons and *n*-alkanes) are comparable to those in the literature.

INTRODUCTION

Supercritical-fluid chromatography (SFC), especially capillary-column SFC, suffers from many of the problems inherent in capillary-column gas chromatography (GC). One area of SFC research is the (reproducible) injection of the sample into the capillary column. Owing to transport phenomena and diffusion effects in the supercritical fluid, capillary columns have inner diameters of 100 μm or less. In order to achieve a good separation and to avoid column overloading, the injected sample is split, and only a portion is loaded on to the column. This loss of detectable analyte consequently limits applications in trace analysis.

Under SFC conditions, the retention times of analytes are much higher than those in GC owing to the much higher density of the eluent inside the column and the limited flow through the column restrictor. The use of shorter capillary columns (2–10 m) reduces the retention times of analytes and the residence times of solvents, but the column efficiency is also reduced. With short and very narrow columns, the injection volume becomes very important. A simple calculation shows that a 1-μl plug injected into a 100-μm diameter column would result in a 127-mm long plug inside the column. A 60-nl plug still results in a length of 7.6 mm, which is much longer than 1 HETP in capillary SFC. In other words, a 7.6-mm plate height in a 2-m long capillary column would yield only 263 theoretical plates; a 127-mm plate height gives 15.7

[a] Present address; Physikalisches Institut, Westfälische-Wilhelms-Universität Münster, Wilhelm-Klemm-Strasse 10, D-4400 Münster, F.R.G.

0021-9673/89/$03.50

theoretical plates. As the flow-rates are usually much higher than the optimum value, the chromatogram becomes very poor.

Much effort has been expended on overcoming such injection problems. A constant splitting device is currently the most common approach in capillary SFC. Unfortunately, the splitting changes with any change in the experimental conditions, *e.g.*, pressure and temperature[1], and there are many problems in quantitative applications[2]. Instead of a split-injection technique, direct injection or time-controlled direct injection is now more often used[2]. This allows better reproducibility of injection and the amount injected can therefore be more easily optimized for efficient chromatography.

We have taken a new approach to split injection in SFC. A controller has been developed that can be used on injection valves with different internal or external sample-loop volumes. It can also be time-programmed in order to save supercritical fluid. Preliminary results are reported.

EXPERIMENTAL

The SFC system was made in-house (Fig. 1, bottom) and consisted of a heated carbon dioxide cylinder, which gave pressures of up to 20.0 MPa (*ca.* 200 atm), with either a 0.2-μl or (in most instances) a 2-μl Valco C14W injection valve (Valco, Houston, TX, U.S.A.)[3]. The splitting system was similar to those described elsewhere[4], with the exception that the split outlet was connected to a Nupro type SS2-A needle valve (BEST. Ventil + Fitting, Dortmund, F.R.G.), which was driven by a stepping motor. The stepping motor was controlled via a two-point control program of a CBM 64 (Commodore) personal computer. A simple schematic diagram explains the split control system (Fig. 1, top). The disturbance $e(t)$ is the difference between the reference input x_w (keyboard value) and the actuating signal $y(t)$ (pressure gauge value). The manipulated variable $U(t)$ adjusts the disturbance to small values; in the apparatus this means control of the direction of the stepping motor and the period of motor action. The software was written in-house. The split-outlet system and the software can easily be modified for column pressure and density control under SFC conditions; this will be reported in a subsequent paper.

The flow diagram of the two-point controller is shown in Fig. 2. The hysteresis becomes important if rapid changes are required, as every change requires (motor run) time. Once the deviation between $y(t)$ and x_w has been determined, the control program is set for no changes ("Yes"), open valve or close valve.

The columns used were either a 10 m × 100 μm I.D. BP-1 or 12 m × 100 μm I.D. BP-10 fused-silica capillary column (Scientific Glass Engineering, Weiterstadt, F.R.G.). The column was kept inside a Carlo Erba Fractovap HRGC 4160 instrument (Erba Science, Hofheim/Taunus, F.R.G.). The column end restrictor was a 90-mm length of 10 μm I.D. fused-silica capillary, connected with a butt connector and inserted into a flame ionization detector (FID) which was kept at 300°C.

Two samples were used: one contained a mixture of three polycyclic aromatic hydrocarbons (PAHs) (naphthalene, biphenyl and phenanthrene) dissolved in various solvents and the other contained six *n*-alkanes (C_{12}–C_{16} and C_{18}).

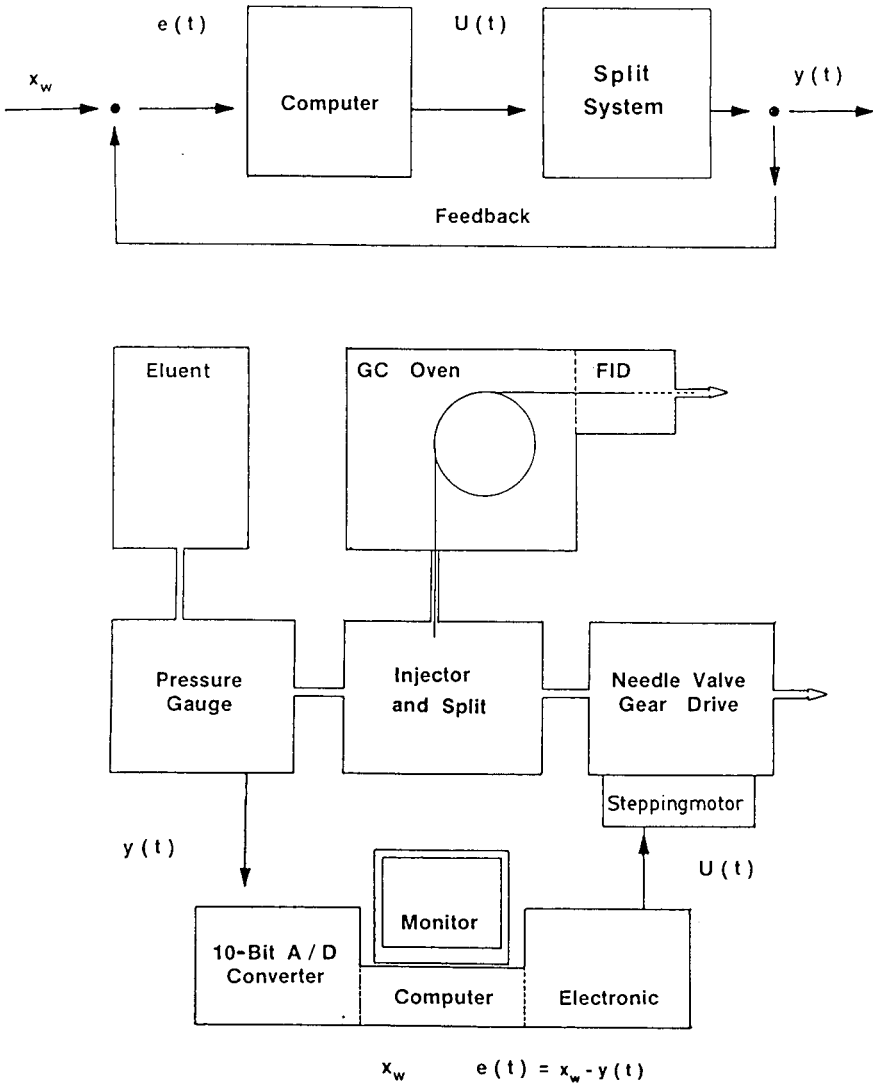

Fig. 1. Schematic diagrams of (top) theoretical control system and (bottom) SFC apparatus and computer control system. A/D = Analog-to-digital.

RESULTS AND DISCUSSION

During an experiment the SFC system was maintained at constant pressure, but for different experiments the pressure was varied by changing the temperature of the carbon dioxide cylinder. The pressure was monitored with a pressure gauge to provide $y(t)$ so that the splitting ratios were kept constant. The reference (input) value (x_w) was compared with $y(t)$ five times per second, which allowed a rapid response for the needle valve positioning. First, the splitting control was used to determine the

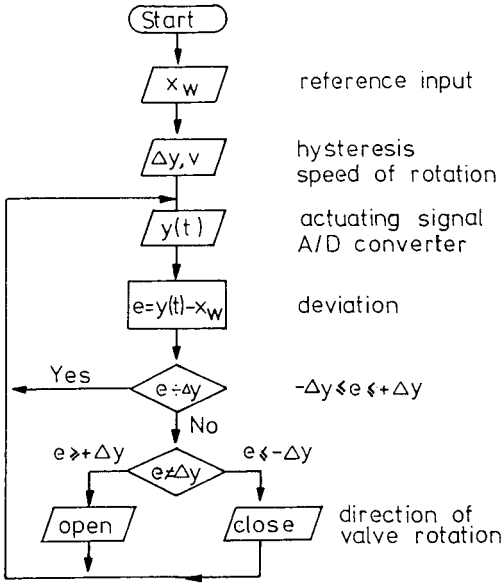

Fig. 2. Flow diagram of the two-point controller. Parallelograms, computer input/output symbol; rectangle, computer calculation symbol; diamonds, computer decision step symbol.

capacity factors (k') of both test mixtures. They were in agreement with data reported in the literature[5]. A slight change in retention times (t_r) at different splitting ratios was observed (Fig. 3). The column outflow remained constant at all times.

A dependence on splitting ratio and sample solvent density was unexpected. At a low splitting ratio (1:3), the retention times of the PAHs increased with increasing

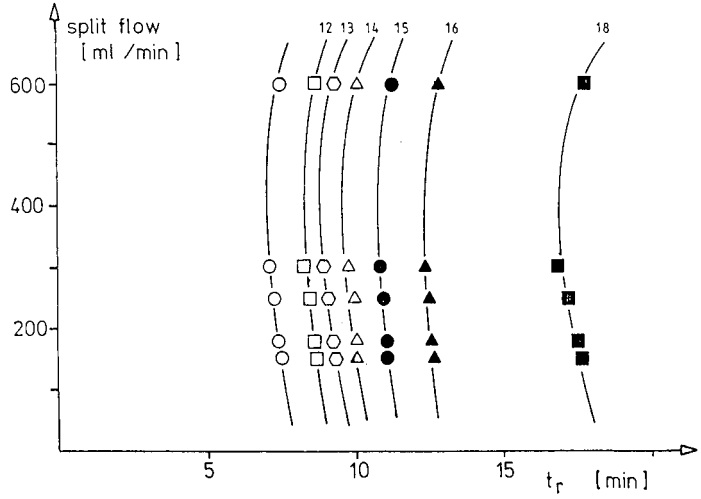

Fig. 3. Dependence of retention time on splitting ratio for six *n*-alkanes (C_{12}–C_{18}, identified by the numbers above the lines) in *n*-heptane (○). Column outflow into detector: 2.1 ml/min.

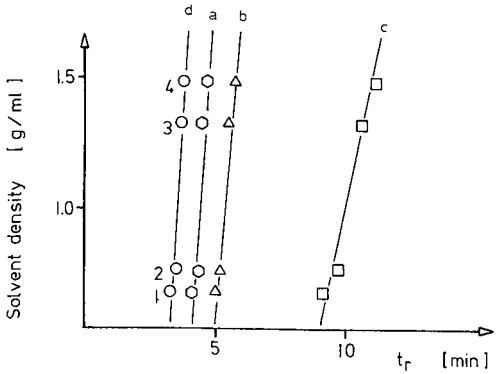

Fig. 4. Effect of solvent density on retention time: a = naphtalene; b = biphenyl; c = phenanthrene; d = solvent (1 = *n*-heptane; 2 = cyclohexane; 3 = dichloromethane; 4 = trichloromethane). Splitting ratio, 1:3; temperature, 85°C; pressure, 11.0 MPa (*ca.* 110 atm).

density of the solvent (Fig. 4). At a high splitting ratio (1:350), the retention times remained constant for every solvent. This could be explained by modification of the column surface at the column head due to the solvent[6] and/or a change in the splitting ratio due to changed flow characteristics in the splitting restrictor. With increasing splitting ratios (up to 1:100), this effect becomes less obvious, but is still apparent. As the concentration was the same in all instances, a solubility effect can be excluded. A solvent and/or density effect is, therefore, more likely than a flow effect. All of these experiments were performed under isodensic conditions, and phenanthrene was eluted with a leading peak, which accounts for its different slope in Fig. 4. From the preliminary experiments is can be concluded that: (1) variable splitting control is one alternative to constant splitting in SFC; (2) large splitting ratios are one alternative to time-controlled injection; and (3) at low splitting ratios a solvent and/or density effect is observed.

In the future, further evaluation of the system and more data are needed to confirm its general applicability. The use of the computer-controlled splitting valve allows much greater and more easily adjustable ranges of splitting ratio, which, as our current data show, can be easily reproduced. In addition, splitting control might also be useful in GC applications.

REFERENCES

1 W. P. Jackson, K. E. Markides and M. L. Lee, *J. High Resolut. Chromatogr. Chromatogr. Commun.*, 9 (1986) 213–217.
2 M. L. Lee and K. E. Markides, *J. High Resolut. Chromatogr. Chromatogr. Commun.*, 9 (1986) 652–656.
3 M. Bohm, *MS Thesis*, Westfälische-Wilhelms-Universität Münster, Münster, 1986.
4 P. A. Peadon, J. C. Fjeldsted, M. L. Lee, S. R. Springston and M. Novotny, *Anal. Chem.*, 54 (1982) 1090–1093.
5 K. Jinno, M. Saito, T. Hondo and M. Sanda, *Chromatographia*, 21 (1986) 219–222.
6 K. Grob, Jr. and B. Schilling, *J. Chromatogr.*, 260 (1983) 265–275.

Journal of Chromatography, 465 (1989) 23–33
Elsevier Science Publishers B.V., Amsterdam — Printed in The Netherlands

CHROMSYMP. 1554

SUPERCRITICAL FLUID CHROMATOGRAPHY WITH SULFUR CHEMILUMINESCENCE DETECTION

WILLIAM T. FOREMAN[a], CURTIS L. SHELLUM[b], JOHN W. BIRKS* and ROBERT E. SIEVERS
Cooperative Institute for Research in Environmental Sciences (CIRES), and Department of Chemistry and Biochemistry, Campus Box 215, University of Colorado, Boulder, CO 80309 (U.S.A.)

SUMMARY

The newly commercialized sulfur chemiluminescence detector, originally designed for gas chromatography, has been successfully interfaced to a capillary-column supercritical fluid chromatograph used with carbon dioxide as the mobile phase. Interfacing was accomplished by inserting the capillary column through a heated (100–125°C) interface tube, and carefully positioning the integral restrictor end of the column within the chemiluminescence reaction chamber. This coupling resulted in direct transfer of the column effluent into the chamber, which minimized the dead volume and provided acceptable sensitivity and peak shape. Example chromatograms are presented to demonstrate the feasibility of this new separation–detection scheme, in which sulfur compounds are detected by the chemiluminescence emitted upon reaction with molecular fluorine. Some observed detection limits and linearity of response are also presented.

INTRODUCTION

The chemiluminescence reaction that occurs when certain sulfur-containing organic compounds react with molecular fluorine forms the basis of detection by the sulfur chemiluminescence detector (SCD)[1]

$$R_1\text{–}S\text{–}R_2 + F_2 \rightarrow \text{products} + h\nu$$

This detector typically exhibits a strong response to organosulfur compounds when the R group bonded to the sulfur is either hydrogen (except for H_2S) or an alkyl group containing hydrogen. Reduced organosulfur compounds having the general structure

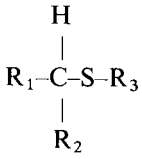

[a] Present address: U.S. Geological Survey, National Water Quality Laboratory, 5293 Ward Road, Arvada, CO 80002, U.S.A.

[b] Present address: University of Graz, Institute for Pharmaceutical Chemistry, Universitätsplatz 1, Graz, Austria.

0021-9673/89/$03.50

and containing hydrogen in the alpha position relative to the sulfur have displayed particularly strong responses, especially when the R groups are short-chain alkyl groups[1–3]. Nelson *et al.*[1] proposed that addition of fluorine gas to an organosulfur compound having the general structure shown above could result in a hydrogen abstraction reaction to form vibrationally excited $HF^{\dagger}$ ($v' < 6$), which provides a chemiluminescence signal at wavelengths higher than 450 nm. Spectroscopic investigations of the chemiluminescent products formed upon reaction of F_2 with the low-molecular-weight hydrogen-bearing organosulfur compounds studied revealed the formation of excited $HF^{\dagger}$ and HCF* as emitting species[4]. Phosphorescent emission from electronically excited thioformaldehyde was observed when at least one of the R groups was $-CH_3$[4,5]. Emissions from a species ascribed to FCS* were also observed for many analytes[4]. In addition to organosulfur compounds, some organoselenium species have been found to respond in the SCD, although their response is about an order of magnitude less than the corresponding sulfur compound[1]. For dimethyl-diselenide the principal emitting species was identified as selenoformaldehyde[6]. Some olefins also show a fairly strong response[1–3].

The SCD was first developed for packed-column gas chromatography (GC), and in that apparatus a short, heated section of PTFE-lined 1/8 in. stainless-steel tubing was utilized as an interface between the GC column and the SCD. This GC–SCD was found to be very sensitive to alkyl sulfides, disulfides, and thiols[1,2]. Subsequently, the SCD was successfully interfaced to a capillary-column system by inserting the column through a section of 1/16 in. I.D. × 1/8 in. O.D. stainless-steel interface tube and up into the chemiluminescence chamber[7]. The interface was heated to temperatures typically in excess of 200°C to maintain analyte volatility in the transfer from the column into the SCD. Detection limits of < 10 pg for methanethiol, ethanethiol, 1- and 2-propanethiol, dimethyl sulfide, and dimethyl disulfide have been determined recently[8], using capillary-column GC–SCD. This combination is at least one order of magnitude more sensitive than the same GC system used with a flame-photometric detector.

While GC can provide excellent separation of analytes, it is not applicable to a large number of organosulfur compounds that are relatively polar, non-volatile, and/or thermally unstable. Several attempts have been made to extend the utility of the SCD to these analytes by interfacing the detector to a high-performance liquid chromatography (HPLC) system[3,9]. These HPLC–SCD systems have provided the necessary liquid-phase separation, but they rely on a heated (typically 300°C or higher) transfer line to introduce the mobile phase and analytes into the chemiluminescence chamber in the vapor phase. While HPLC–SCD systems have been shown to work well, even for some thermally unstable compounds, the development of new interface designs which do not require excessive heating is desirable.

Supercritical fluid chromatography (SFC), a technique complementary to GC and HPLC, shows the potential of separating a variety of thermally labile and higher-molecular-weight organosulfur compounds, and has been found to be relatively easy to interface to a number of detectors used in GC and/or HPLC[10–12]. Recently, Foreman *et al.*[13] succesfully interfaced a capillary-column supercritical fluid chromatograph to the redox chemiluminescence detector and demonstrated some potential applications of the system. Those findings suggested that a supercritical fluid chromatograph might also be directly coupled to other chemiluminescence-based

detectors. This paper describes our successful efforts in interfacing a supercritical fluid chromatograph with the SCD.

EXPERIMENTAL

The SFC system was assembled in-house from commercially available components. Liquid CO_2 was supplied to the chromatograph pump from a siphon tank pressurized to 100 atm with He. A Brownlee Labs. microgradient system syringe pump (Applied Biosystems, Santa Clara Analytical Div., Santa Clara, CA, U.S.A.) with pressure programming capability, was used to deliver the CO_2 mobile phase. All separations were carried out in a 3.5 m × 0.10 mm I.D. DB-5 fused-silica capillary column with a 0.4-μm film thickness (J & W Scientific, Folsom, CA, U.S.A.). The mobile phase was maintained at supercritical temperatures (typically 80–125°C) by housing the column inside the oven of a Model 5890 GC (Hewlett-Packard, Avondale, PA, U.S.A.). Direct injections of 60 nl of sample were made with an unheated Model C2I4W valve (Valco Instrument, Houston, TX, U.S.A.). The column pressure was maintained through use of an integral restrictor[14] at the detector end of the column. CO_2 flow-rates, measured at the column outlet, ranged from *ca.* 0.75 ml/min at 100 atm to 2 ml/min at 300 atm.

A Model 300 SCD (Sievers Research, Boulder, CO, U.S.A.) was connected to the chromatograph oven by an insulated 42.5-cm-long section of a 1/8 in. O.D. × 1/16 in. I.D. stainless-steel tubing which housed part of the chromatograph's capillary column. The detector end of the capillary column was first inserted through a 1/16-in.–1/8-in. stainless-steel reducing union fitting, attached to the supercritical-fluid chromatograph oven end of the interface tube. The restrictor end of the column was carfully positioned to extend 2 mm beyond the detector end of the interface tube, and the reducing union fitting with graphite ferrule was tightened to maintain the column position. The detector end of the tube was then inserted through the 3.2-cm-thick wall of the chemiluminescence chamber and into the chamber another 0.5 cm, and connected to the chamber wall with a 1/8-in. stainless-steel nut and ferrule (see Fig. 1). This nut plus about 2 cm of interface tubing outside the chamber were wrapped

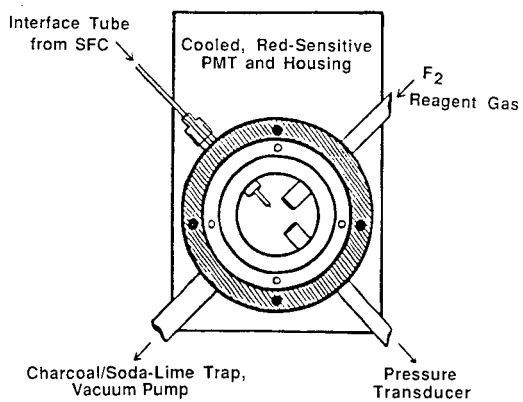

Fig. 1. Diagram of the chemiluminescence reaction chamber of the SCD, showing the positioning of the interface tube within the chamber. The restrictor end of the capillary column extends 2 mm beyond the end of the interface tube (not to scale).

with heating tape and heated to 100–125°C to maintain the column restrictor in the chamber above the critical temperature of CO_2. The remainder of the transfer line was not heated, since heat from the chromatographic oven and the heating tape was enough to maintain the insulated transfer line at or above 40°C.

The column effluent from the supercritical fluid chromatograph was mixed with F_2 reagent gas in the chemiluminescence chamber, the pressure of which was maintained at 1 Torr using a vacuum pump and monitored with a pressure transducer. The F_2 was generated *in situ* prior to entering the chamber by passing SF_6 at 0.5 ml/min through a high-voltage electrical discharge. Light resulting from the chemiluminescent reaction of the reagent gas with each analyte was monitored by photon counting with a red-sensitive photomultiplier tube, cooled to −15°C. A trap, containing charcoal and soda-lime, was positioned between the chamber and the vacuum pump to remove residual organics, HF and F_2. As an additional safety measure, the vacuum pump exhaust was vented to a hood. Additional SCD operational procedures are detailed in refs. 1–3 and 15.

All solvents were of chromatography grade obtained from various commercial sources. Other reagents were benzyl sulfide, benzyl disulfide, and polycyclic aromatic hydrocarbons from Chem Service (West Chester, PA, U.S.A.), and Malathion Insect Control formulation from Dexol Industries (Torrance, CA, U.S.A.). All other pesticide standards were obtained from the Environmental Protection Agency's Pesticides and Industrial Chemicals Repository (Research Triangle Park, NC, U.S.A.). The carbon-black extract and the other anti-oxidant standards were gifts from various researchers.

RESULTS AND DISCUSSION

The coupling of capillary-column GC with the SCD[7,16] requires the use of a transfer line, into which the column is inserted, that is commonly heated to at least 225°C to maintain analyte volatility until it reaches the chemiluminescence chamber. Since SFC relies on analyte solubility in the mobile phase and not on intrinsic analyte volatility we assumed that the interface tube would only need to be heated enough to maintain the mobile phase above its critical temperature (above 32°C for CO_2). Experimental evidence has confirmed that this assumption is warranted.

As shown in Fig. 1, the interface tube extended through the chemiluminescence chamber wall 3.2 cm and into the chamber another 0.5 cm, and the restrictor end of the capillary column was carefully positioned to extend 2 mm beyond the end of this tube. When CO_2 expands through the restrictor into the chamber, maintained at reduced pressure, the Joule-Thomson effect[17] can cause the CO_2 to freeze at the end of the column. The resulting freeze–thaw of CO_2 leads to spiking of analyte peaks. Therefore, it was necessary to supply enough heat to the restrictor end of the column to eliminate the freezing effect. To accomplish this, the nut connecting the interface tube to the chamber plus an additional 2 cm of the tube outside the chamber were wrapped and heated to 100–125°C with heating tape. This heat source provided an adequate heat transfer along the tube into the chamber to maintain the restrictor above the critical temperature of CO_2. With this interface tube design, positioning of the column end within the chamber was found to be critical for the achievement of acceptable chromatograms. If the column end extended more than *ca.* 2 mm past the end of the

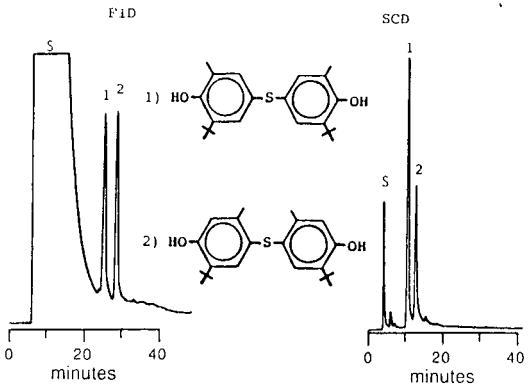

Fig. 2. SFC with flame ionization detection (FID) and sulfur chemiluminescence detection (SCD) of two anti-oxidant isomers: 125 ng of 4,4'-thiobis(*tert.*-butyl-*o*-cresol) (1) and 151 ng of 4,4'-thiobis(*tert.*-butyl-*m*-cresol) (2) in toluene (S). Linear pressure program from 150 atm to 250 atm in 40 min for both chromatograms. FID at 250°C and capillary column at 100°C. SCD at 100°C and capillary column at 80°C. All other conditions as described in the Experimental section.

tube, heat transfer to the restrictor at the end of the column was limited, and spiking and poor peak shape resulted. However, the column had to extend at least beyond the end of the interface tube or else analyte deposition would occur inside the tube, again resulting in poor peak shape. While correct positioning of the column within the chamber was critical, this was easily accomplished, as described in the experimental section.

The responses observed for two sulfur-containing phenolic anti-oxidant isomers analyzed using SFC with a flame ionization detector (FID) and SFC–SCD are compared in Fig. 2. The FID shows a typical, large response to the toluene solvent, whereas the SCD response to toluene was much smaller. This lower response to the solvent allowed chromatographic conditions to be changed to provide faster elution of the analytes by SCD without overlap with the tail of the solvent peak. For the separation in Fig. 2, faster elution was accomplished by increasing the fluid density through reduction of the column temperature to 80°C for the SCD chromatogram (compared with 100°C for the FID). All other conditions for obtaining these two chromatograms were identical, although column flow-rates probably varied slightly due to differences in temperatures at the restrictor (FID at 250°C and SCD heated to 100°C outside the chamber, as described above.) The molar responses in the FID to the two anti-oxidant isomers, which differed only in the position of their two methyl groups [both methyl groups in the *ortho*-position (1) or both in the *meta*-position (2)], were approximately equivalent and typical of this detector. However, in the SCD the molar response of the *ortho*-isomer was about twice that of the *meta*-isomer. The dissimilar SCD responses are likely due to differences between the two isomers in their reactivity with F_2.

In Fig. 3 is shown a chromatogram obtained by SFC–SCD of thermally labile benzyl sulfide and benzyl disulfide. Again, the SCD response to the toluene solvent was relatively small, and due to the complete separation of the two analytes under the conditions of Fig. 3, the chromatographic conditions could be altered to allow

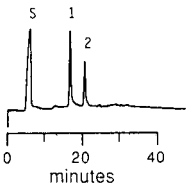

Fig. 3. SFC–SCD of 3.1 ng of benzyl sulfide (1) and 4.5 ng of benzyl disulfide in toluene (S). Linear pressure program from 100 atm to 200 atm in 40 min. SFC column at 80°C. All other conditions as described in the Experimental section.

somewhat faster analysis, while maintaining complete resolution of the analytes. These two analytes possess an alpha hydrogen relative to the sulfur atom, and this renders them reasonably sensitive to detection by the SCD[1–4].

An example analysis of three thermally labile sulfur-containing anti-oxidants by SFC–SCD is shown in Fig. 4. The chloroform used to dissolve these compounds was nearly undetected by the SCD. Of particular interest are the varying responses observed for the three anti-oxidants. Compound **3** (see Fig. 4), while possessing the greatest number of sulfur atoms, gave the least response, exemplifying that the chemiluminescence reactions in the SCD are largely based on hydrogen abstraction reactions, which form vibrationally excited $HF^{\dagger}$ (refs. 1–4), and not on reactions that are specifically related to the number of sulfur atoms. The strongest response was exhibited by compound **2**. This was an unexpected observation since compound **1** contains a hydrogen which is in the alpha position relative to a sulfur atom (but attached to a N atom instead of a C atom), and organosulfur compounds having an alpha-hydrogen configuration (with the H attached to a C atom) have been reported to be very responsive in the SCD[1,3,16]. However, compound **2** does not contain an alpha hydrogen relative to a sulfur atom, and compound **1** was expected to give a greater response than compound **2**, but this is not the case. Since all three of the anti-oxidants in Fig. 4 contain hydrogen atoms, the formation of vibrationally excited $HF^{\dagger}$ is likely for the reactions of these analytes with F_2. In addition, electronically excited HCF* and FCS* reaction products, which have been previously observed in reactions

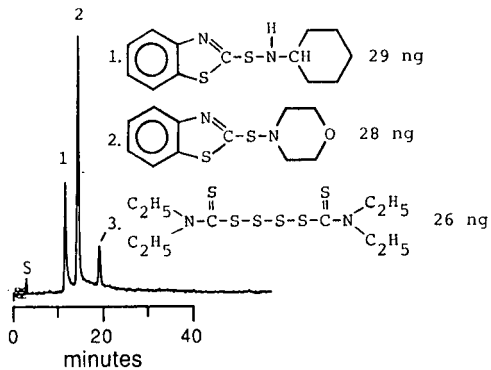

Fig. 4. SFC–SCD of three sulfur-containing anti-oxidants in $CHCl_3$ (S). Linear pressure program from 110 atm to 250 atm in 40 min. All other conditions same as for Fig. 3.

Fig. 5. Isoconfertic SFC–SCD of 28 ng of malathion (*) from a dilution in toluene of a commercial malathion formulation. Pressure at 115 atm, SFC column at 100°C. All other conditions as described in the Experimental section.

between F_2 and organosulfur compounds[4], may be contributing to the chemiluminesc ence signal. The examples in Fig. 2–4 reemphasize that the molar response in the SCD is compound-dependent[1,3,16], and the use of compound-specific standards would be required to do accurate quantitative work with the SCD.

A number of sulfur-containing organophosphate pesticides are thermally unstable, which renders it difficult to determine them by GC; therefore, analysis by SFC–SCD could be of benefit. An isoconfertic analysis of malathion is shown in Fig. 5. This sample was prepared by dilution of a commercial malathion insecticide formulation with toluene. Other inert ingredients besides the xylene solvent were reported to be in this formulation. The two early peaks in the chromatogram are responses to the toluene and xylene solvents and possibly to another ingredient. This SFC–SCD analysis is comparable to a previously reported HPLC–SCD analysis of this formulation[3]. Five other sulfur-containing organophosphate pesticides, carbophenothion, dioxathion, fenitrothion, and methyl and ethyl parathion, were successfully chromatographed and detected by SFC–SCD.

In Table I are shown the detection limits observed in this study for malathion,

TABLE I

DETECTION LIMITS BY SCD[a]

	SFC–SCD		
	ng	*pg/s*	*pg S/s*
1-Octanethiol	1.3	27	6
1-Dodecanethiol	5.0	89	14
Malathion	4.5	77	15
Methyl parathion	39	65	72
Anti-oxidant 1[b]	1.0	26	6
Anti-oxidant 2[b]	0.45	11	3
Anti-oxidant 3[b]	5.0	170	90

[a] Detection limits determined at a 3:1 signal-to-noise ratio as described in the Discussion section.
[b] Structures of anti-oxidants are shown in Fig. 4.

methyl parathion, and a number of other compounds by SFC–SCD. These detection limits were all determined at a 3:1 signal-to-noise (S/N) ratio using the following equation:

$$\text{detection limit} = \frac{3N}{S_i/m_i}$$

where N is the peak-to-peak noise, S_i is the peak signal obtained from the chromatogram for species i, and m_i is the mass of species i injected. The detection limits were calculated from chromatograms in which the analyte signals were *ca.* 5 times greater than the baseline peak-to-peak signal. This detection limit calculation method is identical to that previously described[3]. The detection limits are reported in nanograms of compound injected, picograms of compound per peak width (pg/s), and picograms of sulfur per second (pg S/s). As noted above, however, the number of sulfur atoms present in the analyte does not appear as important as the overall structural configuration to the reactivity of F_2 with analytes. As a result, the pg S/s values likely provide less useful information than the ng compound injected and pg compound injected/s data presented in Table I, but they are included to allow comparison with previous work. The SCD response appears to be compound specific, probably due to different activation energies for the reaction between the analytes and F_2 and due to the formation of a number of different excited-state products that produce distinct chemiluminescence emission spectra. The latter results in a varied response when monitored by the photomultiplier tube in the SCD[4]. Calculated SFC–SCD detection limits were typically in the high-picogram to low-nanogram range of analyte injected.

Using a capillary-column SFC system with dual-flame photometric detector (FPD), Markides *et al.*[19] reported a detection limit of 0.5 ng (S/N = 2) for ethyl parathion in the phosphorous mode. While no detection limit was reported specifically for ethyl parathion in the sulfur mode, they found that the FPD in the sulfur mode was less sensitive (detection limit of 25 ng for benzo[*b*]thiophene) and more noisy than when operated in the phosphorus mode and exhibited a baseline rise during pressure programming, requiring baseline correction procedures. In comparison, the sulfur chemiluminescence detector exhibited no additional noise and only minimal baseline drift during pressure programming, and was found to have a detection limit of 39 ng (S/N = 3) for methyl parathion.

The SFC–SCD detection limits of several analytes reported here can be compared to detection limits previously determined using GC–SCD or HPLC–SCD systems. Compared to the 1-dodecanethiol detection limits determined by SFC–SCD (Table I), a capillary GC–SCD system[18] with a He mobile phase was two orders of magnitude more sensitive, based on the absolute amount of analyte injected (0.06 ng) and one order of magnitude more sensitive when the amount per peak width values (9.5 pg/s) were used to compensate for chromatographic differences between capillary GC and SFC. Signal quenching by CO_2 in the SFC–SCD may account for some of these differences, since triatomic CO_2 is generally a much more effective quencher of chemiluminescence signals than monoatomic He[20,21]. The use of packed-column SFC with SCD was not investigated here. However, outlet flow-rates in packed-column SFC are typically >20 ml/min, and in earlier studies of SFC with another chemiluminescence-based detector, the redox chemiluminescence detector, these

higher mobile phase flow-rates were found to cause substantial signal quenching[13,22]. Whether a similar reduction in response by the SCD will be observed under packed-column SFC mobile phase flow-rates remains to be determined. In 1986, Mishalanie and Birks[3] reported a detection limit of 77 pg/s for 1-octanethiol using a HPLC–SCD system. Their value is *ca.* three times higher than the 27 pg/s value observed in SFC–SCD. This difference may be due in part to instrumental improvements in the new Model 300 SCD over their earlier SCD design. More recently, Legier and Birks[9] reported a detection limit of 390 pg/s of malathion by HPLC when using the Model 300 SCD. Their value is *ca.* five times higher than that found with the SFC–SCD system (77 pg/s). Additional signal quenching from the volatilized mobile phase may account for the slightly lower detection limits observed with HPLC–SCD using acetonitrile–water or methanol–water mobile phases, compared to SFC–SCD with CO_2.

A plot of response (peak area) *versus* amount of 1-octanethiol injected into the SFC–SCD system shows linearity ($r^2 = 0.999$) over the one order of magnitude variation in amount injected. This finding is consistent with calibration curves obtained in the GC–SCD system, which exhibits excellent linearity over approximately four orders of magnitude down to the detection limit for a variety of analytes[2,16]. Linear response up to three orders of magnitude has also been observed recently by another research group, which used an SFC–SCD system similar to the one described here[23].

A number of industrial and environmentally relevant materials contain organosulfur compounds, many at trace levels. One example is carbon black, which has been reported to contain trace quantities of sulfur-containing polycyclic aromatic heterocycles[24,25]. In Fig. 6 is shown an SFC–SCD chromatogram of a dichloromethane extract of carbon black, prepared according to the procedure of Lee and Hites[24]. Again, the minimal response by the SCD to the dichloromethane solvent should be noted. Some of the peaks obtained may be sulfur-containing heterocyclic species. However, the SCD has been found to be not as responsive to sulfur heterocyclic compounds as it is to alkyl sulfur compounds[2,26]. Since carbon black is reported[27] to contain up to nearly 1 part per thousand of individual polycyclic aromatic hydrocarbons (PAHs), we suspected that these hydrocarbons in the carbon black

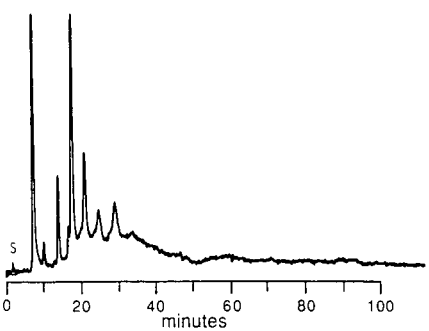

Fig. 6. SFC–SCD of a dichloromethane (S) extract of carbon black. Pressure held for 2 min at 136 atm, then linearly programmed at 4.1 atm/min to a final hold of 374 atm. SFC column at 100°C. All other conditions as described in the Experimental section.

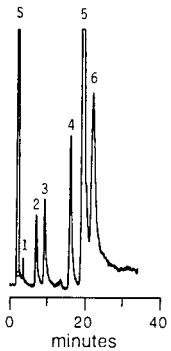

Fig. 7. SFC–SCD of a standard containing six polycyclic aromatic hydrocarbons in toluene (S). Linear pressure program from 100 atm. to 300 atm in 40 min. SFC column at 100°C. All other conditions as described in the Experimental section. Peaks: 1 = naphthalene, 77.4 ng; 2 = fluorene, 95.4 ng; 3 = phenanthrene, 59.4 ng; 4 = chrysene, 58.8 ng; 5 = benzo[*a*]pyrene, 57.0 ng; and 6 = 1,2,5,6-dibenzanthracene, 69.0 ng.

extract might be producing most of the peaks in this chromatogram. In Fig. 7 is shown an SFC–SCD chromatogram of a mixed standard of six PAHs in toluene, run under different chromatographic conditions than Fig. 6. All the PAHs responded with an overall increase in response with increasing number of aromatic rings. The differences in response observed between PAHs of equivalent number of aromatic rings is probably due to varying levels of reactivity of the PAHs with F_2. The substantial response to PAHs, especially those of higher molecular weight, coupled with the reported high concentrations of PAHs in carbon black extracts, suggests that the peaks in Fig. 6 were likely due principally to response by the SCD to PAHs. Potential interferences from olefins and PAHs may therefore present a problem when attempting to determine organosulfur compounds in some matrices. However, the fairly high degree of sensitivity to olefins and some PAHs may be advantageous in some selected analyses.

CONCLUSIONS

The examples shown in this study demonstrate the feasibility and potential applicability of supercritical fluid chromatography coupled with sulfur chemiluminescence detection to the analysis of many thermally labile, polar, and/or high-molecular-weight organosulfur compounds in a variety of fields. Continued refinements of the new SCD will likely further improve detector selectivity and sensitivity, and additional developments and applications using SFC–SCD by another research group are reportedly forthcoming[23].

ACKNOWLEDGEMENTS

The loan of a Model 300 sulfur chemiluminescence detector from Sievers Research, Boulder, CO, U.S.A., and partial financial support is gratefully acknowledged. We thank Applied Biosystems, Santa Clara Analytical Division, Santa Clara,

CA, U.S.A., for a loan of their microgradient system pump. Special thanks also to Steve Montzka for technical assistance and to Herb Schwartz and Randy Shearer for supplying some of the analytes. W.T.F. gratefully acknowledges the support of the Cooperative Institute for Research in Environmental Sciences for a visiting scientist fellowship. Support of the National Science Foundation under Grant ATM-8618793 to the University of Colorado is gratefully acknowledged.

REFERENCES

1 J. K. Nelson, R. H. Getty and J. W. Birks, *Anal. Chem.*, 55 (1983) 1767.
2 J. K. Nelson, *Ph.D. Dissertation*, University of Colorado, Boulder, CO, U.S.A., 1984.
3 E. A. Mishalanie and J. W. Birks, *Anal. Chem.*, 58 (1986) 918.
4 R. J. Glinski, E. A. Mishalanie and J. W. Birks, *J. Photochem.*, 37 (1987) 217.
5 R. J. Glinski, J. N. Getty and J. W. Birks, *Chem. Phys. Lett.*, 117 (1985) 359.
6 R. J. Glinski, E. A. Mishalanie and J. W. Birks, *J. Am. Chem. Soc.*, 108 (1986) 531.
7 J. E. Tavernier, *M.S. Thesis*, University of Colorado, Boulder, CO, U.S.A., 1987.
8 R. Dominguez, South Coast Air Quality Management District Laboratory, El Monte, CA, personal communication, Aug. 1988.
9 M. Legier and J. W. Birks, *Sensitive HPLC method for the Detection of Pesticides Using a Novel Sulfur-Selective Detector*, presented at the *30th Rocky Mountain Conference, July 31–August 5, 1988, Denver, CO, U.S.A.*
10 J. C. Fjeldsted and M. L. Lee, *Anal. Chem.*, 56 (1984) 619A.
11 M. Novotny, *J. High Resolut. Chromatogr. Chromatogr. Commun.*, 9 (1986) 137.
12 D. W. Later, D. J. Bornhop, E. D. Lee, J. D. Henion and R. C. Wieboldt, *LC/GC*, 5 (1987) 804.
13 W. T. Foreman, R. E. Sievers and B. W. Wenclawiak, *Fresenius' Z. Anal. Chem.*, 330 (1988) 231.
14 E. J. Guthrie and H. E. Schwartz, *J. Chromatogr. Sci.*, 24 (1986) 236.
15 *Sievers Model 300 SCD Operation Manual*, Sievers Research, Boulder, CO, 1988.
16 R. S. Hutte, R. E. Sievers and J. W. Birks, *J. Chromatogr. Sci.*, 24 (1986) 499.
17 I. N. Levine, *Physical Chemistry*, McGraw-Hill, New York, NY, 1978, p. 56.
18 L. A. Jones, *Sievers Model 300 SCD Detection Limit Data Application Note 001, Feb. 1988*, Sievers Research, Boulder, CO, 1988.
19 K. E. Markides, E. D. Lee, R. Bolick, M. L. Lee, *Anal. Chem.*, 58 (1986) 740.
20 M. A. A. Clyne, B. A. Thrush and R. P. Wayne, *Trans. Faraday Soc.*, 60 (1964) 359.
21 R. L. Shearer, *Ph.D. Dissertation*, University of Colorado, Boulder, CO, U.S.A., 1987.
22 B. W. Wenclawiak, R. E. Sievers and W. T. Foreman, in M. Perrut (Editor), *Int. Symposium on Supercritical Fluids Proceedings, Nice, 17–19 October, 1988*, Vol. 1, Institut National Polytechnic de Lorraine, 1988, p. 433.
23 D. J. Bornhop, Lee Scientific, Salt Lake City, UT, personal communication, 1988.
24 M. L. Lee and R. A. Hites, *Anal. Chem.*, 48 (1976) 1980.
25 P. A. Peaden, M. L. Lee, Y. Hirata and M. Novotny, *Anal. Chem.*, 52 (1980) 2268.
26 R. S. Hutte, Sievers Research, Boulder, CO, personal communication.
27 U. R. Stenberg and T. E. Alsberg, *Anal. Chem.*, 53 (1981) 2067.

30th Rocky Mountain Conference (Ion Chromatography and Supercritical Fluid Chromatography Symposia), Denver, CO (U.S.A.) July 31–August 5, 1988

END OF SYMPOSIUM PAPERS

The Treasury Building, Washington, DC, U.S.A.; wood engraving, 1884

SYMPOSIUM ISSUE

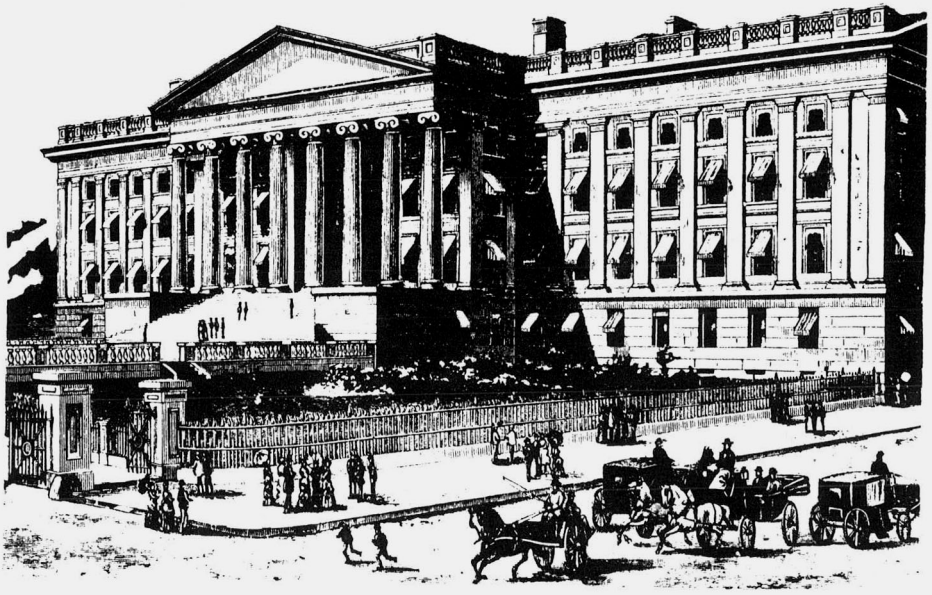

TWELFTH INTERNATIONAL SYMPOSIUM ON COLUMN LIQUID CHROMATOGRAPHY

LATE PAPERS

Washington, DC (U.S.A.), June 19–24, 1988

SYMPOSIUM VOLUMES

Guest Editor

G. GUIOCHON

(Knoxville and Oak Ridge, TN)

The proceedings of the *Twelfth International Symposium on Column Liquid Chromatography, Washington, DC, June 19–24, 1988*, are published in three volumes of the *Journal of Chromatography*: Vols. 458 and 459 (1988) and 461 (1989). The Foreword to the proceedings, and information on the Sponsoring Scientific Organizations and the Scientific and Organization Committees only appear in Vol. 458. Vol. 459 is dedicated to the memory of **Dr. István Halász**, and opens with an obituary. Due to the tight publication schedule for these proceedings volumes, the final versions of a number of papers arrived too late to be included; these "late papers" are published in the following pages [Vol. 465 (1989) pp. 39–119].

CONTENTS

TWELFTH INTERNATIONAL SYMPOSIUM ON COLUMN LIQUID CHROMATOGRAPHY, WASHINGTON, DC, JUNE 19–24, 1988 (LATE PAPERS)

H. Giesche, K. K. Unger, U. Esser, B. Eray, U. Trüdinger and J. N. Kinkel, Packing technology, column bed structure and chromatographic performance of 1–2-μm non-porous silicas in high-performance liquid chromatography 39

T. P. Bridge, M. H. Williams and A. F. Fell, Artificial intelligence techniques for peak homogeneity validation in liquid chromatography 59

P. L. Desbène, B. Desmazieres, J. J. Basselier and A. Desbène-Monvernay, Polarographic detection of non-ionic surfactants analyzed by reversed-phase partition chromatography 69

K. T. Lin, G. E. Rivard and J.-M. Leclerc, High-performance liquid chromatographic determination of mitoxantrone in plasma utilizing non-bonded silica gel for solid-phase isolation to reduce adsorptive losses on glass during sample preparation 75

M. Petrarulo, S. Pellegrino, O. Bianco, M. Marangella, F. Linari and E. Mentasti, Derivatization and high-performance liquid chromatographic determination of urinary glycolic acid . . . 87

A. Marzo, N. Monti, M. Ripamonti, G. Cardace and E. Arrigoni-Martelli, High-performance liquid chromatographic evaluation of PCF 39, a new immunomodulator agent 95

X. Poiesi, A. Tamanini, S. Ghielmi and A. Albertini, Protein A, hydroxyapatite and diethylaminoethyl: evaluation of three procedures for the preparative purification of monoclonal antibodies by high-performance liquid chromatography 101

G. Grossi, A. Bargossi, R. Battistoni, A. Lippi and G. Sprovieri, Full automation of catecholamine metabolite determination by column switching and high-performance liquid chromatography 113

Journal of Chromatography, 465 (1989) 39–57
Elsevier Science Publishers B.V., Amsterdam — Printed in The Netherlands

CHROMSYMP. 1539

PACKING TECHNOLOGY, COLUMN BED STRUCTURE AND CHROMATOGRAPHIC PERFORMANCE OF 1–2-μm NON-POROUS SILICAS IN HIGH-PERFORMANCE LIQUID CHROMATOGRAPHY

H. GIESCHE*,[a], K. K. UNGER, U. ESSER, B. ERAY and U. TRÜDINGER
Institut für Anorganische und Analytische Chemie, Johannes Gutenberg-Universität, D-6500 Mainz (F.R.G.)
and
J. N. KINKEL
Chemicals and Reagents Division, E. Merck, D-6100 Darmstadt (F.R.G.)

SUMMARY

This work is aimed at further elucidating the aggregation behaviour of micron- and submicron-size non-porous silicas and the column performance of 1–2-μm C_{18} silicas in reversed-phase high-performance liquid chromatography of low-molecular-weight compounds. It is demonstrated that highly ordered, dense, porous aggregates of such silica beads were obtained by gravity settling and centrifugation. The slurry techniques applied at constant flow-rate and a pressure up to 50 MPa provided less-ordered aggregates, but generated an acceptable performance of columns when 1–2-μm C_{18} silica beads were employed. To operate columns of 53 mm × 4.6 mm I.D., the maximum flow-rate needs to be *ca.* 2.5 ml/min at an inlet pressure of 50 MPa. To keep extra-column effects to a minimum, the injection volume should be about 0.6 μl, the volume of the detector cell about 0.3 μl and the time constant of the detector < 50 ms. Such columns enable fast separations of mixtures of low-molecular-weight substances in less than 30 s.

INTRODUCTION

The slurry, axial- and radial-compression techniques have been widely accepted as standard packing procedures in analytical and preparative high-performance liquid chromatography (HPLC)[1,2]. Each technique is applied in a number of variations, depending on the type of packing and column configuration. For instance, the slurry technique is carried out both with low- and high-viscosity solvent mixtures, at constant pressure or at constant flow-rate, upwards or downwards.

The main goal of a packing procedure is to achieve a homogeneous, dense and stable column bed, which generates the expected chromatographic performance and

[a] Present address: c/o Professor E. Matijević, Department of Chemistry, Clarkson University, Potsdam, NY, 13676, U.S.A.

0021-9673/89/$03.50

provides an adequately long column lifetime. It has been demonstrated that columns packed with spherical particles exhibit better chromatographic properties than those with irregularly shaped particles of the same size and size distribution[3]. Yet, it is still a matter of debate to which extent the width and the shape of the particle size distribution and the porosity of the packing affects the column quality[4,5].

In order to examine the bed structure and performance of analytical HPLC columns, we used as model packings non-porous 1–2-μm silicas, which were recently developed in our laboratory[6]. The material consists of uniform and monodisperse non-porous spheres. The mean particle diameter could be adjusted between 0.5 and 3.5 μm with a standard deviation of the mean, based on the number average, of less than $\pm 5\%$. The material is composed of amorphous silica of a bulk density of 2.20–2.25 g/ml. It possesses a hydroxylated surface. Thus, the traditional chemical modification procedures can be applied to make any type of bonded phase. The lack of internal surface area and porosity makes the beads less susceptible to compression during packing than porous particles. The small particle size of about 1 μm generates a high back pressure and limits the column length to about 50 mm. On account of the extremely small particles, the columns are able to perform highly rapid and efficient separations, provided the HPLC equipment is properly designed. The low surface area of about 1–3 m^2/ml, compared to *ca.* 100 m^2/ml for porous silicas, decreases the mass loadability for low-molecular-weight substances by a factor of 50, as the mass loadability is proportional to the surface area of the packing.

This study falls into two parts. In the first part, we attempted to assess the column bed structure of compacted non-porous silica beads by applying various established techniques in powder agglomeration and in HPLC. The data permit to compare the packed aggregates in terms of the interstitial pore volume, the mean pore diameter and the packing structure, and to judge the performance of the various aggregation techniques. The packing structure is directly related to the column performance, in particular to the column plate height (via the A-term of the Knox equation) and to the column pressure drop (via the column resistance factor Φ)[4,3].

Thus, in the second part the peak height–linear velocity dependencies measured on slurry-packed 1–2-μm columns and the pressure drop are compared with the theoretically predicted values. In addition, the chromatographic performance data obtained are discussed under the aspects of the practical limitations where short columns packed with these particles are used for fast separations.

Results on 1–2-μm spherical porous silicas have also been reported by Dewaele and Verzele[7], Unger *et al.*[8] and Danielson and Kirkland[9,10].

EXPERIMENTAL

Materials

The silica spheres were prepared by hydrolyis of tetraethoxysilane in ethanol–water–ammonia mixtures in two ways[6].

Procedure A

Silica spheres of a projected area diameter, $d_{p_n}^{p,a}$, of <0.5 μm were synthesized following the Stöber process[11].

Procedure B

Spheres of $d_{p_n}^{p.a.}$ in the range 0.2–3.5 μm were prepared by subjecting the silica suspensions made according to procedure A to a slow, controlled size-growth process, applying a dilute tetraethoxysilane solution[6]. By careful control of the experimental conditions a layer-by-layer growth of the native particles occurred without a second nucleation.

The suspensions were allowed to settle, and the particles were obtained by removing the supernatant solution. In separate experiments, an *in situ* silanization of the external surface of the silica spheres was performed by substituting the dilute tetraethoxysilane solution in the controlled size-growth process by a solution of ethyltriethoxysilane and *n*-octyltriethoxysilane[6]. The products are abbreviated as C_2 modified and C_8 modified. The native silica beads "as made" were subjected to the following treatments: (1) calcination at 823 K over a period of 48 h; (2) rehydroxylation by refluxing the beads in an aqueous suspension or in 1 *N* nitric acid at 373 K for 4 days; (3) silanization by a reaction of the dried silica beads with N,N-dimethylaminodimethyl-*n*-octylsilane according to a procedure described elsewhere[12]. The batches prepared are listed in Table II.

Tetraethoxysilane, obtained from Wacker (Burghausen, F.R.G.), was distilled over calcium oxide (b.p. = 441 K, n_D^{20} = 1.383). Water was quartz-distilled and deionized. Ammonia solution (25%, w/w), ethanol and acetonitrile were of analytical grade (Merck, Darmstadt, F.R.G.). Test substances were benzene, naphthalene, biphenyl, fluorene, anthracene, pyrene and chrysene (analytical grade, Merck).

METHODS

Aggregation techniques

Gravity settling and centrifugation. For gravity settling, either the actual silica suspension was used or the beads were isolated by freeze-drying and then suspended in deionized water or aqueous solution of pH 2.6, 5.3 or 10.9 at a concentration of about 1% (w/w). The suspensions were allowed to settle under vibration-free conditions. After settling was completed, the excess of solvent was carefully decanted. Drying was carried out sequentially in air, in a dessiccator over silica gel, at a vacuum of about 10 mbar at room temperature (24 h), and at 373 K (24 h).

As settling by gravity was extremely slow for batch B241/I of d_p = 89.6 nm, aggregation was performed by centrifugation. A centrifuge was applied with a rotor diameter of 15 cm at 680 (75 *g*) and 3000 (1450 *g*) rpm. After settling, the cake was carefully removed and dried under the previously described conditions.

Slurry technique. A stainless-steel HPLC column, 53 mm × 4.6 mm I.D. (Bischoff, Leonberg, F.R.G.), fitted at the lower end with metal frits and filter paper No. 827 (Schleicher & Schüll, Dassel, F.R.G.), was connected with its upper open end to a 100-ml autoclave. A 1% (w/w) suspension of the silica beads was made in ethanol–water (50:50, v/v) by ultrasonic treatment and poured into the autoclave with the column attached. After closing the autoclave, the suspension was pumped through the column at a constant flow-rate, raising the pressure to 50 (in the first experiment) or 100 (in the second) MPa. After filling, the pressure was slowly reduced. The column content was pressed out and dried as described for the gravity settling and centrifugation experiments.

Isostatic compression (dry bag). A tube made of poly(vinyl chloride) was filled with silica beads. It was then closed at both ends with rubber stoppers and placed in a high-pressure autoclave (Nova Suisse, Effretikon, Switzerland). The autoclave was filled with deionized water. After closing the autoclave, the pressure was raised stepwise. Four experiments were run with final pressures of 1.28, 8.0, 50 and 313 MPa, which were maintained over a period of 12 h. Then the pressure was released step-wise to atmospheric pressure over several hours, and the compacted spheres carefully removed after cutting the plastic tube.

Transmission electron microscopy (TEM) and scanning electron microscopy (SEM)

TEM was employed to assess the particle size distribution of the silica beads, and SEM served as a means of analyzing the packing structure of porous aggregates. TEM micrographs were obtained on a Philips (Kassel, F.R.G.) Model EM 300 electron microscope. The acceleration voltage of the electron beam was 80 kV. Magnification was $\times 1000$ to $\times 52\,000$. SEM micrographs were obtained on a Philips Model PSEM 500 electron microscope. The electron beam was focussed to 8–64 nm. For each sample, several micrographs were taken at a series of angles.

The micrographs were analyzed by an image analyzer (Videoplan; Kontron, Munich, F.R.G.). The mean particle diameter of the silica spheres calculated was the projected area diameter, based on the number-average $d_{p_n}^{p,a}$ at 50% of the cumulative distribution curve. The precision in the particle size determination was less than $\pm 1\%$. The error of the calculated x,y,z coordinates of the beads was less than $\pm 5\%$.

Sorption measurements

Nitrogen sorption isotherms at 77 K were determined gravimetrically, using a microbalance (Model 4102 or 4433; Sartorius, Göttingen, F.R.G.). Samples were degassed until the sample mass remained constant (473 K, 10 h, final vacuum 10^{-4} Pa). Nitrogen was of 99.999% purity (Linde, Düsseldorf, F.R.G.). The saturation vapour pressure of nitrogen was measured close to the sample, employing a specially constructed device[13]. The pressure was recorded with a piezo-resistive pressure transducer (Model 4043A1; Kistler, Ostfildern, F.R.G.). From nitrogen sorption data the specific surface area according to the BET equation, a_s (BET) was calculated, using the molecular cross-sectional area of nitrogen, a_m (N_2) = 0.162 nm^2 (ref. 14).

Sorption isotherms of helium and xenon (purity 99.999%; Messer, Griesheim, F.R.G.) were performed on the dried and calcined silica beads at 298 K, using a magnetic suspension balance (Sartorius).

Mercury porosimetry

The porosimeter was constructed in our laboratory, as described in refs. 13 and 15.

The sample was weighed into the penetrometer, degassed and then filled with freshly distilled mercury. The volume of intruded mercury, v_p^{MP}, was measured as a function of increasing pressure. The pressure was recorded when equilibrium was achieved. The v_p^{MP} value was corrected by the compression of mercury and the penetrometer device[15]. After intrusion, the retraction branch was measured by releasing the pressure in steps. For some measurements, the intrusion was repeated after refraction.

The following parameters were calculated:

v_p^{MP} = the specific pore volume corresponding to the intruded volume of mercury at p_{max}.
PSD = the pore size distribution, calculated from the Washburn equation with a surface tension of mercury of 480 mN/m and a contact angle of mercury of 140° at 298 K (ref. 14).
pd_{50}^{MP} = the mean pore diameter, corresponding to the 50% value of the cumulative distribution.

Apparent helium, mercury and water densities

The apparent density of helium, d_{app} (He), was determined on a helium pycnometer (Model 930; Beckman, Munich, F.R.G.). The apparent mercury and water densities, d_{app} (Hg) and d_{app} (H_2O) were measured at 298 K, using a pycnometer of 0.8 ml volume[8]. The reproducibility of the density measurements was ±0.15%. The total specific pore volume was calculated by

$$v_p \text{ (total)} = \frac{1}{d_{app} \text{ (Hg)} - d_{app} \text{ (H}_2\text{O)}} \quad (1)$$

(or d_{app} (He) instead of d_{app} (H_2O))

Column packing procedures

For chromatographic tests, two batches of silicas were employed with $d_p^{p.a.}$ = 1.5 and 2.1 μm. The silica beads were modified with monochlorodimethyl-*n*-octylsilane according to a procedure described elsewhere[12]. Suspensions of the *n*-octyldecyl-bonded beads were made in tetrachloromethane–paraffin (50:50, v/v) mixtures by ultrasonic treatment. The concentration of C_{18}-bonded silica was 5% (w/w). The silica was packed into columns of 33 mm × 8 mm and 53 mm × 4.6 mm (Bischoff) at a constant flow-rate and a maximum pressure of 50 MPa. The end-fittings were filter papers No. 827 (Schleicher & Schüll) supported by metal frits No. 22800812 (Bischoff).

Chromatographic measurements

The HPLC equipment consisted of a Model 2200 pump (Bischoff), a Model 7413 injection system (Rheodyne, Cotati, CA, U.S.A.) with a 0.5-μl sample loop, a variable-wavelength UV detector from Shimadzu (Düsseldorf, F.R.G.) with a detector cell volume of 0.6 μl and a time constant of 50 ms. The separation was repeated at 150 ms and 1.5 s. A Model C-R3A integrator from Shimadzu was used.

Thiourea was employed as unretained compound (t_m marker) to calculate the capacity factor of the test substances and the linear velocity, u.

The plate height, H, of the test substances was measured by means of the equation

$$H = \frac{L}{16} \left(\frac{w_t}{t_R}\right)^2 \quad (2)$$

where L is the column length, t_R the retention time and w_t the peak width in time units at 13.5% of the peak height.

RESULTS AND DISCUSSION

Characterization of the silica beads

The silica beads were synthesized by hydrolytic polycondensation of tetraethoxysilane in a two-step procedure[6]. The first step followed the procedure developed by Stöber *et al.*[11], yielding a suspension of colloidal silica particles up to about 0.5 μm of mean particle diameter. In a consecutive reaction, the particles were subjected to a slow, controlled size-growth process by means of hydrolysis of a dilute tetraethoxysilane solution, avoiding nucleation. In this way, particles up to a mean diameter of 3.5 μm were synthesized and isolated from the supernatant by sedimentation. The procedure developed has several attractive features, in particular, when the material is intended to be used in HPLC. The size of the beads covers a range that is still usable, with regard to column back pressure, in columns operated under normal HPLC conditions. No sizing is needed, as is essential in the manufacture of microparticulate porous silicas. The procedure described has been scaled up to batches of several kilograms. The size distribution is extremely narrow, i.e. the standard deviation of the mean particle diameter is smaller than ±5%. Fig. 1 shows the probability plot of the cumulative size distribution curve of two batches. The median projected diameter, based on a number average, and the standard deviation of the median were: batch B241/III (431 ± 9.2) nm, batch B241/IV (1002 ± 21.2) nm. The shape factor, f, being the axial ratio of an ellipsoid with the same inertial moment, varied between 0.95 and 0.98.

Characteristics of aggregated 1-μm and submicron silica beads

Colloidal silica particles of submicron size have a tendency to aggregate, due to

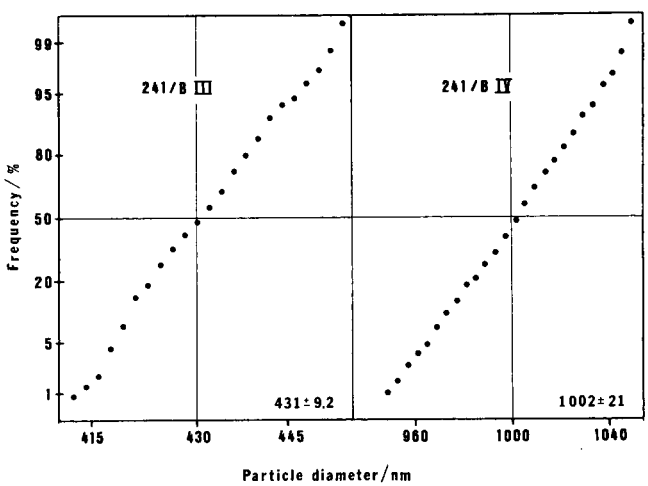

Fig. 1. Probability plot of the cumulative size distribution curve of sample B241/III (d_p = 431 ± 9.2 nm) and B241/IV (d_p = 1002 ± 21.2 nm).

their high surface area-to-volume ratio. Aggregation of colloidal silica is usually accomplished by gelling, coagulation, flocculation and coacervation, in which the assembled particles form a less-ordered three-dimensional network[16]. Aggregation must be clearly distinguished from agglomeration. By definition, in aggregates, the particles are loosely coherent, while in agglomerates they are rigidly joined together[17]. Correspondingly, the processes applied for aggregation and agglomeration differ. Agglomeration processes can be divided into hard- and soft-based, depending upon whether excess pressure is applied or not[18,19]. Soft processes comprise bead granulation and spray-drying, while agglomeration under pressure is carried out by isostatic compression, extrusion, and other modes employing the dry or wet powder, a paste or a suspension.

Aggregation procedures applied in this study were gravity settling and centrifugation. To prepare dense aggregates, the traditional HPLC slurry technique was employed, with pressures between 50 and 100 MPa, and the dry-bag isostatic compression technique, with pressures between 1 and 300 MPa. On account of the small size of the colloidal particles and of the relatively high pressures, particle bridging might occur in the latter. In addition to 1-μm particles, smaller beads were chosen down to a d_p of 90 nm. The silica beads were used in their native state, calcined, and *n*-alkyl-silanized.

Model structures originating from packed, uniform spheres have been examined by Heesch and Laves[20], Manegold[21], Kadaner *et al.*[22], Meissner *et al.*[23], Ridgeway and Tarbuck[24], and Karnaukhov[25]. Characteristic parameters describing these close-packed spheres were the type of structure, the contact number per sphere, the void volume or porosity, the diameter of a sphere inscribed in the cavities, and the diameter of the circle inscribed in the throats connecting the cavities[26]. In order to estimate these parameters on aggregates of uniform spheres the following methods were applied: nitrogen sorption, mercury porosimetry (MP), SEM, and optical diffraction. In a previous study at this laboratory, the pore structure of synthetic opal of a particle size of $d_p = 220$ nm and of an aggregate of colloidal silica particles made by the Stöber process of $d_p = 310$ nm were analyzed[26]. The synthetic opal displayed the closest packing of spheres with a contact number of 12 and a porosity of 26.3%.

Porosity and mean pore diameter of the aggregates. To study the effect of the soft and hard aggregation techniques on the porosity and pore diameter, a batch of 1-μm silica beads was employed and subjected to heat treatment at 473 K. The properties of the product were: d_p, 954 ± 22 nm, $f = 0.95$, $d_{app}(He) = 2.04$ g/ml.

The porosities of bodies of packed uniform spheres have been reported as: hexagonal and cubic close-packed, 25.95%; body-centered tetragonal, 30.18%; primitive hexagonal, 39.54%; primitive cubic, 47.64%; and tetrahedral, 66.01%[27]. The pore diameter, expressed as the diameter of the inscribed circle in the throats, pd_{th}, calculated according to Karnaukhov[28,29] for an aggregate of regularly packed uniform spheres, is

$$pd_{th} = 2.8\ v_p/a_{s(ext)} \cdot 10^3/\text{nm} \tag{3}$$

where v_p is the specific pore volume in ml/g and $a_{s(ext)}$ the external surface area in m^2/g, given by

$$a_{s(ext)} = 6/d_p d_{app}(He) \quad (4)$$

Using $d_{app}(He) = 2.04$ g/ml and $d_p = 954$ nm, $a_{s(ext)}$ is calculated to be 3.1 m^2/g. Thus, the closest-packed structure of spheres with porosity, $P = 26\%$ and $v_p = 0.172$ ml/g would result in a pore diameter of $pd_{th} = 147$ nm $= 0.147$ μm.

Table I lists the values of v_p, P, and the mean pore diameter pd_{50}^{MD}, assessed by mercury porosimetry, of aggregates obtained by gravity settling, centrifugation and the two pressure compaction methods. When aqueous suspensions of the silica beads are used, the surface charge of the particles comes into play. The point of zero charge of suspended silica particles lies in the range between pH 1 and 2, although higher values have been reported[30], measured by the electrokinetic mobility of silicas in suspensions of different pH. With increasing pH, the negative charge of the particles increases, the particles repel each other, and the suspension becomes more stable. As a result, notably higher packing densities and corresponding lower porosities were achieved with aggregates settled by gravity and by centrifugation at pH 10.9 than at pH 2.6. In spite of the favourable conditions, the porosities found were slightly higher than those for the densest array of packed spheres (26%). The decrease in porosity with rising pH of the suspension is accompanied by a diminution in the pore diameter. The mean pore diameters, measured by MP, were in the order of those calculated by eqn. 4, using $a_{s(ext)} = 3.1$ m^2/g.

The porosities of aggregates obtained by the slurry technique reflect the same tendency with regard to the pH of the suspension as was observed for aggregates made by settling and centrifuging. As expected, the dry-bag isostatic compression technique led to a densification of aggregates with rising pressure. At a pressure of 313 MPa, some of the particles were seen to show cracks and fissures. This phenomenon did not occur with silanized silica beads when ethyltriethoxysilane was used as a reagent under otherwise constant conditions. In general, the porosities of aggregates made of the silanized beads were slightly lower than those for beads made of parent silica (see values in Table I in parentheses). This might be a result of the weaker particle-to-particle interactions of the silanized beads, which cause a higher lateral mobility under the compression forces.

Batches of silica beads of $d_p = 89.6$, 199, 431 and 1002 nm in the native, thermally treated, rehydroxylated and silanized state were chosen to examine the effect of the nature of the surface on the settling behaviour and on the properties of the aggregates (see Table II). Rehydroxylation of the calcined beads slightly increased the mean pore diameter due to the hydrothermal treatment of porous aggregates (*cf.* batches B241/I and B241/II). The consecutive silanization with *n*-octyldimethylaminosilane narrowed the pore diameter by nearly the thickness of a fully extended *n*-octyl layer (about 2 nm) and also decreased the porosity. Silica beads, modified with ethyltriethoxysilane *in situ* and aggregated, gave generally higher packing densities and lower porosities than those made from beads modified *in situ* with *n*-octyltriethoxysilane. It is probable that the long-chain alkyl groups hinder a close attachment of the spheres during settling in aqueous suspensions. Burning off the carbon layer by calcination at 823 K slightly increased the packing density. The aggregated C_2 product, subjected to calcination at 823 K, showed the same porosity or even smaller porosity than the native calcined material without any modification, whereas the aggregated C_8 product could not be densified by calcination to such an extent.

TABLE I

RESULTS OF AGGREGATION EXPERIMENTS WITH *CA.* 1-μm NATIVE AND SILANIZED MONODISPERSE SILICA PARTICLES

v_p^{MP} = Specific pore volume from the mercury intrusion curve at p_{max}; P = porosity; pd_{50}^{MP} = mean pore diameter at 50% of cumulative distribution curve from mercury porosimetry. The batch of $d_p = 954 \pm 20$ nm was prepared according to the same procedure as batch B241/IV (see Table II). Values in parentheses refer to the silanized silica particles.

Mode of aggregation	d_p *of starting silica (nm)*	*Variable*		v_p^{MP} *(ml/g)*	*P (%)*	pd_{50}^{MP} *(nm)*
		pH of suspension	*Pressure (MPa)*			
Centrifugation	954 ± 20	2.6		0.456	48.3	337
		5.3		0.372	43.2	284
		7.0		0.351	41.8	293
		10.9		0.305	38.4	275
Gravity settling	954 ± 20	2.6		0.428	46.7	367
		10.9		0.33	40.3	279
Slurry technique (100 MPa)	954 ± 20	2.6		0.437	47.2	371
		5.3		0.380	43.7	334
		7.0		0.370	43.1	307
		10.9		0.353	41.9	290
Isostatic compression	954 ± 20		1.28	0.481	49.6	489
			8.0	0.422 (0.354)	46.3 (42.0)	466 (355)
			50	0.409 (0.376)	45.5 (43.5)	449 (364)
			313	0.285 (0.273)	38.3 (35.8)	344 (282)

Structure of aggregates. Two methods were chosen to elucidate the structure of aggregates: SEM and MP. SEM has the advantage of providing direct images of the aggregates. Disadvantages are that small domains of the exterior structure are always seen and, hence, sufficiently many photographs are required to get a representative image of the whole material. Also stereo-SEM should be applied to avoid false interpretations of the structure.

In MP mercury as a non-wetting liquid is intruded into the void space of the aggregates by gradually raising the pressure. Frevel and Kressley[31] have computed theoretical porosimetry curves for aggregates of uniform microspheres on the basis of the interconnected-void model. The characteristic feature is an abrupt threshold mercury penetration. It is assumed that this phenomenon is attributed to the sudden penetration throughout the interconnected voids, followed by a gradual filling of toroidal voids around the point of contact between two particles. Mayer and Stowe[32,33] have improved the model, introducing the breakthrough pressure as a decisive parameter, which was defined in terms of the porosity of the aggregate and the contact angle of mercury. Their model structure was an assembly of spheres, grouped in hexagonal close-packed layers, with vertically stacked layers above and below.

It is common to normalize the pressure by means of the equation

$$p^* = p\, d_p / 2\gamma_{L,v} \tag{5}$$

where p^* is the normalized pressure, p the equilibrium pressure, d_p the diameter of the

TABLE II

RESULTS OF AGGREGATION EXPERIMENTS WITH NON-POROUS SILICAS OF VARIOUS PARTICLE SIZES, NON-SURFACE-MODIFIED AND SILANIZED, NON-CALCINED AND CALCINED AT 823 K

Batch No.	d_p *(nm)*	*Procedure*	*Mode of aggregation*	*Aggregates of*	v_p^{MP} *(ml/g)*	*P (%)*	pd_{50}^{MP} *(nm)*
B241/I	89.6 ± 6.6	A	Centrifugation	Native beads	0.249	33.1	20.6
				In situ C_2-modified beads	0.220	30.4	17.1
				In situ C_8-modified beads	0.273	35.2	25.9
				Native beads calcined at 823 K and rehydroxylated	0.218	32.8	21.1
				Native beads calcined at 823 K and rehydroxylated, C_8-modified	0.190	29.8	19.1
B241/II	199 ± 6.8	B (batch B241/I)	Gravity settling	*In situ* C_2-modified beads	0.201	31.1	30.7
				In situ C_2-modified beads calcined at 823 K	0.195	30.4	31.8
				In situ C_8-modified beads	0.244	35.3	40.2
				In situ C_8-modified beads calcined at 823 K	0.231	34.1	42.9
				Native beads calcined at 823 K	0.208	31.8	38.8
				Native beads calcined at 823 K, rehydroxylated	0.203	31.3	40.0
				Native beads calcined at 823 K, rehydroxylated, C_8-modified	0.191	29.2	37.5
B241/III	431 ± 9.2	B (batch B241/II)	Gravity settling	*In situ* C_2-modified beads	0.183	26.7	69.9
				In situ C_2-modified beads calcined at 823 K	0.179	28.6	86.0
				In situ C_8-modified beads	0.207	29.2	77.7
				In situ C_8-modified beads calcined at 823 K	0.173	30.3	91.2
				Native beads calcined at 823 K	0.173	27.9	141
B241/IV	1002 ± 21.2	B (batch B241/III)	Gravity settling	*In situ* C_2-modified beads	0.231	31.5	259
				Native beads calcined at 823 K	0.203	31.3	307

primary particles of the aggregates and $\gamma_{L,v}$ the surface tension of mercury. Values of p^* for the breakthrough pressure reported in the literature, are 4.06 (ref. 31), 4.0 (ref. 34) and 3.18–4.41 (ref. 35).

The mercury intrusion curves were measured for a number of aggregates, made by gravity settling, and plotted as the intruded volume of mercury against the normalized breakthrough pressure. Usually the breakthrough into the pore system occurred at p^* values of 8 to 10. In the case of some less dense packings, the breakthrough started at more or less lower values of about 4.5 to 5.0. Occasionally, a two-step intrusion was observed. According to Mayer and Stowe[32,33], the first value corresponds to a close-packed structure of spheres, assuming a contact angle of mercury of 130–140°C. The first value fits a structure with a packing angle σ = 70–80°, where the layers are laterally displaced and show defects.

The high value of the breakthrough pressure of 9–10 has never been reported before in the literature. It appears, that it is associated with the highly regular and dense structure of aggregates. Iczkowski[36] has shown, that the breakthrough pressure is a function of the free distance between the assembled spheres. In the calculated function of the breakthrough pressure against the particle–particle distance, p^* approximates a value of 9.5 at zero distance, with a contact angle of mercury of 140°.

The two-step intrusion curve results in a bimodal pore size distribution when the Washburn equation is applied. This is exemplified by Fig. 2, showing the cumulative and relative pore size distribution of aggregates, made of batch B241/IV by gravity settling.

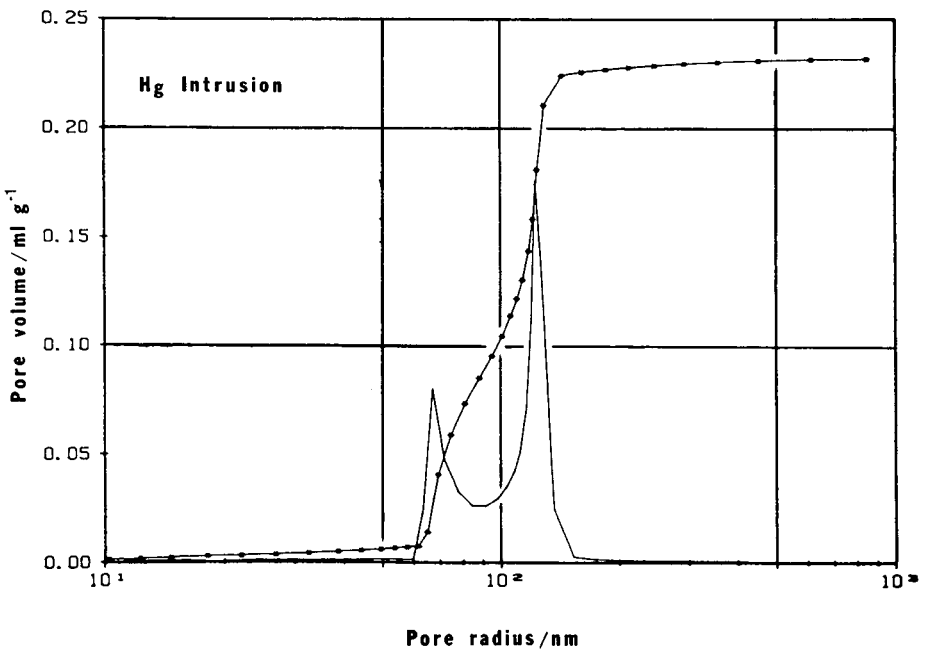

Fig. 2. Cumulative pore size distribution curve of batch B241/IV (d_p = 1002 ± 21.2 nm), obtained by mercury porosimetry (intrusion branch, surface tension of mercury = 480 mN/m, contact angle of mercury = 140°C).

The highly ordered structure of aggregates made by settling was evidenced by the SEM images (see Fig. 3b). There are domains with a close-packed structure within the layers and a vertical stacking of spheres in the layers above and below. This structure is identical to that postulated by Mayer and Stowe[32,33] in their model. The ordered domains are interrupted by defects. A preferred formation of densest horizontal layers and a more open structure between the layers was also observed in the flocculation of silica sols in the presence of detergents. According to Iler[37], the aggregates "grow as sheetlike layers and attach themselves to the growing sheet only around the edges of the sheet, where ionic repulsion is least". The preferred attachment of spheres at the edges of aggregates was also confirmed by potential-energy calculations[38]. Luck *et al.*[39] examined the structure of packed spheres of styrene lattices of 0.8 μm diameter. Their experiments and calculations showed that the cubic structure is energetically slightly preferred over the hexagonal. Similar observations were made for the samples described in this paper. In contrast to the aggregates made by settling, the arrays of silica beads obtained by the slurry technique looked highly disordered and displayed a much more open structure (Fig. 3a).

A more reliable structure analysis was performed by applying stereo-SEM to the aggregates. Images and photographs were taken from a series of different angles to assess the position of the beads in the x,y and z coordinates of the structure. A typical result is shown in Fig. 4. This approach allowed us to compute the sequence of layers as well as the layer-by-layer distance. Again, the close-packed structure was confirmed in the horizontal layers.

In conclusion, the detailed diagnosis of the aggregates has shown that gravity settling provides the densest structure within and between the layers and also less defects between the ordered domains than other techniques. The latter seem to be responsible for not approaching the theoretical porosity of 26% of a close-packed assemblage of spheres. By employing submicron silica beads it was further evidenced that long *n*-alkyl silanes, bonded to the external surface, inhibit dense packing of aggregates.

Packing procedures and performance of columns packed with 1–2-μm non-porous monodisperse C_{18}-bonded silicas

For application in reversed-phase HPLC, the calcined and rehydroxylated silica beads were subjected to silanization by reaction with *n*-octadecyldimethylchlorosilane according to a procedure described elsewhere[12]. As the carbon content of the C_{18}-bonded phase was about 0.2% (w/w) and hence in the range of the reproducibility of the carbon elemental analysis (which is *ca.* $\pm$0.2%), the ligand density could not be calculated from the carbon content. An indirect means is to compare the capacity factors of solutes on the non-porous C_{18}-bonded phase with those on a porous C_{18}-bonded silica of known surface area and ligand density under constant eluent conditions, taking into account the differences in the specific surface areas between the two phases. A direct method of assessing the ligand density is to employ a ^{14}C-enriched silane in the surface reaction and to derive the carbon content of the bonded phase by means of scintillation measurements. Nonetheless, comparison of the retention data showed no difference in the selectivity of the non-porous and porous C_{18}-bonded silicas when the same surface modification procedure and identical chromatographic conditions were used. In order to achieve the same capacity factors with the

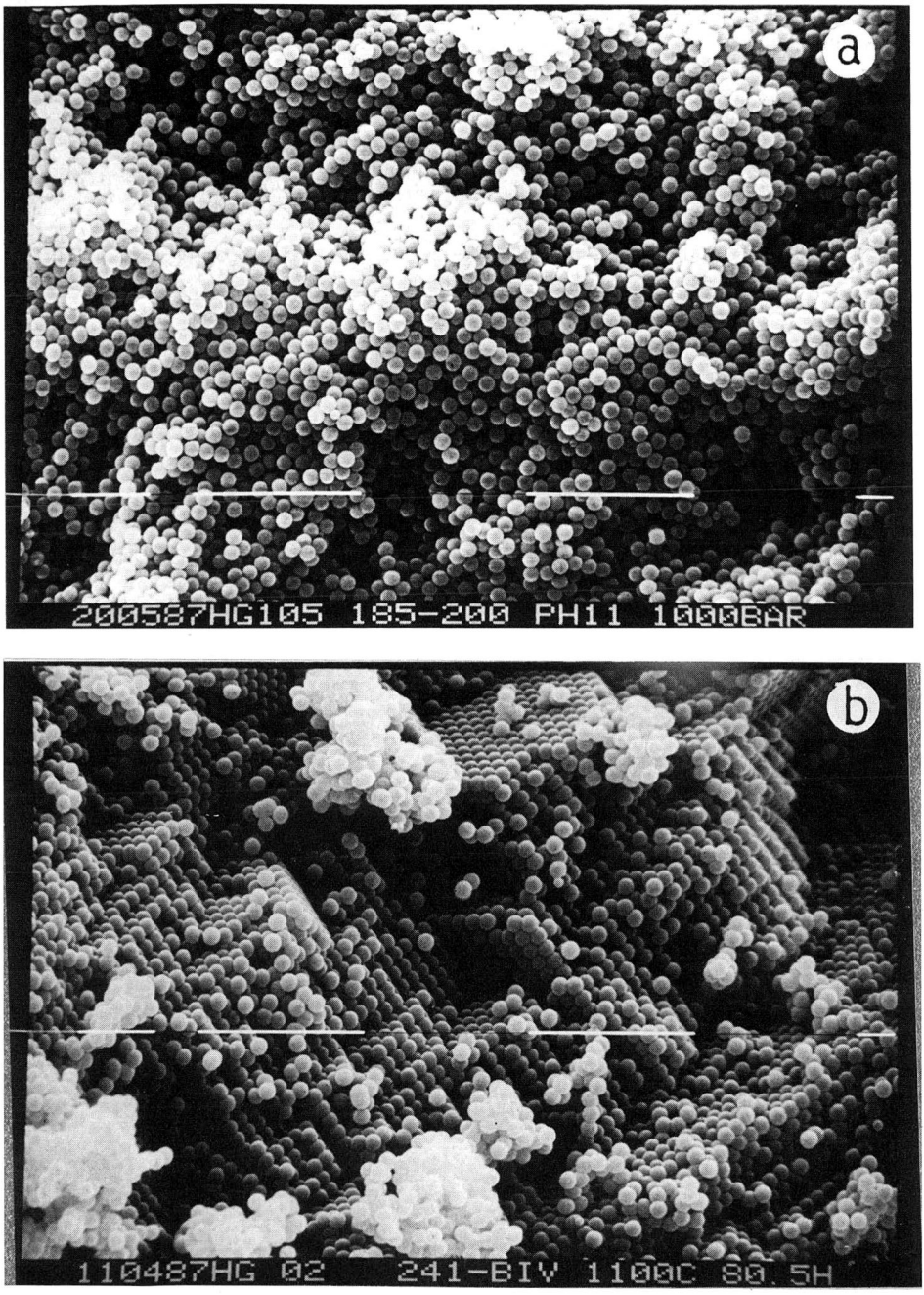

Fig. 3. Scanning electron micrographs of compacted spheres, obtained by (a) the slurry technique and (b) centrifugation. (Batch B241/IV). Bar = 10 μm.

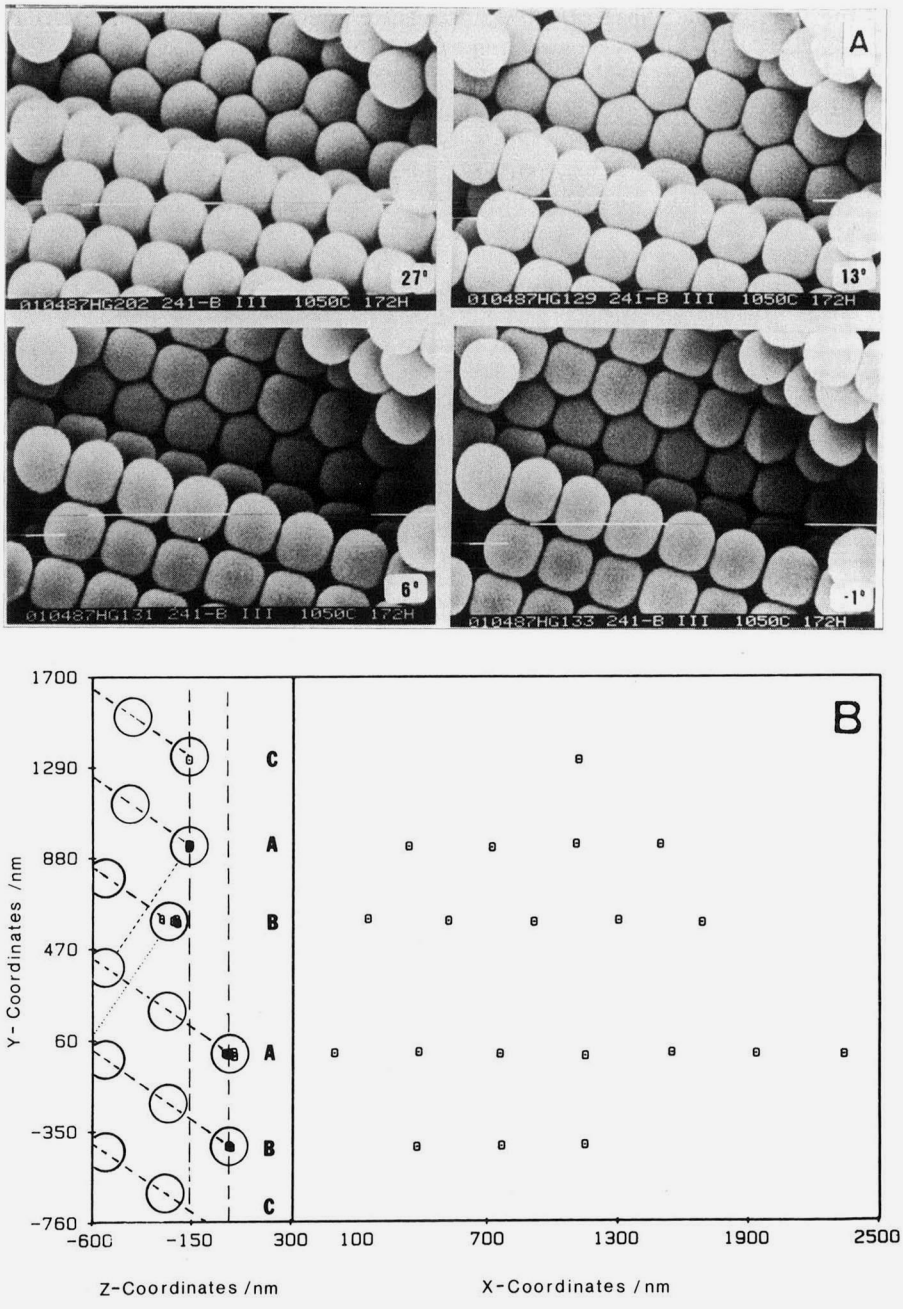

Fig 4. (A) Stereo scanning electron micrograph of aggregates spheres (batch B241/III, $d_p = 431 \pm 9.2$ nm). (B) Assessment of the position of beads in the x,y,z coordinates in the structure.

non-porous C_{18}-bonded silica as with the porous C_{18}-bonded silica, *e.g.*, Hypersil ODS (Shandon, U.K.), the water content of the water–acetonitrile eluent must be increased to 80% (v/v) compared to 40% (v/v) with the Hypersil column.

Although in the aggregation experiments the soft techniques, like gravity settling and centrifugation, gave superior packing structures and higher packing densities than the hard techniques, the slurry technique applied at constant flow-rate and moderate pressures up to 50 Pa and gravity settling in an ethanol–water suspension resulted in nearly the same performance characteristics. In time experience showed that the absence of dead volumes at the column ends was of decisive importance for the column performance. Best results were obtained with Hyperchrom columns (Bischoff) and endfittings made of paper filters, supported by metal frits. The total porosity of the fittings was less than 0.2 μm.

In order to utilize the performance of the 1–2-μm particle columns fully, the HPLC equipment has to meet a number of specifications and requirements which were treated in depth by Guiochon[40].

The use of short columns, *ca.* 50 mm long, first limits the maximum value of the sample volume $V_{S,M}$

$$V_{S,M} = \lambda \Theta \pi \frac{d_c^2}{4} \varepsilon_t (1 + k') (L H)^{\frac{1}{2}} \tag{6}$$

where λ is a numerical factor, reflecting the shape of the injection profile, Θ a factor characterizing the relative increase of the zone width, d_c the column inner diameter, ε_t the total porosity of the column and k' the solute capacity factor. Setting $\lambda = 2$, $\Theta = 0.1$, $d_c = 4.6$ mm, $\varepsilon_t = 0.35$, $k' = 0$, $L = 53$ mm and $H = 6$ μm, $V_{S,M}$ is calculated to be 0.65 μl. The value corresponds to the volume of the sample loop of the Rheodyne injection system employed.

The sample mass to be injected is equal to the product of the sample volume and the sample concentration. On account of the difference in the surface of stationary phase between the porous and the non-porous C_{18}-bonded silicas of about 50, the applicable sample concentration is correspondingly reduced. Column mass loadability for low-molecular-weight compounds thus decreases from about 1 mg per g of porous reversed-phase packing to about 20 μg for the non-porous packing.

When 1–2-μm particles are used, the column back pressure, ΔP, is a limiting factor with regard to the column length. ΔP is given by

$$\Delta P = u \eta L \Phi / d_p^2 \tag{7}$$

where u is the linear velocity of the eluent, η the eluent viscosity, and Φ the column resistance factor. Setting $u = 5$ mm/s, $\eta = 1$ mNs/m^2, $L = 53$ mm, $\Phi = 620$ ($\varepsilon_t = 0.35$), and $d_p = 2.1$ μm, a column back-pressure of 37.3 MPa results. A pressure drop of 37.3 MPa = 373 bar corresponds to a volume flow-rate of 1.74 ml/min. Plots of the column back-pressure against the flow-rate, f_v, were measured for a column of 53 × 4.6 mm, packed with 2.1-μm particles upwards and downwards in several cycles, and gave a straight line with values exactly as predicted by eqn. 7. The equipment used in this study allowed a maximum pressure of about 60 MPa.

On columns packed with 1–2-μm particles, operated at high flow-rates, frictional

heat effects become noticeable. They lead to an additional band broadening[41]. As a rule-of-thumb, the temperature difference, ΔT, between the column head and column exit is related to d_c and d_p as[42]

$$\Delta T = \Psi \, (d_c^2 \, v \, / \, d_p^4) \tag{8}$$

where Ψ is a constant and v the reduced linear velocity of the eluent. Eqn. 8 shows that ΔT increases by a factor of 30 in going from a 5- to a 2-μm particle column under otherwise constant conditions (column dimensions, eluent composition).

To keep the contribution of the volume of the connecting tubes to the column performance to a minimum, capillaries of 0.1 mm I.D. and 50 mm total length were employed.

The cell volume and the response time of the detector are critical parameters in the operation of short 1–2-μm particle columns. According to Guiochon[40], the maximum allowable cell volume is calculated to be

$$V_{d,M} = \Theta \frac{\pi \, d_c^2}{4} (1 + k') \, h \, d_p \, N^{\frac{1}{2}} \tag{9}$$

where h is the reduced plate height and N the plate number of the column. Setting $\Theta = 0.1$, $d_c = 4.6$ mm, $\varepsilon_t = 0{,}35$, $k' = 0$, $h = 3$, $d_p = 2.1$ μm and $N = 8800$, $V_{d,M}$ is calculated to be 0.3 μl. The cell volume of the UV detector employed in this study was

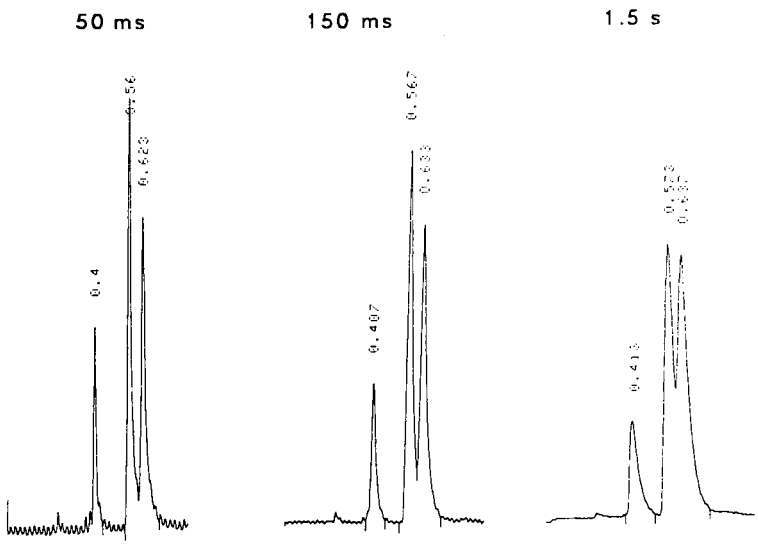

Fig. 5. Effect of the time constant, τ, of the UV detector on the chromatographic resolution. Conditions: column, 53 mm × 4.6 mm I.D. Monospher RP-18, $d_p = 2.1$ μm; eluent, water–acetonitrile (60:40, v/v); flow-rate, 1.25 ml/min; detection, UV at 254 nm, $\tau = 50$ ms, 150 ms or 1.5 s. Sequence of analytes: naphthalene, biphenyl, fluorene. The numbers at the peaks represent retention times in min.

0.6 μl. The maximum permissible time constant, τ_M required to avoid a noticeable loss in column efficiency is given by

$$\tau_M = \Theta \, t_R / N^{\frac{1}{2}} \tag{10}$$

Setting $\Theta = 0.1$, $N = 8800$ and $t_R = 10\,(60)$ s, τ_M is calculated to be 10 (60) ms. No UV detectors are commercially available with time constants smaller than 50 ms. Fig. 5 demonstrates the influence of the time constant at $\tau = 5$ ms, 150 ms and 1.5 s on the chromatographic resolution of a three-compound mixture on a 53 × 4.6 mm column, packed with 2.1-μm non-porous C_{18}-bonded silicas.

Predicted and actual column performance

Inspection of the plots of h against v indicates optimum values at $h \approx 3$ and $v \approx 5$ (ref. 43). The reduced linear velocity is given by

$$v = \frac{u \, d_p}{D_{im}} = 5 \tag{11}$$

where D_{im} is the solute diffusion coefficient in the eluent.

Setting $D_{im} = 2 \cdot 10^{-9}$ m^2/s for a low-molecular-weight compound in a water–acetonitrile (60:40, v/v) eluent and $d_p = 2.1$ μm, gives $\hat{u} = 5$ mm/s. The reduced plate height of $h = 3$ generates a plate height of $H = 3\,d_p = 6$ μm for particles of $d_p = 2.1$ μm or a plate number of 8800 at a column length of 53 mm.

Fig. 6 shows a plate height *versus* linear velocity plot, obtained with a 53 mm × 4.6 mm column, packed with non-porous 2.1-μm C_{18}-bonded silica beads. The plate height values between $2 < u < 5$ mm/s are scattered in the range from 5 to 8 μm and reflect the excellent performance of the columns. It is further evident that the plate height at a constant u value increases with decreasing solute capacity factor. This is a clear indication that extra-column contributions to the plate height are present and, hence, affect the peak width of the early-eluted compounds more than that of the late-eluted compounds.

Due to extra-column contributions to the plate height and due to the fact that H was determined by the tangent method, the parameters A, B and C of the Knox equation cannot be reliably estimated by fitting the experimental H *versus* u curves in Fig. 6.

CONCLUSION

As shown in the aggregation experiments of non-porous 1-μm silica beads by centrifugation, gravity settling and the slurry technique, stable suspensions of about pH 10 are required to achieve a high packing density. The dry-bag isostatic compression technique gave dense aggregates only when pressures in excess of 300 MPa were applied. Silica beads with bonded ethylsilyl groups aggregated by gravity settling resulted in denser bodies than those with bonded *n*-octylsilyl groups and even untreated silica. Of all techniques employed, gravity settling gave aggregates with the densest and most highly ordered structure; *i.e.*, a close-packed structure in the horizontal layers and a vertical stacking in between the layers. This was evidenced by

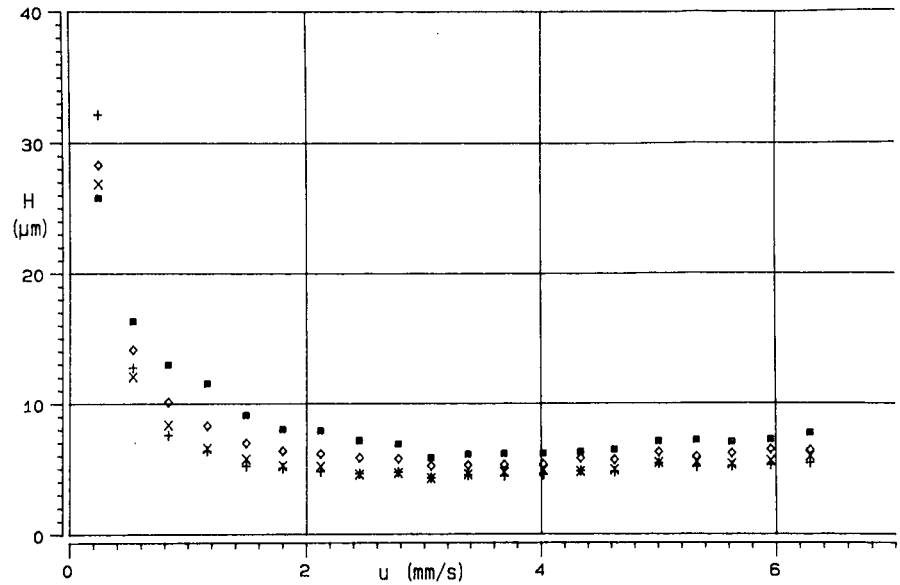

Fig. 6. Plot of the theoretical plate height, H, against the linear velocity of the eluent, u. Conditions: column, 53 mm × 4.6 mm I.D. Monospher RP-18, d_p = 2.1 µm; eluent, water–acetonitrile (60:40, v/v); detection, UV at 254 nm, flow-cell volume 0.6 µl, τ = 50 ms; injection volume, 0.5 µl. Solutes: □ = naphthalene (k' = 0.39); ◇ = anthracene (k' = 1.18); × = pyrene (k' = 1.74); + = chrysene (k' = 2.99).

stereo-SEM images. The high breakthrough pressure p^* of 8–10 obtained by mercury intrusion on these aggregates served as an additional indication. In contrast, the aggregates made by the slurry technique displayed a more open, random-type structure.

Batches of *n*-octadecyl-modified non-porous 1–2-µm silicas were employed for chromatographic studies. Columns of 53 mm × 4.6 mm I.D. were packed by gravity settling and by the slurry technique (constant flow-rate, end pressure 60 MPa). The columns packed by the two techniques gave nearly the same performance characteristics in terms of pressure–flow-rate and plate height–linear velocity dependence. The generation of less dense column beds by gravity settling compared to the previously described aggregates is probably attributed to the fact that the extent of free settling when the particles sediment in a column is somewhat reduced. As a consequence, all columns used were slurry-packed. In order to use the short columns for fast separations of less than 1 min, the injection volume must be about 0.6 µl, the volume of the UV detector cell about 0.3 µl and the time constant of the detector <50 ms. In addition, dead volume contributions must be avoided. Even then the peak dispersion (plate height) of the early-eluted peaks was found somewhat lower than those of the late-eluting peaks, indicating the presence of extra-column effects. This might be caused by the type of injection system employed which did not permit a fast injection.

In general, the plate height–linear velocity plots showed the expected performance characteristics for micron-size packings: a plate height value corresponding to two to five times the mean particle diameter and at a linear velocity of $u \gg 3$ mm/s

with nearly no loss in column efficiency up to 6.0 mm/s. At about 6.4 mm/s corresponding to a flow-rate of 2.2 ml/min the pressure limit of the HPLC equipment was reached.

REFERENCES

1 L. R. Snyder and J. J. Kirkland, *Introduction to Modern Liquid Chromatography*, Wiley, New York, 1979, pp. 202–218.
2 G. Guiochon and A. Katti, *Chromatographia*, 24 (1987) 165–189.
3 M. Verzele, J. van Dijck, P. Musche and C. Dewaele, *J. Liq. Chromatogr.*, 5 (1982) 1431–1448.
4 C. Dewaele and M. Verzele, *J. Chromatogr.*, 260 (1983) 13–21.
5 M. Verzele, C. Dewaele and D. Duquet, *J. Chromatogr.*, 391 (1987) 111–118.
6 K. K. Unger, H. Giesche and J. N. Kinkel, *Ger. Pat.*, DE-3534 143.2 (1985).
7 C. Dewaele and M. Verzele, *J. Chromatogr.*, 282 (1983) 341–350.
8 K. K. Unger, G. Jilge, B. Eray and I. Novak, paper presented at the *10th International Symposium on Column Liquid Chromatography, San Francisco, CA, May 18–23, 1986*, paper 502.
9 N. D. Danielson and J. J. Kirkland, paper presented at the *10th International Symposium on Column Liquid Chromatography, San Francisco, CA, May 18–23, 1986*, paper 503.
10 N. D. Danielson and J. J. Kirkland, *Anal. Chem.*, 59 (1987) 2501–2506.
11 W. Stöber, A. Fink and E. Bohn, *J. Colloid Interface Sci.*, 26 (1968) 62.
12 K. D. Lork, K. K. Unger and J. N. Kinkel, *J. Chromatogr.*, 352 (1986) 199–211.
13 K. K. Unger, E. Schadow and H. Fischer, *Z. Phys. Chem. (N.F.)*, 99 (1976) 245–256.
14 S. J. Gregg and K. S. W. Sing, *Adsorption, Surface Area and Porosity*, Academic Press, London, 1982.
15 E. Schadow and K. K. Unger, *High Temp.–High Pressures*, 9 (1977) 591–594.
16 R. K. Iler, in E. Matijevič (Editor), *Surface and Colloid Science*, Vol. 6,Wiley, New York, 1973, pp. 39–65.
17 G. D. Parfitt and K. S. W. Sing, *Characterization of Powder Surfaces*, Academic Press, London, 1976, p. 10.
18 H.Rumpf, *Chem.–Ing.–Tech.*, 46 (1974) 1–11.
19 H.Schubert, *Chem.–Ing.–Tech.*, 51 (1979) 266–277.
20 H. Heesch and F. Laves, *Z. Kristallogr.*, 85 (1933) 443.
21 E. Manegold, *Kapillarsysteme*, Vol. 1, Strassenbau, Chemie & Technik Verlag, Heidelberg, 1955.
22 D. G. Kadaner, V. M. Lukjanovich and L. V. Radushkevich, *Dokl. Akad. Nauk SSSR*, 87 (1952) 1001.
23 H. P. Meissner, A. S. Michaels and R. Kaiser, *Ind. Eng. Chem. Prod. Res. Dev.*, 3 (1964) 202.
24 K. Ridgway and K. J. Tarbuck, *Br. Chem. Eng.*, 12 (1967) 385.
25 A. P. Karnaukhov, in S. Modry and M. Svata (Editors), *Pore Structure and Properties of Materials, Proc. RILEM/IUPAC Conf., Prague, 1973; Preliminary Report*, Part I, Academia, Prague, pp. A3–A33.
26 S. Buckowiecki, B. Straube and K. K. Unger, in J. M. Haynes and P. Rossi-Doria (Editors), *Principles and Applications of Pore Structural Characterization*, Arrowsmith, Bristol, 1985, pp. 43–55.
27 R. G. Avery and J. D. F. Ramsay, *J. Colloid Interface Sci.*, 42 (1973) 597.
28 A. P. Karnaukhov, *Kinet. Katal.*, 12 (1971) 1025.
29 A. P. Karnaukhov, *Kinet. Katal.*, 12 (1971) 1235.
30 J. Rouqerol, personal communication.
31 L. K. Frevel and L. J. Kressley, *Anal. Chem.*, 35 (1963) 1492.
32 R. P. Mayer and R. A. Stowe, *J. Colloid Sci.*, 20 (1965) 893.
33 R. P. Mayer and R. A. Stowe, *J. Phys. Chem.*, 70 (1966) 3867.
34 S. Kruyer, *Trans. Faraday Soc.*, 54 (1958) 1758.
35 D. M. Smith and D. L. Stermer, *J. Colloid Interface Sci.*, 111 (1985) 160.
36 R. P. Iczkowski, *Ind. Eng. Chem.*, 5 (1966) 516; 6 (1967) 263.
37 R. K. Iler, in E. Matijevič (Editor), *Surface and Colloid Science*, Vol. 6, Wiley, New York, 1973, pp. 58–60.
38 I. L. Thomas and K. H. McCorkle, *J. Colloid Interface Sci.*, 36 (1971) 110.
39 W. Luck, M. Klier and H. Wesslau, *Naturwissenschaften*, (1963) 37.
40 G. Guiochon, in Cs. Horváth (Editor), *HPLC —Advances and Perspectives*, Vol. 2, Academic Press, New York, 1980, pp. 1–54.
41 H. Poppe and J. C. Kraak, *J. Chromatogr.*, 282 (1983) 399–412.
42 S. J. Van der Waal, *LC, Mag. Liq. Chromatogr. HPLC*, 3 (1985) 488–496.
43 J. H. Knox and H. P. Scott, *J. Chromatogr.*, 282 (1983) 297–313.

Journal of Chromatography, 465 (1989) 59–67
Elsevier Science Publishers B.V., Amsterdam — Printed in The Netherlands

CHROMSYMP. 1534

ARTIFICIAL INTELLIGENCE TECHNIQUES FOR PEAK HOMOGENEITY VALIDATION IN LIQUID CHROMATOGRAPHY

T. P. BRIDGE and M. H. WILLIAMS
Department of Computer Science, Heriot-Watt University, 79 Grassmarket, Edinburgh EH1 2HJ (U.K.)
and
A. F. FELL*
School of Pharmaceutical Chemistry, University of Bradford, Bradford, BD7 1DP (U.K.)

SUMMARY

A problem area in the interpretation of chromatographic data is the determination of the purity of a detected peak. The problem arises in deciding whether a peak is due solely to one component, or is caused by the simultaneous elution of two or more components. Whilst a number of multivariate statistical techniques are available to assess the number of components contributing to a given signal, they may require a significant amount of computer power to provide an answer, and are prone to noise-induced errors. As part of a programme of research aimed at developing an intelligent system for mobile phase optimisation, we have developed a knowledge-based systems approach to the problem of peak homogeneity assessment. The expert system applies a number of simple numerical tests to the three-dimensional dataset produced by a photodiode-array detector and assess the results in light of the chromatographic signal.

INTRODUCTION

The authors are engaged in the development of an expert system to assist in the development of an optimum separation for a mixture in reversed-phase liquid chromatography[1,2]. The expert system determines the appropriate solvent strength by means of a gradient elution experiment, and subsequently establishes the mobile phase composition to achieve optimum selectivity. The selectivity optimisation is achieved by adjusting the relative concentrations of three organic modifiers according to either a modified simplex[3] or iterative regression optimisation strategy[4].

The choice of optimisation strategy is guided by the amount of reliable information which can be extracted from the isoeluotropic chromatograms. The iterative regression method relies on the ability of the system to determine capacity factors for each solute under a number of different elution conditions, to provide a basis from which a mathematical model of the effect of changes in mobile-phase composition on selectivity, can be produced. The optimum composition for the mobile

0021-9673/89/$03.50

phase may then be identified by examination of the modelled response surface. The basis for identification of each solute in each chromatogram, and hence for allowing the variation in capacity factor with mobile-phase composition to be tracked, is the spectral information derived from a linear photodiode-array detector. The system compares the spectrum associated with one component with the spectra derived from other separations of the same mixture. If the matching process is successful, the variation in retention time, and hence capacity factor, can be determined for each detected solute.

However, this matching process may fail for reasons which include the variation in spectral profile caused by the change in solvent, the inability to discriminate between two or more components with similar spectral profiles, or the masking of components as a result of simultaneous elution. In such cases, the optimisation process is directed by a modified simplex algorithm, which requires no spectral information until sufficient additional information has been acquired to allow the iterative regression procedure to resume control of the optimisation process.

The reliance of the overall optimisation on the simplex method will be reduced if spectra can be extracted from peaks resulting from the simultaneous elution of two or more components. This may be achieved by the use of appropriate chemometric tools, such as factorial analysis[5]. A disadvantage of employing such techniques is the amount of computer power required to produce meaningful spectral profiles. The overall computer power requirement can be reduced significantly if the use of factorial analysis is restricted to heterogeneous peaks, where the spectral information is only available after deconvolution, and not on homogeneous peaks, from which no additional information can be derived by the application of such techniques.

To this end, the knowledge-based system is provided with the means to call upon a number of rapid homogeneity screening tests, the results of which are used in combination to assess the need for applying full matrix-based deconvolution methods.

METHODS FOR ASSESSING PEAK HOMOGENEITY

The peak homogeneity tests provided for use by the knowledge-based system were selected on the basis of their rapidity and reliability[6]. Whilst no single test is capable of detecting all cases of simultaneous elution, the use of a number of different tests in combination will increase the probability of correctly identifying heterogeneous peaks. The tests available within the system are described briefly below.

Determination of difference in spectral profile

The normalised profiles of spectra taken from the leading and trailing edges of the peak are compared. Spectra are extracted from the data matrix at times before and after the peak maximum, where the amplitude of the total absorbance signal is one third of that recorded at the peak maximum. These spectra are normalised at the wavelength of maximum absorption of the leading edge spectrum. The square root of the sum of the squares (RSS) of the differences between the two profiles is calculated, and this value is passed to the logic-processing element of the knowledge-based system.

Derivative total absorbance chromatograms

The profile of a differentiated curve is often a more sensitive indicator of the

existence of an otherwise hidden minor component than is the original zero-order curve[7]. To make use of this effect, an approximation to the time-domain derivative of the total absorbance chromatogram is calculated, and the number of zero crossings in the derivative profile is determined. For a pure peak, only one zero crossing will be produced. To reduce the effect of noise in the derivative signal in determining the true number of such crossings, a crossing is only accepted as valid if the value of the total absorbance chromatogram at that time is above a predefined threshold. First-derivative chromatograms of pure and composite peaks are illustrated in Fig. 1.

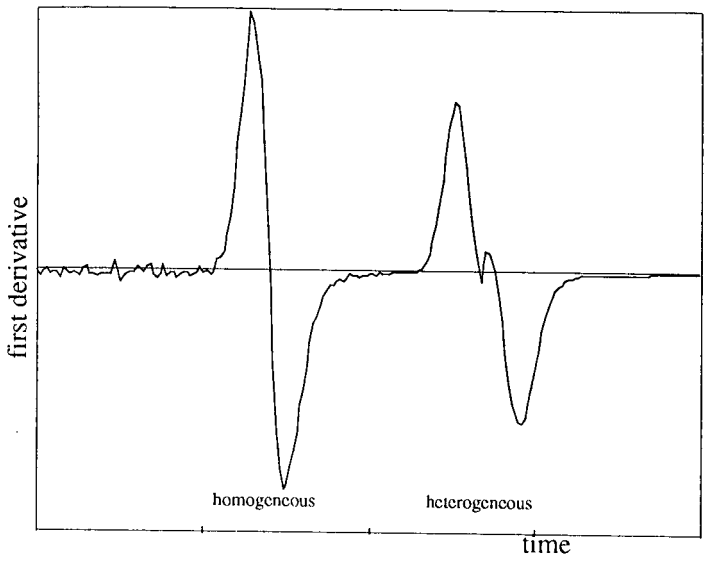

Fig. 1. First-derivative chromatogram.

As a consequence of the band-sharpening produced by differentiation, the second-derivative profile is more sensitive to the presence of minor components than is the first derivative. To produce the second-derivative profile, the first-derivative chromatogram is further differentiated numerically. As for the first-derivative profile, the number of zero crossings is used as an indicator of homogeneity. Two such crossings will be produced by a pure peak. Second-derivative chromatograms of pure and composite peaks are illustrated in Fig. 2.

Absorbance ratio chromatogram

The ratio of absorbances measured at two wavelengths should be invariant with time for a homogeneous peak[8]. This test locates the time at which maximum absorbance occurs in the total absorbance chromatogram and identifies the wavelength of maximum absorbance as well as the wavelength associated with an absorbance of half the maximum, at this time. The ratio of the signals at these two wavelengths is then calculated as a function of time across the peak. As the ratio is not evaluated for signals below a pre-determined threshold, to reduce the effect of noise on the output ratiogram, and as the ratio of the absorbances is independent of

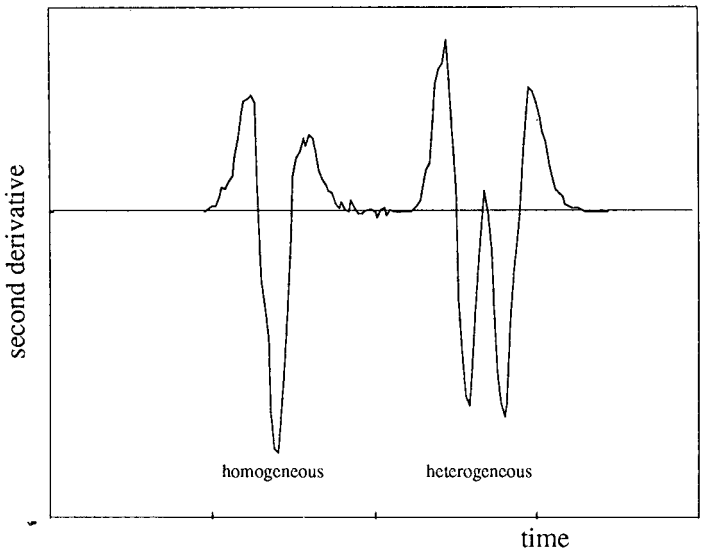

Fig. 2. Second-derivative chromatogram.

concentration, and therefore time, a pure peak produces a ratiogram with a square-wave profile. To assess the variation from this ideal profile, the RSS deviation from the value of the ratio at the midpoint of the peak is determined and reported. For a pure peak this should be zero, or for a real system it should not exceed the variation in signal due to detector noise. Ratiograms derived from homogeneous and heterogeneous peaks are illustrated in Fig. 3.

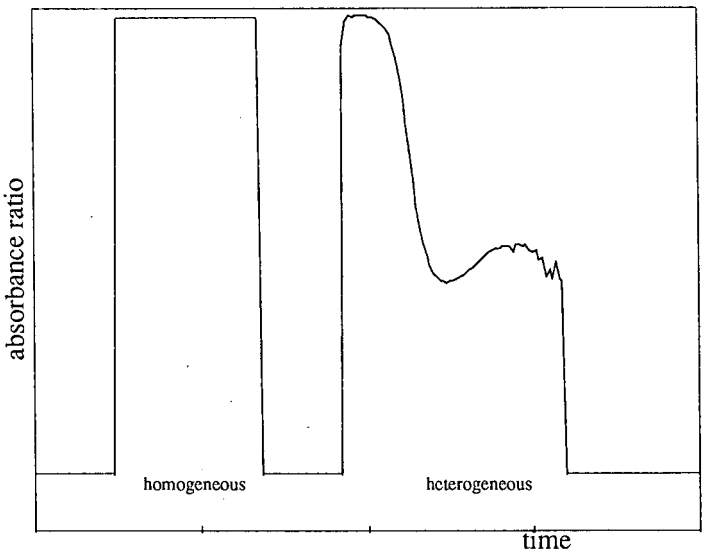

Fig. 3. Ratiogram of pure and impure peaks.

The idea of absorbance ratio evaluation may be extended into the derivative domain[9] if the chromatograms extracted, as above, at the wavelengths of maximum absorbance and half-maximum absorbance respectively, are differentiated before the ratio is evaluated. This may offer improved sensitivity towards certain cases of peak overlap, but at the cost of reduced indifference to noise in the spectrum.

Variation of apparent retention time

The observed retention time of a pure component will be independent of the wavelength used to monitor the chromatogram. However, in the case of a peak resulting from the simultaneous elution of two or more components, a variation in apparent retention time may be observed[10]. The degree of variation depends on the difference in the spectral profiles of the components, their separation and relative amplitudes. To quantify this variation for a single peak, the times of maximum absorbance are determined for each detector channel, and the difference between the largest and smallest values reported. Plots of retention time as a function of wavelength for two peaks are given in Fig. 4.

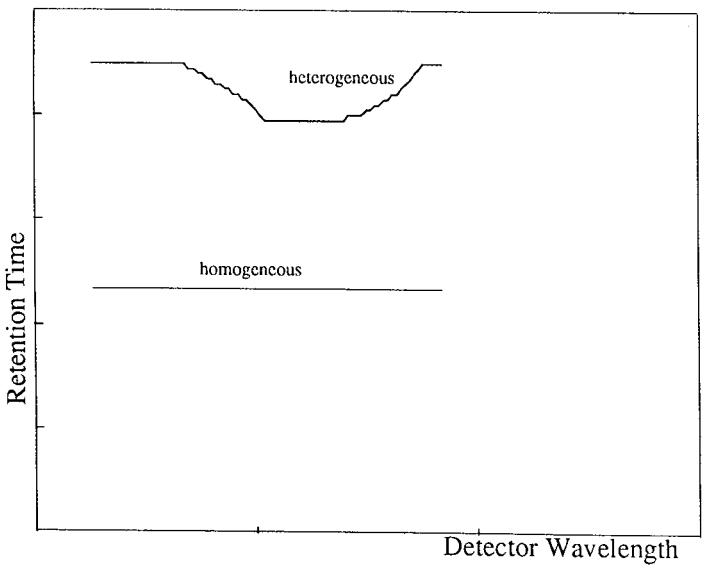

Fig. 4. Variation of retention time for pure and impure peaks.

THE EXPERT SYSTEM

The software forming the knowledge-based system is hosted on an IBM PS/2 micro-computer, operated with PC-DOS 3.30. The software is arranged in a highly modular fashion to facilitate development. Such a structure also allows the use of languages appropriate to the local task. Thus, whilst the logic processing is performed by modules written in microProlog, the homogeneity tests are coded in Pascal. The selection and execution of the various modules is controlled by a supervisory

Prolog Code for Peak Evaluation

```
The query is: ?((homogeneity assessed))

                ((homgeneity assessed)
                 (peak_is_pure yes))

                ((homgeneity assessed)
                 (peak_is_impure yes))

                ((peak_is_impure yes)
                 (NOT derivative_check ok)
                 (NOT spectrum_check ok))

                ((peak_is_impure yes)
                 (NOT derivative_check ok)
                 (NOT ratio_check ok))

                ((peak_is_impure yes)
                 (NOT derivative-ratio_check ok)
                 (NOT derivative_check ok))

                 ...

                ((derivative_check ok)
                 (first_derivative_test ok)
                 (second_derivative_test ok))

                ((derivative-ratio_check ok)
                 (Evaluate derivative_error x)
                 (x LESS limit_deriv_ratio))

                ((first_derivative_test ok)
                 (Evaluate d1_zero_crossings x)
                 (x LESS 2)
                 (0 LESS x))

                 ...

                ((Evaluate x y)
                 (EXECUTE x)
                 (OPEN "result_file")
                 (READ "result_file" y)
                 (CLOSE "result_file"))
```

Fig. 5. Extract from the PROLOG code used to interpret the homogeneity tests.

microProlog program. A section of the logic routine used to interpret the results of the homogeneity tests is reproduced in Fig. 5. The logic employed by the expert system to evaluate peak homogeneity is illustrated by the flowchart of Fig. 6.

EVALUATION

The operation of the expert system was evaluated by assessing the homogeneity of 33 chromatographic peaks of known composition. The composition of each of these

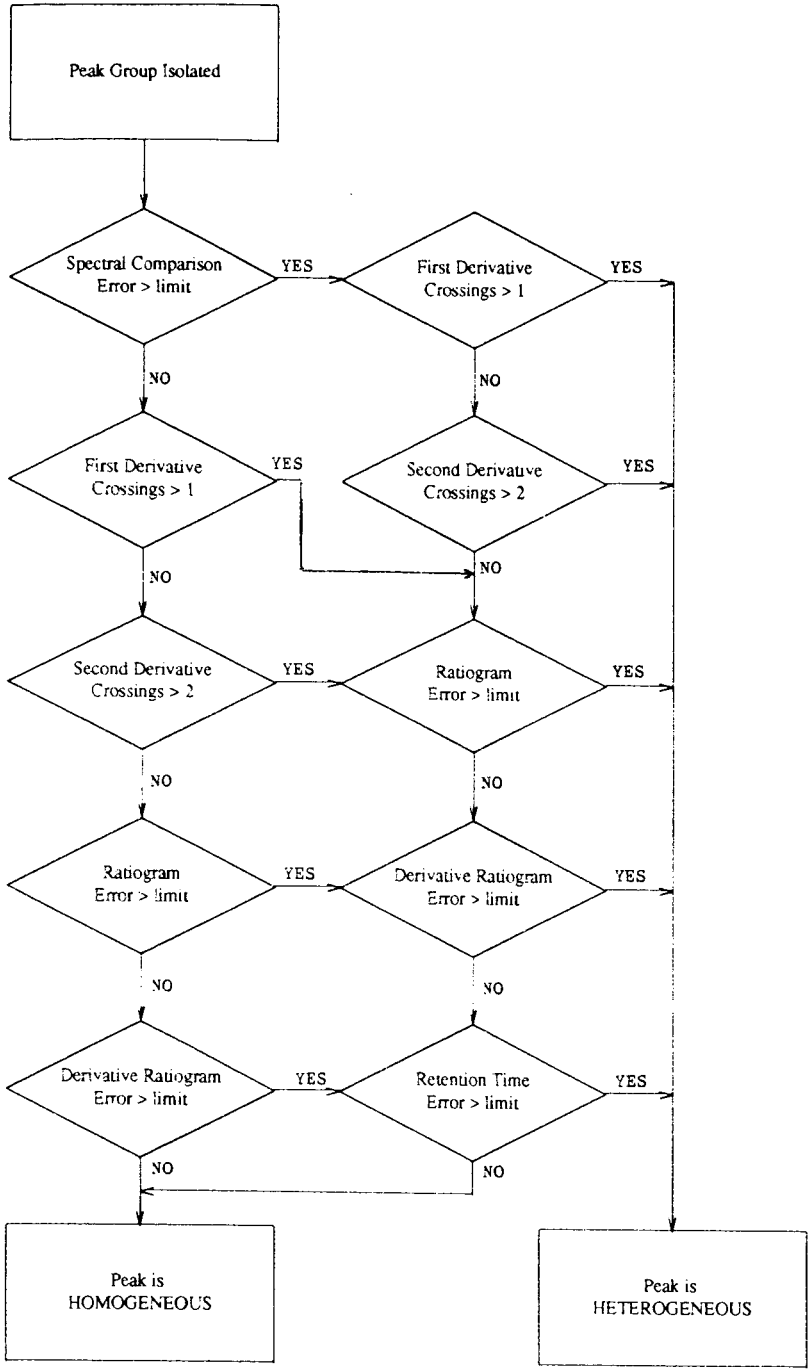

Fig. 6. Flowchart of the logic used to assess peak homogeneity.

TABLE I

COMPOSITION OF THE TEST CHROMATOGRAMS

No. of components	*Component*	*Relative amplitude*	*Separation (s)*	*No. of components*	*Component*	*Relative amplitude*	*Separation (s)*
1	Fluoranthrene	1		1	1,3-Xylenol	1	
1	Biphenyl	1		1	3,4-Xylenol	1	
1	Fluorene	1		1	2,3-Xylenol	1	
1	Pyrene	1		1	2,5-Xylenol	1	
2	Fluorene	1		2	2,3-Xylenol	1	
	Pyrene	1	20		3,4-Xylenol	1	20
2	Fluoranthrene	1		2	1,3-Xylenol	1	
	Biphenyl	1	20		2,5-Xylenol	1	20
3	Pyrene	1		3	2,3-Xylenol	1	
	Biphenyl	1	20		1,5-Xylenol	1	20
	Fluorene	1	20		1,3-Xylenol	1	20
4	Fluoranthrene	1		4	2,3-Xylenol	1	
	Biphenyl	1	20		3,4-Xylenol	1	20
	Fluorene	1	20		2,5-Xylenol	1	20
	Pyrene	1	20		1,3-Xylenol	1	20
2	Biphenyl	1		2	1,3-Xylenol	1	
	Pyrene	1	40		2,5-Xylenol	1	40
2	Biphenyl	1		2	1,3-Xylenol	1	
	Pyrene	1	20		2,5-Xylenol	1	30
2	Biphenyl	1		2	1,3-Xylenol	1	
	Pyrene	1	10		2,5-Xylenol	1	10
2	Biphenyl	1		2	1,3-Xylenol	1	
	Pyrene	1	5		2,5-Xylenol	1	5
2	Fluorene	1					
	Biphenyl	1	20				
2	Fluorene	1					
	Biphenyl	1	10				
2	Fluorene	1					
	Biphenyl	1	5				
2	Fluorene	2					
	Biphenyl	1	20				
2	Fluorene	2					
	Biphenyl	1	10				
2	Fluorene	2					
	Biphenyl	1	5				
2	Fluorene	4					
	Biphenyl	1	20				
2	Fluorene						
	Biphenyl	1	10				
2	Fluorene	4					
	Biphenyl	1	5				

peaks is indicated in Table I. As a comparative exercise the same chromatographic data were interpreted by a number of chromatographers in our laboratories. The results of the evaluation are expressed in Table II.

TABLE II

COMPARISON OF PEAK HOMOGENEITY ASSESSMENT BY THE EXPERT SYSTEM AND HUMAN EXPERTS

Analyst 1	*Analyst 2*	*Analyst 3*	*Analyst 4*	*Expert system*
Homogeneous peaks correctly assessed (from a total of 8)				
2	4	2	5	8
Heterogeneous peaks correctly assessed (from a total of 25)				
25	24	21	24	22

DISCUSSION

In the limited evaluation exercise reported above, the knowledge-based system out-performs the human analysts in the recognition of homogeneous peaks, and is of comparable performance in the detection of heterogeneous peaks caused by the simultaneous elution of two or more components. In such an exercise the human analysts might be expected to out perform the computer system, since they are using a visual interpretation of the complete chromatographic profile, rather than the limited numerical sample available to the expert system.

The use of a limited degree of artificial intelligence in the interpretation of rapid numerical tests offers a method for improving the reliability of peak homogeneity assessment in cases where the resources are not available for more comprehensive analysis by chemometric methods, such as iterative target testing factor analysis.

REFERENCES

1 T. P. Bridge, M. H. Williams, G. G. R. Seaton and A. F. Fell, *Chromatographia*, 24 (1987) 691.
2 T. P. Bridge, M. H. Williams and A. F. Fell, *Anal. Proc.*, 25 (1988) 43.
3 J. C. Berridge, *Analyst (London)*, 109 (1984) 291.
4 A. C. J. H. Drouen, *Ph.D. Thesis*, Technical University of Delft, Delft, 1985.
5 G. G. R. Seaton and A. F. Fell, *Chromatographia*, 24 (1987) 208.
6 T. P. Bridge, M. H. Williams and A. F. Fell, *Anal. Chim. Acta*m (1988) in press.
7 T. P. Bridge, A. F. Fell and R. H. Wardman, *J. Soc. Dyers Colour.*, 103 (1987) 17.
8 A. F. Fell, H. P. Scott, R. Gill and A. C. Moffa, *J. Chromatogr.*, 282 (1983) 123.
9 A. F. Fell, T. P. Bridge and M. H. Williams, *J. Pharm. Biomed. Anal.*, 6 (1988) 555.
10 A. G. Wright, A. F. Fell and J. C. Berridge, *Chromatographia*, 24 (1987) 533.

Journal of Chromatography, 465 (1989) 69–74
Elsevier Science Publishers B.V., Amsterdam — Printed in The Netherlands

CHROMSYMP. 1551

POLAROGRAPHIC DETECTION OF NON-IONIC SURFACTANTS ANALYZED BY REVERSED-PHASE PARTITION CHROMATOGRAPHY

P.L. DESBENE*, B. DESMAZIERES and J.J. BASSELIER
Laboratoire de Chimie Organique Structurale, UA 455, Université P. et M. Curie, 4 Place Jussieu, 75230 Paris Cédex 05 (France)
and
A. DESBENE-MONVERNAY
ITODYS, LA 34, Université Paris VII, 1 rue Guy de la Brosse, 75005 Paris (France)

SUMMARY

The analysis of non-ionic polyoxyethylenic surfactants used in enhanced oil recovery was performed by reversed-phase partition chromatography with polarographic detection after derivatization using 3,5-dinitrobenzoyl chloride. The optimization of the electrochemical detection was studied by varying the different parameters (organic solvent, supporting salt and reduction potential). Determinations were performed by chromatography on a Nucleosil C_8 column with acetonitrile–water (3:2) as the eluent containing 0.01 *M* $(C_4H_9)_4NClO_4$ as the supporting salt, at -1 V*vs.* Ag/AgCl in the direct current mode or at -0.8 V*vs.* Ag/AgCl in the differential pulse mode which improved the sensitivity. With polarographic detection, which is 50 times more sensitive than ultraviolet detection, surfactants can be reliably measured in the range of 10 to 1000 ppm.

INTRODUCTION

We have previously analyzed non-ionic polyoxyethylene surfactants used in enhanced oil recovery by reversed-phase partition chromatography and UV detection[1]. The non-ionic surfactants were obtained by condensation of a mixture of natural C_{16} and C_{18} fatty alcohols with ethylene oxide. The mean lengths of the polyoxyethylene chains are 6, 11 and 20 ethylene oxide units for the surfactants KL 6, KM 11 and KM 20 respectively. In order to analyze these surfactants in crude oil phases, a specific and sensitive detection method, such as electrochemical detection[2], is required. This paper describes the optimization of the electrochemical detection of non-ionic surfactants, achieved with a polarographic detector, and compares its performance with that of an UV detector.

0021-9673/89/$03.50

EXPERIMENTAL

Reagents

Acetonitrile was obtained from Prolabo (Paris, France) and tetrahydrofuran (THF) from BDH Chemicals (Poole, U.K.); both were high-performance liquid chromatography (HPLC) grade. The water was purified in a Milli RO and Millie Q system. Different mixtures of organic solvent and water, containing 0.01 *M* of a supporting salt, $NaClO_4$ or $(C_4H_9)_4NClO_4$ (Fluka, Buchs, Switzerland), were used as the mobile phases. They were vacuum-filtered through a 0.45-μm Millipore HA filter (Millipore, Molsheim, France) prior to use. Continuous deoxygenation of the solvent reservoir was accomplished by purging with argon. The surfactant standards with six ethylene oxide units and either a C_{16} or a C_{18} moiety were obtained from Nikko (Tokyo, Japan). The surfactants studied, KL 6, KM 11, KM 20 and S 385 (of technical grade), were provided by Marchon France (Saint Mihiel, France) and the Institut Francais du Pétrole. The derivatization with the 3,5-dinitrobenzoyl chloride (Prolabo, RP grade) has been described elsewhere[3].

Instrumentation

The chromatographic separation was performed on a 250 mm × 4.6 mm I.D. column packed in our laboratory with 5-μm C_8 bonded silica (Nucleosil; Macherey-Nagel, Düren, F.R.G.) using the method reported by Coq *et al.*[4]. The 6000 A pump (Waters, Milford, MA, U.S.A.) was connected to two pulse dampers (Touzart et Matignon, Ivry, France). The mobile phase flow-rate varied from 1 to 1.5 ml/min. The injector, Model 7010 (Rheodyne, Cotati, CA, U.S.A.), was equipped with a 20-μl sample injection loop. Detection at a dropping mercury electrode was accomplished with an EGG PAR Model 310 polarographic detector (EG/G Princeton Applied Research, Princeton, NJ, U.S.A.), which incorporated an Ag/AgCl reference electrode and a platinum auxiliary electrode. A drop size providing both sensitivity and reproducibility was selected. The 310 electrode was equipped with an argon inlet in order to deoxygenate the detection cell.

For current–potential (i–E) curves the "circulation" cell was replaced by a normal cell. The EGG PAR Model 364 potentiostat was employed in both voltammetry and detection experiments. The IFELEC IF 3802 recorder (Chauvin Arnoux, Paris, France) was used in the XY mode for polarograms and in the XT mode to obtain chromatograms.

In order to compare polarographic detection with UV detection, a Philips PU 4025 UV–VIS detector (Philips Analytical, Cambridge, U.K.) was inserted before the 310 electrode, and its signal was recorded on a recorder (Kipp & Zonen, Delft, The Netherlands).

RESULTS AND DISCUSSION

The chromatographic analysis using isocratic elution requires *ca.* 2 h. In order to gain time, various parameters (nature and electroactivity range of the medium, electrode material) were studied by means of voltammetry.

Electrochemical detection requires the use of conducting media that offer a wide electroactivity range. Acetonitrile–water and THF–water mixtures which ap-

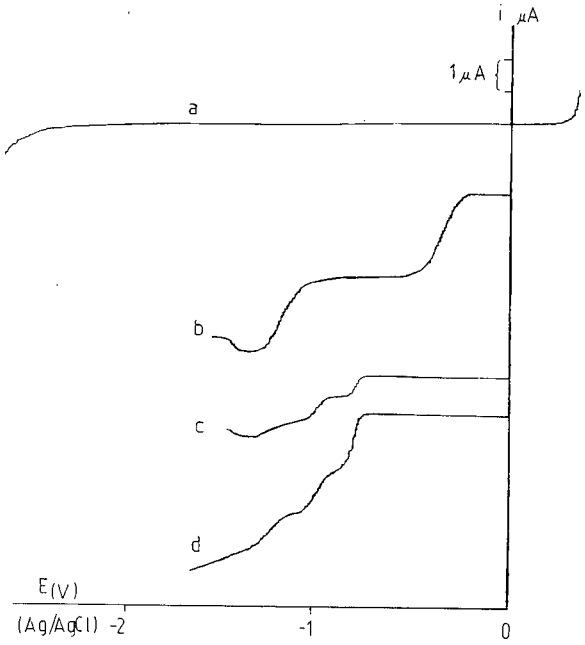

Fig. 1. Polarograms obtained in acetonitrile–water (1:1) + 0.01 *M* $(C_4H_9)_4NClO_4$ with a potential scan rate of 5 mV/s in the SDC mode. (a) Supporting salt only; (b) 3,5-dinitrobenzoyl chloride; (c) derivatized standard (6 ethylene oxide units, C_{16} chain); (d) derivatized surfactant KM 20.

peared to be the best mobile phases for the reversed-phase partition chromatography of the surfactants studied[1] showed an electroactivity range from -1 to -1.5 V *vs.* Ag/Ag^+ when using a glassy carbon electrode and 0.01 *M* $NaClO_4$ or $(C_4H_9)_4NClO_4$ as the supporting salt. The electroactivity range can be extended to -2.2 V *vs.* Ag/AgCl when using a dropping mercury electrode in the presence of $(C_4H_9)_4NClO_4$ (Fig. 1a). The polyoxyethylene surfactants KL 6, KM 11 and KM 20 as well as the ionic surfactant S 385 (which can be encountered in the media studied) do not show any oxidation wave on glassy carbon nor a reduction wave on mercury. This was not surprising, because the polyoxyethylene surfactants KM 11 and KM 20 possess only saturated C_{16} and C_{18} chains. The surfactant KL 6 also has an unsaturated C_{18} chain, while the ionic S 385 results from the sulphonation of a petroleum fraction, so they are also inactive. Consequently it appeared necessary to introduce an electroactive group in order to detect the surfactants electrochemically[5,6]. The introduction of nitro groups was accomplished by esterification of the alcohol function of the polyoxyethylene chain with 3,5-dinitrobenzoyl chloride. Derivatized surfactants showed a series of reduction waves for the standards (Fig. 1c) and for the samples (Fig. 1d), while the derivatization reagent was reduced more easily (Fig. 1b). The waves appeared more distinct in acetonitrile than in THF. Because electrochemical detection seemed more difficult on glassy carbon than on a mercury electrode, we chose a polarographic detector, although the detection in the reduction mode requires the elimination of oxygen from the medium. Although the potential reduction could be

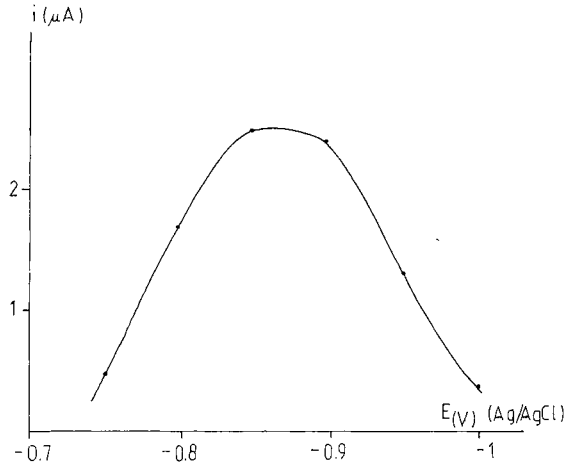

Fig. 2. Hydrodynamic polarogram of the derivatized standard (6 ethylene oxide units, C_{16} chain), obtained in the SDC mode. Chromatographic conditions: mobile phase, acetonitrile–water (3:2); flow-rate, 1.5 ml/min; column, C_8 Nucleosil (25 cm × 0.46 cm, $d_p = 5$ μm); injected volume, 20 μl; concentration, 100 ppm.

approximated from the *i–E* curves, it had to be optimized under the same hydrodynamic conditions.

The polarographic detector was tested in aqueous acetonitrile and THF with percentages of the organic solvent not exceeding 65% because above this value the detector underwent deterioration. This implicated the use of a C_8 column, which is less retentive than a C_{16} column. The salt $(C_4H_9)_4NClO_4$ was preferred as supporting electrolyte to $NaClO_4$, which rapidly altered the performance of the column packing.

The EGG PAR potentiostat offered four modes of measuring current intensity, only two of which are of interest for electrochemical detection: sampled direct current (SDC) and differential pulse (DP). As the analysis of the surfactants requires *ca.* 2 h, optimization of the detection was performed with an esterified standard having six ethylene oxides and a C_{18} chain. The hydrodynamic polarogram of this compound obtained in acetonitrile–water is shown in Fig. 2. As the noise increases when the

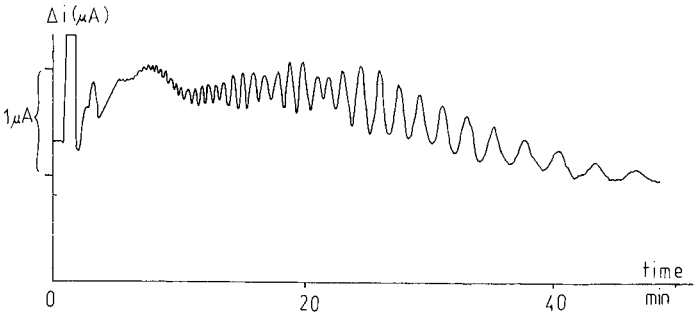

Fig. 3. Chromatogram of the derivatized surfactant KM 20, obtained in the SDC mode. Chromatographic conditions: as in Fig. 2, except flow-rate 1 ml/min, concentration 1000 ppm and detection potential −0.85 V *vs.* Ag/AgCl.

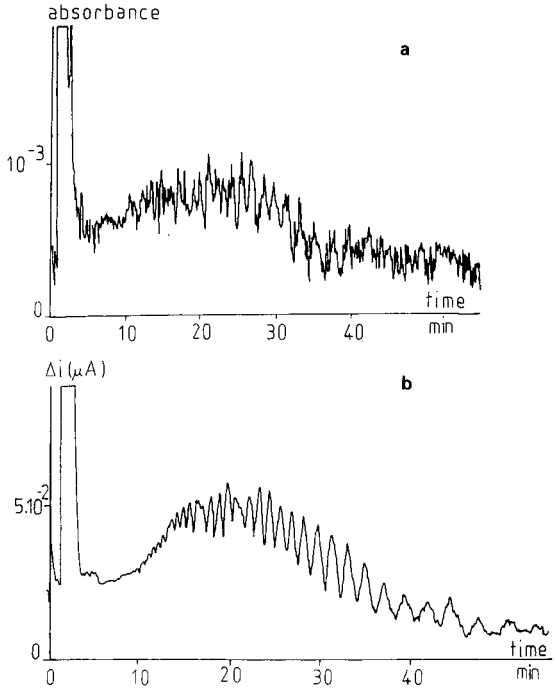

Fig. 4. Chromatograms of the derivatized surfactant KM 20: (a) polarographic detection (DP mode) potential −0.76 V *vs.* Ag/AgCl; (b) UV detection wavelength, 254 nm. Chromatographic conditions: as in Fig. 2.

potential becomes more negative, −0.85 V *vs.* Ag/AgCl was used for the detection in SDC mode. Under analogous conditions, a signal ten times less intense was recorded when acetonitrile was replaced by THF. This can be attributed to the weaker dielectric constant of this solvent (7.4) compared to that of acetonitrile (38.0). In the DP mode the optimum potential was −0.76 V *vs.* Ag/AgCl, and the sensitivity was increased by a factor of ten. The surfactants analysis under the previously established conditions led to satisfactory chromatograms, as shown in Fig. 3. The presence of an ionic surfactant (S 385) and/or inorganic ions (Ca^{2+}, Mg^{2+}, SO_4^{2-}, Cl^-) in the mixtures used for enhanced oil recovery did not change the appearance of this chromatogram, these species being electroinactive at the detection potential employed.

The performance of the polarographic detector in quantitative analysis was tested and compared to that of an UV detector, mounted in series before the Model 310 electrode. The dynamic ranges of the two detectors were initially established with the esterified standard (6 ethylene oxide units, C_{16} chain). The linear dynamic range extended from 0.5 to 100 ppm for the polarographic detector used in DP mode and from 5 to 10 000 ppm for the UV detector. The Model 310 electrode appeared more sensitive than the UV detector, having an absolute detection limit of 0.1 ppm compared to 1 ppm at a signal-to-noise ratio of 2.0, but it was saturated for concentrations exceeding 500 ppm.

For the surfactants studied the linear range extended from 10 to 1000 ppm, the detection limit of the polarographic detector being 10 ppm, while the UV detector

offered a linear dynamic range from 1000 to 10 000 ppm and a detection limit of 500 ppm.

In conclusion, polarographic detection is superior to UV detection in trace analysis of the surfactants KL 6, KM 11 and KM 20 (Fig. 4). Moreover, it can be used with complex mixtures, absorbing in the UV range, particularly, in the petroleum phases which we are now considering.

REFERENCES

1 P. L. Desbène, B. Desmazieres, J. J. Basselier and A. Desbène-Monvernay, *J. Chromatogr.*, 461 (1989) 305.
2 A. M. Krstulovic, H. Colin and G. A. Guiochon, *Adv. Chromatogr. (N.Y.)*, 24, (1984) 83.
3 P. L. Desbène, B. Desmazieres, V. Even, J. J. Basselier and L. Minssieux, *Chromatographia*, 24 (1987) 857.
4 B. Coq, C. Gonnet and J.-L. Rocca, *J. Chromatogr.*, 106 (1975) 249.
5 P. T. Kissinger, K. Bratin, G. C. Davis and L. A. Pachla, *J. Chromatogr. Sci.*, 17 (1979) 137.
6 P. Leroy and A. Nicolas, *Analusis*, 14 (1986) 263.

Journal of Chromatography, 465 (1989) 75–86
Elsevier Science Publishers B.V., Amsterdam — Printed in The Netherlands

CHROMSYMP. 1535

HIGH-PERFORMANCE LIQUID CHROMATOGRAPHIC DETERMINATION OF MITOXANTRONE IN PLASMA UTILIZING NON-BONDED SILICA GEL FOR SOLID-PHASE ISOLATION TO REDUCE ADSORPTIVE LOSSES ON GLASS DURING SAMPLE PREPARATION

KUN T. LIN*, GEORGES E. RIVARD and JEAN-MARIE LECLERC
Centre de Recherche, Hôpital Ste-Justine, Montreal, Quebec, H3T 1C5 (Canada)

SUMMARY

Mitoxantrone, a highly active antineoplastic agent, was found to bind strongly to non-bonded silica gel and glassware. When a Hamilton syringe was used to load and inject a mitoxantrone solution (0.4 μg/ml in water) on to a high-performance liquid chromatographic (HPLC) system, about 95% of the loaded compound was found to bind to the glass surface of the syringe barrel and could not be removed by rinsing with water. It could, however, be removed slowly with an acidic solution and thus a small peak of mitoxantrone was present on the chromatogram whenever a blank acidic solution was injected with the syringe. The bound mitoxantrone could be removed effectively from the syringe surface with a solution of tetramethylammonium chloride, citric acid, methanol and water (elution solvent). This binding introduces a large error in assay results and might be one of the major factors responsible for contradictory pharmacokinetic data that have been reported. A new plasma preparation scheme and an HPLC method for mitoxantrone were developed to address this binding problem. Mitoxantrone was extracted directly from plasma samples with a plastic mini-column packed with non-bonded silica gel and eluted with the above elution solvent. The eluent was analysed by HPLC on an ODS column with an absorbance detector at 658 nm. The mobile phase was 0.1 *M* triethylamine phosphate (pH 3.0) in water–tetrahydrofuran–methanol (69:1:30) containing 0.02 *M* tetramethylammonium chloride. Methylene blue was added as an internal standard. Preliminary results showed that mitoxantrone levels in human plasma followed a triphasic decay curve after an intravenous bolus injection. The terminal elimination half-lives measured in three patients (mean $t_{\frac{1}{2}}\gamma$ = 25 min) were all shorter than the published values which ranged from 56 min to 9 days.

INTRODUCTION

Mitoxantrone [1,4-dihydroxy-5,8-bis({2[(2-hydroxyethyl)amino]ethyl}amino)-9,10-anthracenedione dihydrochloride; CAS 70476-82-3; NSC 301739; Novantrone; Fig. 1] is an affective chemotherapeutic agent currently used against a wide variety of neoplastic diseases in humans[1–5]. Although many pharmacokinetic studies

0021-9673/89/$03.50

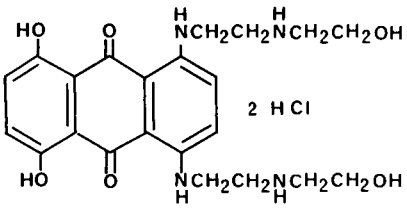

MITOXANTRONE

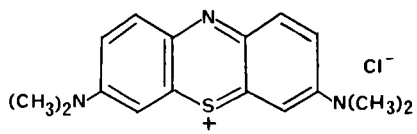

METHYLENE BLUE

Fig. 1. Structures of mitoxantrone and methylene blue.

have been carried out, the reported data are controversial with the elimination half-life varying widely from 56 min to 9 days[6–10]. Most of the data were obtained by high-performance liquid chromatographic (HPLC) analysis with some differences in the experimental conditions, such as mobile phase or absorption wavelength for detection[10–15]. The differences in the HPLC systems do not appear to be sufficient to account for such large discrepancies in the reported data. The largest differences among these assay methods lies in the sample preparation procedures which include extraction by liquid–liquid partition[11,12], by solid-phase retention with a hydrophobic resin[10,13] or with reversed-phase silica gel[14], or by a column-switching technique[15,16]. We initially tried to find a possible explanation for the discrepancies by comparing the various sample clean-up procedures. In the process, we found that mitoxantrone bound strongly to silica gel and to laboratory glassware. This property appears to have escaped the attention of previous workers and may be responsible to a great extent for the differences reported.

In this paper we present evidence to show that the binding of mitoxantrone to the laboratory glassware can result in erroneous assay data. We also describe a new plasma sample preparation scheme and an HPLC assay system for mitoxantrone that addresses the binding problem. The proposed system involves the use of methylene blue (Fig. 1) as an internal standard and a solid-phase extraction technique for sample preparation.

EXPERIMENTAL

Materials

Mitoxantrone was obtained form Cyanamid Canada (Toronto, Canada) with a purity of 101.1% as its dihydrochloride salt (free base content, 86.9%). Methylene blue was purchased from Mallinckrodt (St.Louis, MO, U.S.A.), tetramethylammonium chloride and triethylamine from Fluka (Ronkonkoma, NY, U.S.A.), methanol, acetonitrile and monobasic ammonium phosphate (all of HPLC grade) from Fisher Scientific (Fair Lawn, NJ, U.S.A.), tetrahydrofuran (distilled-in-glass grade) from Caledon Laboratories (Georgetown, Canada), orthophosphoric acid (85.9%, analytical reagent grade), *l*-ascorbic acid (biochemical-reagent grade) and citric acid monohydrate (analytical grade) from J. T. Baker (Phillipsburg, NJ, U.S.A.) and citrated normal human plasma from American Hospital Supply (Miami, FL, U.S.A.).

Plastic mini-columns (65 × 6 mm I.D., Bond-Elut), aspiration apparatus (Vac-Elut) and non-bonded silica gel (Sepralyte, 40 μm) were obtained from Analytichem International (Harbor City, CA, U.S.A.).

A stock solution of triethylamine phosphate (1 *M*) was prepared by mixing 67.8 ml of orthophosphoric acid with 800 ml of deionized water, titrating to pH 3.0 with triethylamine and then diluting to 1000 ml with deionized water. It was filtered through a 0.45-μm type HA filter (Millipore, Bedford, MA, U.S.A.) and stored at 4°C. The deionized water used throughout the experiments was obtained by connecting the distilled water system of the hospital to a Barnstead three-module Nanopure II system (Bybron/Barnstead, Boston, MA, U.S.A.).

HPLC system

The apparatus consisted of an LKB (Bromma, Sweden) Model 2150 pump, a Waters Assoc. Model 441 absorbance detector at 658 nm (Millipore, Bedford, MA, U.S.A.), a Hitachi (Tokyo, Japan) Model 561 chart recorder, a Rheodyne (Cotati, CA, U.S.A.) injection valve with a 50μl sample loop and a Waters Nova-pak ODS 4-μm column (75 × 3.9 mm I.D.). The mobile phase was prepared by mixing 10 parts (v/v) of triethylamine phosphate (1 *M*, pH 3.0), 1 part of tetrahydrofuran, 30 parts of methanol, 2 parts of tetramethylammoniumchloride (1 *M*) and 57 parts of deionized water. It was filtered through a 0.5-μm Type FH filter (Millipore) under maximum suction from a hydraulic pump and used without further degassing. HPLC was carried out at room temperature (22–23°C) with a flow-rate of 1.0 ml/min.

Binding on to syringes

Before injection of any solution the Hamilton syringe (Type A; size 100 μl) was rinsed three times with the elution solvent (see *Isolation procedures*) and each time the solvent was allowed to fill up to the full capacity of the syringe. The syringe was then rinsed three times with deionized water, five times with 0.1 *M* Cl in 50% aqueous methanol and again rinsed ten times with deionized water. The syringe was then used to load and inject 100 μl of the elution solvent on to the HPLC system to verify that no interfering peak was detected on the chromatogram. The syringe was again rinsed ten times with deionized water. It was then used to load 100 μl of test solution, the solution was allowed to remain in the syringe for 1 min at room temperature and then all 100 μl were injected on to the HPLC system (which was equipped with a 50-μl sample loop). The syringe was rinsed ten times with deionized water and used to inject 100 μl of the solution as described or subjected to the cleaning procedures as described above before injection of a new test solution. A plastic syringe (plastic tuberculin syringe, capacity of 1 ml in divisions of 0.01 ml; Becton-Dickinson, Rutherford, NJ, U.S.A.) fitted with a Hamilton removable needle for the Rheodyne injector was also used in the experiment. Great care was taken to fill up the solution to the 0.1-ml mark and all other conditions were followed precisely as those for the Hamilton syringe described above.

Collection of plasma samples

Venous blood (2.5 ml) was withdrawn with a polypropylene syringe and transferred into a polypropylene test-tube (100 × 17 mm I.D.) which contained 0.06 ml of 15% ascorbic acid (prepared in 0.6 *M* citrate buffer, pH 3.0) and chilled in ice–water

immediately. The mixture was centrifuged at 2000 *g* for 5 min at 4°C (with a Model NH-SII centrifuge; IEC, Needham Heights, MA, U.S.A.) and the plasma was stored at −20°C in a 1.5-ml Eppendorf polypropylene centrifuge tube equipped with a cap until analyzed. All plasma samples were frozen at least overnight before assay.

Isolation procedures

Plastic mini-columns, each containing 100 ml of non-bonded silica gel, were inserted into Luer fittings of the aspiration apparatus (Vac-Elut). Each column was then washed with 1 ml of 1 *M* hydrochloric acid, followed by 3 ml of water and finally with 0.5 ml of 2 *M* monobasic ammonium phosphate (pH unadjusted). The frozen plasma sample was thawed at 4°C and an aliquot (1.0 ml) was pipeted into a 1.5-ml Eppendorf polypropylene centrifuge tube. A 5-μl volume of methylene blue solution (5 μg/ml) was added to each sample as an internal standard. After centrifugation at 12 000 *g* for 1 min at 4°C (with a Model 5412 Eppendorf centrifuge; Brinkmann, Westbury, NY, U.S.A.), the supernatant was transferred into the above-mentioned mini-column and allowed to pass through at a flow-rate of about 1 ml/min by adjusting the suction of the pump. The precipitate remaining in the centrifuge tube was resuspended in 0.5 ml of 0.3% ascorbic acid solution (1:50 dilution of the aforementioned 15% ascorbic acid in 0.6 *M* citrate buffer, pH 3.0) by vortexing and subsequently transferred into the same mini-column. This two-step transfer of plasma sample was found to be essential to ensure a good flow of sample through the mini-column, which was frequently blocked by the small clots that invariably formed after the plasma sample was stored. The column was then washed with 0.5 ml of water followed by 0.5 ml of acetonitrile saturated with tetramethylammonium chloride and suction was applied for a further 5 min. It was subsequently removed from the aspiration unit, suspended above a plastic test-tube (100 × 7.5 mm I.D.) and eluted with 0.3 ml of elution solvent by centrifugation at 2000 *g* for 5 min at 4°C with an IEC Model NH-SII centrifuge. The elution solvent was prepared by mixing 10 parts (v/v) of tetramethylammonium chloride solution (1 *M*), 32 parts of methanol, 20 parts of citric acid solution (1 *M*) and 38 parts of deionized water.

Quantitation

The minimum quantifiable concentration for mitoxantrone by the detector was 1 ng/ml at a peak height-to-noise ratio of 5. The baseline on the chart recorder was very stable (fluctuation 0.3 mm; full-scale = 25 cm) with the recorder at its maximum sensitivity ($R=0.005$) and the mobile phase running at a flow-rate of 1.0 ml/min. Citrated normal human plasma blank together with those spiked with mitoxantrone at concentrations of 2.5, 5, 10, 25, 100 and 500 ng/ml were each added to 20 μl of 15% ascorbic acid (in 0.3 *M* citrate buffer, pH 3.0) and then prepared as described under *Isolation procedures*. After HPLC analysis, a calibration graph of the peak-height ratio of mitoxantrone to methylene blue *versus* mitoxantrone concentration was constructed. The graph was linear over the range 2.5–500 ng/ml with $Y = 0.056x + 0.22$, and a correlation coefficient (r) = 1.001. The mitoxantrone concentrations in clinical samples were obtained from the calibration graph by reference to the peak-height ratio of mitoxantrone to methylene blue determined by HPLC.

Pharmacokinetic study

An intravenous bolus of mitoxantrone (10 mg/m^2 body surface area) was given at 0 min and the blood samples were taken at 1, 2, 5, 10, 15, 20, 30, 45, 60, 120, 180 and 480 min. A blank sample was also taken immediately before drug administration. For those at 1, 2 and 5 min, the diluted samples (1:10 in 0.3% ascorbic acid) and also the undiluted samples were analyzed. For all other samples, only the undiluted plasma were analyzed. As the timing gap between the first three samples was narrow, sampling times were varied appropriately from the schedule owing to slow blood flow.

RESULTS AND DISCUSSION

It is well known that protonated amines can be strongly retained by the surface of silica gel and the mechanism for the retention is thought to involve interaction with the silanol groups of the gel[17,18]. With four amino groups present on its molecule (Fig. 1), it is therefore not surprising that mitoxantrone binds very strongly to silica gel and glassware.

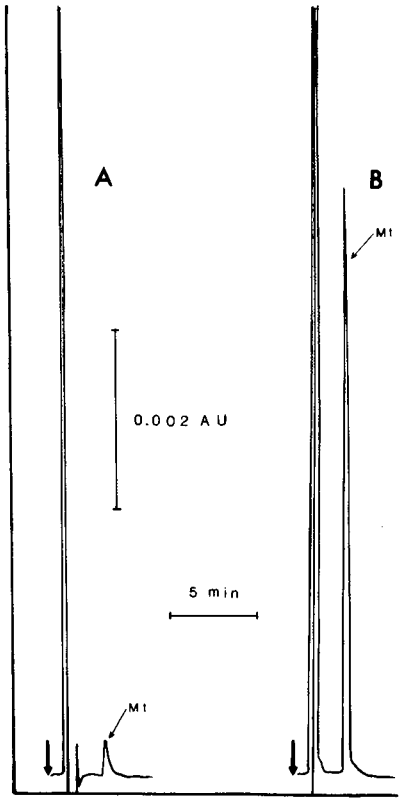

Fig. 2. Chromatographic profiles of (A) mitoxantrone solution (0.4 μg/ml in water) and (B) blank elution solvent injected into the HPLC system with a Hamilton syringe.

One of the most commonly used items of glassware in HPLC is the Hamilton syringe. Fig. 2A shows a chromatogram of mitoxantrone solution (0.4 μg/ml) prepared in deionized water and injected into the HPLC system with a Hamilton syringe. After rinsing ten times with deionized water the syringe was used to inject a blank elution solvent (see *Isolation procedures*) and the chromatogram shown in Fig. 2B was obtained. The peak height of mitoxantrone in Fig. 2B is about 16.4 times that in Fig. 2A, indicating that mitoxantrone solution (prepared in deionized water) binds to the glass surface of the syringe barrel and can subsequently be removed by rinsing with a solution containing a competing amine, but not by rinsing extensively with deionized water.

Fig. 3A shows a chromatogram of mitoxantrone solution (0.4 μg/ml) prepared in the elution solvent and injected into the HPLC system with a Hamilton syringe. After the injection the syringe was rinsed ten times with deionized water and a blank elution solvent was then injected. Only a very minor mitoxantrone peak (about 1% of the peak height in Fig. 3A) was detected on injection of the blank elution solvent (Fig. 3B). Another injection of blank elution solvent gave no mitoxantrone peak (not shown). The experiments demonstrated that, if a competing amine is present in the injection solution (such as the elution solvent), very little mitoxantrone is adsorbed on

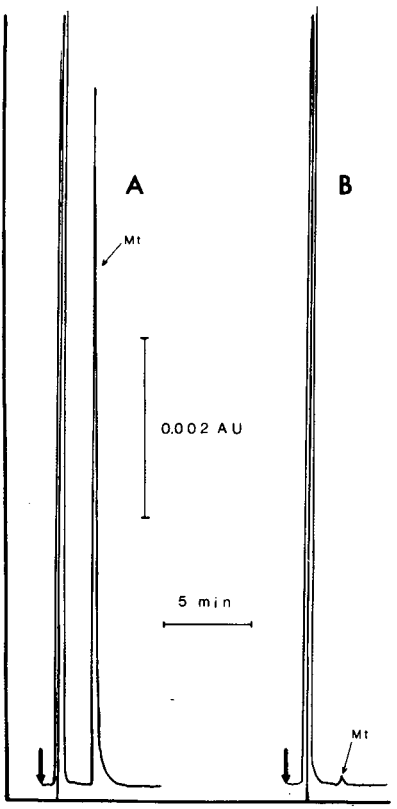

Fig. 3. Chromatographic profile of (A) mitoxantrone solution (0.4 μg/ml in the elution solvent) and (B) blank elution solvent injected into the HPLC system with a Hamilton syringe.

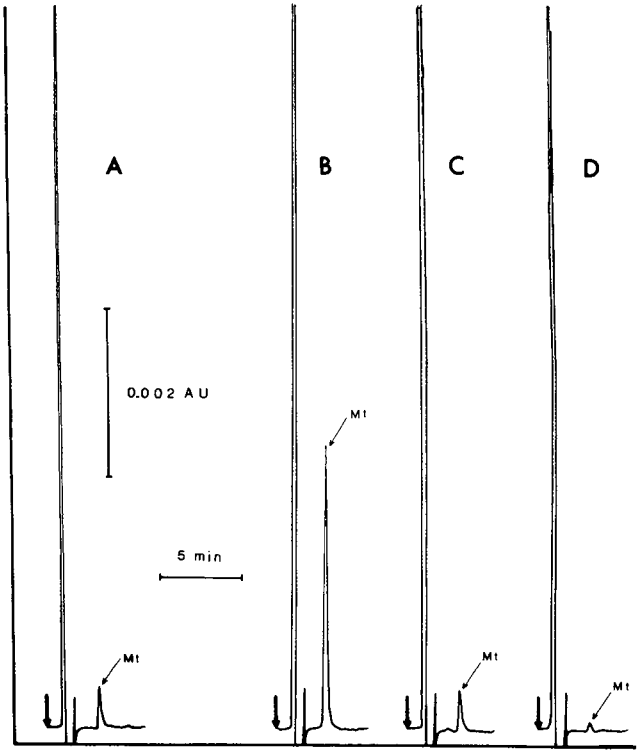

Fig. 4. Chromatographic profiles of (A) mitoxantrone solution (0.4 μg/ml in water) and successive injections of 0.1 *M* hydrochloric acid (B, C and D) with a Hamilton syringe. (B) First injection; (C) second injection; (D) fifth injection.

the syringe wall and if the Hamilton syringe is rinsed with the elution solvent between injections, almost no carry-over contamination of the Hamilton syringe by mitoxantrone will occur. The peak height of mitoxantrone in Fig. 2A is only 5% of that in Fig. 3A, suggesting that about 95% of loaded mitoxantrone in a solution prepared only with deionized water binds to the glass wall of the Hamilton syringe.

Fig. 4 shows the results obtained by injection of mitoxantrone solution (0.4 μg/ml in water) (A) with a Hamilton syringe, followed by a succession of aliquots of 0.1 *M* hydrochloric acid injected with the same Hamilton syringe (B, C and D). The syringe was rinsed ten times with deionized water between each injection. The experiment demonstrates that mitoxantrone adsorbed on the glass surface of the barrel of a Hamilton syringe can be removed slowly and inefficiently with an acidic solution. Thus, if a contaminated Hamilton syringe is used by an unsuspecting analyst to inject an acidic extract, a small mitoxantrone peak will be produced even though no mitoxantrone is present in the extract. One of the consequences of this error will be an artificially long elimination half-life for mitoxantrone in human plasma.

Fig. 5A shows the chromatographic profiles of a mitoxantrone solution (0.4 μg/ml in water) injected with a polypropylene syringe. The syringe was then rinsed with deionized water and the elution solvent was injected (Fig. 5B). There appeared to be some adsorption of mitoxantrone on the syringe, but the extent of the binding was

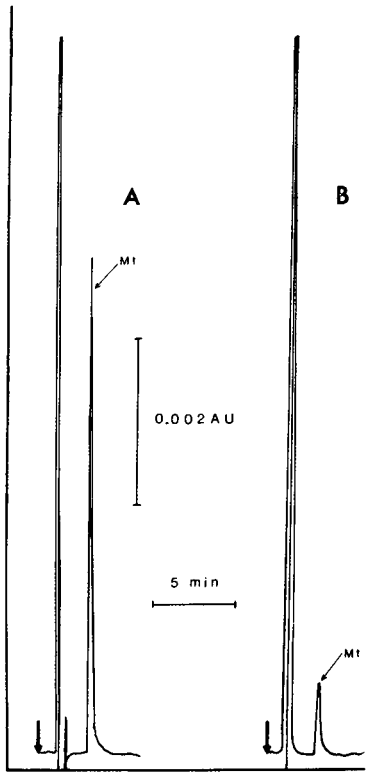

Fig. 5. Chromatographic profiles of (A) mitoxantrone solution and (B) blank elution solvent injected into the HPLC system with a polypropylene syringe.

far less than that observed with a Hamilton syringe. It must be noted that the plastic syringe was equipped with a rubber-tipped plunger, and therefore the source of this minor binding has not been located. The experiment nevertheless suggests that laboratory equipment or hardware made of polypropylene rather than glass should be used in mitoxantrone assays. We also avoid using rubber stoppers for vessels for the storage of plasma samples.

Taking advantage of this property, we isolated mitoxantrone directly from plasma samples with a mini-column packed with non-bonded silica gel and then eluted mitoxantrone and methylene blue (internal standard) from the column with an elution solvent that consisted of tetramethylammonium chloride, citric acid, methanol and deionized water. The composition of the elution solvent was formulated on the basis of three factors, a competing amine, an acid and an organic solvent. The selection of each compound could be carried out visually as both mitoxantrone and methylene blue show a deep blue color. When 1 ml of mitoxantrone or methylene blue solution (1 μg/ml in water) was allowed to pass through the plastic mini-column packed with non-bonded silica gel it formed a sharp blue band on top of the gel. A series of test solutions at different concentrations were added 100 μl at a time to the silica gel to evaluate their efficiency in washing down the blue band from top of the gel. Tetramethylammonium chloride is known to block silanol groups on silica gel[19].

but alone it was found to be not as effective in eluting down the bound mitoxantrone or methylene blue. Addition of citric acid to the tetramethylammonium chloride solution made both blue compounds move down more sharply and faster through the silica gel. Many other acids tested, including hydrochloric, phosphoric, formic and acetic acid, were not as effective. The effectiveness of the elution was also enhanced by the addition of methanol to the solvent, but its concentration could not be too far above that in the HPLC mobile phase otherwise the chromatographic system would be destabilized[20].

Methylene blue serves well as an internal standard. It is a polyamine with an absorption spectrum very similar to that of mitoxantrone and allowed the detection procedure to be carried out at 658 nm. Methylene blue also binds to Hamilton syringes and similar results to those for mitoxantrone in Fig. 2–4 were observed. It binds to silica gel even more strongly than mitoxantrone and required a larger volume of solvent for elution. In order to elute both compounds in a small volume of solvent, the sample-loaded column was washed once with acetonitrile that had been saturated with tetramethylammonium chloride. This washing pushed the methylene blue band so that it moved forward without much effect on mitoxantrone and thus allowed the two compounds to be eluted from the mini-column at about the same time with the elution solvent formulated. It should be noted that when methylene blue was added to the sample as an internal standard it was decolorized immediately by ascorbic acid (added as a stabilizer for mitoxantrone) in the plasma. The reduced form of methylene blue, however, was rapidly reoxidized once it had been injected into the HPLC system, because any residual amount of ascorbic acid that might be present in the injection solution would be separated quickly by the ODS column and the remaining methylene blue was continuously interacting with a mobile phase that contained air (N.B., the mobile phase was only filtered using the hydraulic pump, without further degassing). We verified this fact by injecting into the HPLC system methylene blue solution (100 ng/ml in the elution solvent) with and without 0.3% ascorbic acid and found that identical peaks (same retention time and peak shape and height) were produced.

Fig. 6 shows a representative chromatographic profile from the HPLC analysis of a plasma sample from a leukemic patient who had received an intravenous bolus injection of mitoxantrone. The first plasma sample was taken 2.5 min after administration of the drug. Subsequent plasma samples obtained 5 and 20 min after the injection of the drug showed a rapid decline of the mitoxantrone peaks, whereas the peaks for the internal standard (methylene blue) remained relatively unchanged. There was no interfering peak in blank plasma (Fig. 6, −5 min).

The results obtained in studies on three patients are summarized in Table I. The plasma concentration at 0.5 – 1 min after administration of the drug was 1.2 – 3.4 μg/ml; it then followed a triphasic decay curve with mean half-lives of 2.2 min ($t_{\frac{1}{2}}\alpha$), 8.7 min ($t_{\frac{1}{2}}\beta$) and 25 min ($t_{\frac{1}{2}}\gamma$)[21]. The terminal elimination half-life ($t_{\frac{1}{2}}\gamma$) obtained by us is the shortest that has ever been reported to date. The data, however, do not conflict with the observation that [^{14}C]mitoxantrone "equivalents" could be identified in autopsy tissues that were obtained more than 1 month after drug administration[22], as the workers concerned measured only the recovery of radioactivity without identifying the nature of the compounds (the site of the label on mitoxantrone was not identified).

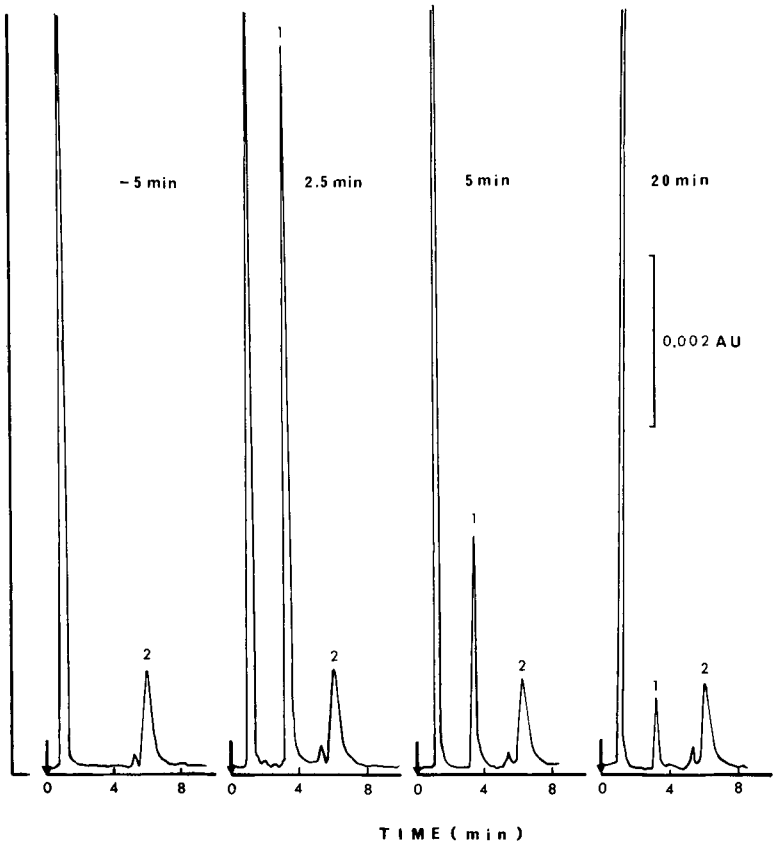

Fig. 6. Representative chromatographic profile for the analysis of plasma samples from a leukemic patient who had received an intravenous bolus of mitoxantrone (10 mg/m^2 body surface area) at 0 min. Plasma samples were taken at 1, 2.5, 5, 10, 15, 20 min continuing up to 4 h. A blank sample (−5 min) was also obtained immediately before administration of the drug. Only the results of −5, 2.5, 5 and 20 min are shown. Peaks: 1 = mitoxantrone; 2 = methylene blue. The minor peak between these two peaks is an impurity carry-over from the methylene blue solution.

Many sample preparation techniques for mitoxantrone, including solid-phase extraction, have been described[10–16]. The advantages for using solid-phase extraction over liquid–liquid extraction are well recognized[23]. Our solid-phase extraction method is superior to other methods in several respects. First, we include in our system an internal standard, in contrast to all other solid-phase extraction methods published so far[10,13,14]. Second, our extraction mechanism is based on adsorption and desorption of an amine with silanol groups, whereas extraction of mitoxantrone using an XAD-2 column [10,13] or a reversed-phase silica gel column[14] was based on hydrophobic interaction or a mixed mechanism. Obviously our method is more selective. Third, our elution solvent for the mini-column has a similar composition to the HPLC mobile phase, and therefore the HPLC system can withstand repeated injections of samples without deterioration. Other methods use a strong organic solvent, such as 30% propanol[10,13] or 0.5 *M* methanolic hydrochloric acid[14], for the elution. Is is well

TABLE I

HPLC ANALYSIS OF PLASMA SAMPLES FROM PATIENTS WHO HAD RECEIVED AN INTRAVENOUS BOLUS INJECTION OF MITOXANTRONE

Patient	*Age (yr)*	*Weight (kg)*	*Peak concentration*[a] *(μg/ml)*	*Half-lives (min)*		
				$t_{\frac{1}{2}}\alpha$	$t_{\frac{1}{2}}\beta$	$t_{\frac{1}{2}}\gamma$
F.D.	16	76	3.4 (0.5 min)	2	9	25
S.B.	16	47	2.1 (1.0 min)	1.5	8	20
I.F.J.	15	70	1.2 (1.0 min)	3	9	30

[a]The peak concentration represents the mitoxantrone concentration in the first plasma sample obtained after administration of the drug. The time in parentheses indicates the time when the sample was taken.

known that injecting a sample in a stronger organic solvent than the mobile phase can result in peak broadening and distortion[20]. Fourth, our method addressed the problem of binding of mitoxantrone to the laboratory glassware and thus avoided potential errors. None of the published methods for the determination of mitoxantrone has addressed this binding problem.

In conclusion, we found that mitoxantrone bound strongly to silica gel and glassware. We have developed a reliable and sensitive HPLC method for monitoring plasma mitoxantrone that addressed the binding problem. We recommend that all future studies on mitoxantrone, including drug monitoring and *in vitro* incubation, should avoid using any glassware to prevent loss of the compound. Polypropylene vessels should be used in a place of glass vessels.

ACKNOWLEDGEMENTS

This work was supported by grants from Cyanamid Canada, from the Medical Research Council of Canada (UI-004), from the Cancer Research Society of Canada and from Leucan. Our sincere thanks are due to Marjolaine Blanchet for technical assistance and to Suzanne Beaudet for secretarial work.

REFERENCES

1 M. McDonald, L. E. Posner, G. Duckart and S. C. Scott, *Cancer Res.*, 39 (1979) 1570.
2 R. H. Adamson, *Cancer Chem. Rep.*, 56 (1974) 293.
3 P. A. Paciucci, T. Ohnuma, J. Cuttner, R. T. Silver and J. F. Holland, *Cancer Res.*, 42 (1983) 3919.
4 J. F. Smyth, M. A. Cornbleet, R. C. Stuart-Harris, I. E. Smith, R. E. Coleman, R. D. Rubens, M. McDonald, H. T. Monnidsen, H. Rainer and A. T. van Dosterom, *Semin. Oncol.*, 11 (1984) 15.
5 G. Robbins, D.D.F. Ma and A. D. Ho, *Semin. Oncol.*, 11 (1984) 32.
6 D. S. Alberts, Y. M. Peng, S. Leigh, T. P. Davis and D. L. Woodword, *Cancer Treat. Rev.*, 10, Suppl. B (1983) 23.
7 K. Lu, N. Savarai, T. L. Loo, in M. Rosencweig, D. D. von Hoff and M. J. Staquet (Editors), *New Anticancer Drugs: Mitoxantrone and Bisantrene*, Raven Press, New York, 1983, p. 71.
8 N. Savaraj, K. Lu, M. Valdivieso, M. Burgess, T. Umsawasdi, R.S. Benjamon and T. L. Loo, *Clin. Pharmacol. Ther.*, 31 (1982) 312.
9 J. A. Stewart, J. J. McCormack and I. H. Krakoff, *Cancer Treat Rep.*, 66 (1982) 1327.
10 G. Ehninger, B. Proks, G. Heinzel, E. Schiller, K.-H. Weible and D. L. Woodward, *Investig. New Drugs*, 3 (1985) 109.

11 Y. M. Peng, T. P. David and D. S. Alberts, *Life Sci.*, 29 (1981) 36.
12 F. Ostroy and R. A. Gams *J. Liq. Chromatogr.*, 3 (1980) 637.
13 D. L. Reynolds, L. A. Sternson and A. J. Repta, *J. Chromatogr.*, 222 (1981) 225.
14 Y. M. Peng, D. Ormberg, D. S. Alberts and T. P. David, *J. Chromatogr.*, 233 (1982) 235.
15 B. Payet, Ph. Arnoux, J. Catalin and J. P. Cano, *J. Chromatogr.*, 424 (1988) 337.
16 M. J. Czejka and A. Georgopoulos, *J. Chromatogr.*, 425 (1988) 429.
17 R. F. Majors, in C. F. Simpson (Editor), *Practical High Performance Liquid Chromatography*, Heyden, London, 1976, p. 92.
18 N. H. C. Cooke, *Chromatogram*, 3 (No. 3) (1980) 1.
19 J. T. Przybytek, in P. A. Krieger (Editor) *High Purity Solvent Guide*, Burdick & Jackson Labs., McGaw Park, IL, 2nd. ed., 1984, p. 149.
20 G. Sivorinovsky, *Chromatogram*, 3 (No. 3) (1980) 6.
21 M. Rowland, in K. L. Melmon and H. F. Morrelli (Editors), *Clinical Pharmacology: Basic Principles in Therapeutics*, Macmillan, New York, 2nd. ed. 1978, Ch. 2, p. 55.
22 D. A. Alberts, *Investig. New Drugs*, 3 (1985) 101.
23 B. Tippins, *Am. Lab. (Fairfield, Conn.)*, 19 (No. 2) (1987) 107.

Journal of Chromatography, 465 (1989) 87–93
Elsevier Science Publishers B.V., Amsterdam — Printed in The Netherlands

CHROMSYMP. 1559

DERIVATIZATION AND HIGH-PERFORMANCE LIQUID CHROMATOGRAPHIC DETERMINATION OF URINARY GLYCOLIC ACID

MICHELE PETRARULO*, SERGIO PELLEGRINO, ORNELLA BIANCO, MARTINO MARANGELLA and FRANCO LINARI
Laboratory of Renal Stone Disease, Ospedale Mauriziano Umberto I, Largo Turati 62, Turin (Italy)
and
EDOARDO MENTASTI
Department of Analytical Chemistry, University of Turin, Via Giuria 5, Turin (Italy)

SUMMARY

A high-performance liquid chromatographic method for the determination of urinary glycolic acid is proposed, based on pre-column derivatization with phenylhydrazine coupled with the enzymatic oxidation of glycolate to glyoxylate. The phenylhydrazone formed is separated by liquid chromatography and detected at 324 nm. The minimum detectable concentration of glycolate was 10.0 μmol/l. The recovery of glycolate added to urine averaged 96.1%. The day-to-day coefficients of variation calculated by analysis of two urine samples with normal and high glycolate contents were 4.6 and 7.5%, respectively. Results of analyses of urine samples from healthy persons, idiopathic calcium stone formers and Type I primary hyperoxaluria patients are reported.

INTRODUCTION

Apart from ascorbate (ASC), glyoxylic (GLX) and glycolic (GLY) acids are the only known precursors of oxalate (OX) in man. In mammalians, the endogenous non-enzymic transformation of ASC into OX accounts for significant amounts of urinary OX[1]. GLY and GLX are connected with the metabolism of glycolaldehyde and serine and are enzymatically interconvertible and easily transformable into OX. The endogenous production of GLX is slower than its oxidation to OX, which is catalysed by lactate dehydrogenase (LDH) and glycolic acid oxidase (GAO), and consequently GLX serum and urine levels are extremely low[2].

An increase in GLX, GLY and OX in either serum or urine occurs in cases of Type I primary hyperoxaluria, vitamin B_6 deficiency and intake of toxic metabolic precursors[1,3–7]. Further, it has been reported that an increase in aromatic amino acid intake produces a mild increase in OX synthesis via GLY and GLX[8]. On the other hand, increases in OX levels may be coupled with normal urinary excretion of GLX and GLY in cases of Type II primary hyperoxaluria, with increased intake of ASC or OX and in a variety of malabsorptive syndromes[1,9–11].

0021-9673/89/$03.50

In a previous paper[2], we described a high-performance liquid chromatographic (HPLC) method for determining GLX in urine as the phenylhydrazone derivative, but the clinical use of the GLX determination in screening for hyperoxaluria syndromes gave partly meaningless results on account of the poor stability of GLX in biological fluids. Therefore, we have developed a new HPLC method for the determination of GLY acid in urine.

Simple colorimetric determination is one of the most widely used methods, in which a purification step with ion exchangers is followed by a colour reaction with chromotropic acid[12]. The use of glycolate oxidase (E.C. 1.1.3.3) for the determination of GLY in urine and plasma was described previously[13]. The method requires the treatment of the sample with charcoal and the determination of lactate for an indirect evaluation of GLY. Some gas chromatographic methods are also available, but they often require complex and lengthy sample processing[14–17].

In this paper we propose a new HPLC procedure for the determination of GLY in urine, based on the enzymatic conversion of GLY to GLX, coupled with the derivatization of the α-keto acid with phenylhydrazine (PH). The phenylhydrazone formed is then isolated and determined by HPLC.

EXPERIMENTAL

Materials

Analytical-reagent grade chemicals were used and water was deionized and distilled. Sodium glyoxylate monohydrate and oxalacetic acid were purchased from Fluka (Buchs, Switzerland) and GAO from spinach (glycolate oxygen oxidoreductase, E.C. 1.1.3.15, lyophilized powder, 3.8 U/mg protein), glycolic acid and phenylhydrazine hydrochloride were obtained from Sigma (St. Louis, MO, U.S.A.). HPLC-grade methanol, L-cysteine hydrochloride, concentrated hydrochloric acid, concentrated acetic acid, 30% ammonia solution, phosphoric acid and dipotassium hydrogenphosphate were obtained from Merck (Darmstadt, F.R.G.). Amino acid calibration standards, Type P-B and P-AN were purchased from LKB Biochrom (Cambridge, U.K.).

A 0.1 *M* L-cysteine solution was prepared weekly by dissolving 439 mg of L-cysteine hydrochloride in 25 ml of water and stored at 4°C. Phenylhydrazine hydrochoride was recrystallized twice from water, dried overnight at 37°C and stored in the dark until used. A 494 mmol/l working solution was prepared daily by dissolving 286 mg of the salt in 4.0 ml of water. Portions of 25 U of enzyme were reconstituted with 1.0 ml of 0.1 *M* potassium phosphate buffer (pH 8.3) by gentle shaking. The lyophilized powder is stable for at least 2 months when stored at 4°C, but the reconstituted portions must be used within 1 week.

Stock solutions of 1.0 *M* glycolic acid were prepared in water and stored in a refrigerator. Working standard solutions, containing 200 and 800 μmol/l, were prepared daily by diluting 50 μl and 200 μl, respectively, of the stock solution with 250 ml of water. An aqueous solution containing approximately 600 μmol/l of oxaloacetate was prepared daily and used as an internal standard.

Methods

Samples from 24-h urines, collected in the presence of 2.0 ml of chlorhexidine

gluconate, were obtained from twenty healthy persons (normals), 60 idiopathic calcium stone formers (ICaSF) and two patients with Type I primary hyperoxaluria (Type I HOx) while on an *ad libitum* diet. The urine samples were stored frozen and analysed within 1 month. Before analysis, the samples were filtered through 0.22-μm cellulose filters (Millipore, Segrate, Milan, Italy).

The derivatives were prepared by adding to 10-ml glass vials 50 μl of standard solution or urine, 50 μl of internal standard solution, 2.0 ml of phosphate buffer, 100 μl of cysteine and 100 μl of 494 mmol/l PH. After vortex mixing, 50 μl of the suspended enzyme were added and the solutions were mixed. The mixtures were left to react for 10 min at room temperature; the light yellow solutions were injected into the liquid chromatograph.

A Varian (Palo Alto, CA, U.S.A.) 5500 liquid chromatograph, equipped with a UV–VIS variable-wavelength detector and a Rheodyne (Berkeley, CA, U.S.A.) 7126 automatic injection valve with a 50-μl loop, was used. Peak heights were measured with a Shimadzu (Kyoto, Japan) R1A recorder–integrator. The detector output was set at 0.002 a.u.f.s. and the recording sensitivity was 8 mV at full scale.

An octadecylsilyl LiChrospher RP-18 (10 μm) column (250 × 4 mm I.D.) (Merck) was used throughout, connected with a Perisorb RP-18 (30–40 μm) (Merck) guard column (30 × 4 mm I.D.). Isocratic elution was performed at a flow-rate of 2.0 ml/min with methanol–0.15 *M* acetic acid (12:88, v/v) adjusted to pH 6.80 with ammonia solution as the mobile phase. Detection was performed at 324 nm. The buffer composition in the mobile phase was accurately controlled and the column was periodically cleaned by flushing with methanol and acetonitrile.

RESULTS AND DISCUSSION

The reactivity of GLX towards PH was detailed in a previous paper[2], in which the respective *syn*- and *anti*-phenylhydrazones were shown to be produced rapidly and quantitatively under the conditions described. The determination of GLY was performed with a reaction system based on the above derivatization. GAO catalyses the oxidation of GLY to GLX by molecular oxygen, producing hydrogen peroxide; oxidation appears to proceed further, making the disappearance of GLX very rapid. GLX is a reaction intermediate which, in the presence of a suitable PH concentration, is converted to the corresponding hydrazone, as described above. The conversion is performed at pH 8.3, where the enzyme activity is highest, and in the presence of an excess of cysteine as a reducing substrate to protect the GLX from the hydrogen peroxide formed:

$$CH_2OHCOOH + O_2 \xrightarrow{GAO} H_2O_2 + CHOCOOH \xrightarrow{PH} C_6H_5NHN{=}CHCOOH$$

$$\begin{array}{lll} & \text{GAO} \\ \text{cysteine} \downarrow & \downarrow O_2 \\ \text{cystine} & \text{unknown} \end{array}$$

The enzymatic conversion requires at least 0.6 U of enzyme per millilitre of reaction mixture to be complete within 10 min for GLY concentrations lower than 1000 μmol/l. Under these conditions, the enzymatic conversion represents the rate-determining step. Longer reaction times are required for the analysis of samples with a high GLY content. The quantitative conversion of GLY at concentrations between 1000 and 3000 μmol/l is achieved within 1 h, but appropriate dilution of the sample is advisable for concentrations up to 1000 μmol/l (see Fig. 1).

Under the chromatographic conditions described, derivatives of GLY and of the less retained internal standard are eluted in *ca.* 5 and 3 min, respectively. Chromatograms of a standard solution and a urinary sample are shown in Fig. 2.

Chromatograms from blanks show the presence of a small peak, eluted at the same retention time of that of the GLX phenylhydrazone. It corresponds to a GLY concentration of approximately 10 μmol/l. Further, PH reacts with other α-keto acids to produce the corresponding hydrazones. The retention times of the derivatives of some α-keto acids of biological relevance are as follows: oxaloacetate, 2.95; α-ketoglutarate, 4.57; glyoxylate, 5.15; and pyruvate, 5.92 min.

Urinary GLY stability was studied by storing two pools of urine, in the presence of 0.1 *M* hydrochloric acid, 0.04% of chlorhexidine gluconate and without stabilizers, either at room temperature or at −20°C. GLY was measured immediately and on subsequent days. The results showed that GLY is stable, irrespective of the means of preservation, for at least 1 month when stored in the frozen state.

Oxaloacetate (600 μmol/l) was used as an internal standard in the determination of GLY in order to minimize the injection error. Its natural concentration in urines was found to be insignificant in comparison with the amount added. Its phenylhydrazone was eluted in a blank zone of the chromatogram. The rate of the reaction between oxaloacetate and PH, under the above conditions, is so rapid that optimum conditions for its use as an internal standard are fulfilled. The instability of the 600 μmol/l oxaloacetate solutions was not considered to cause problems in this context.

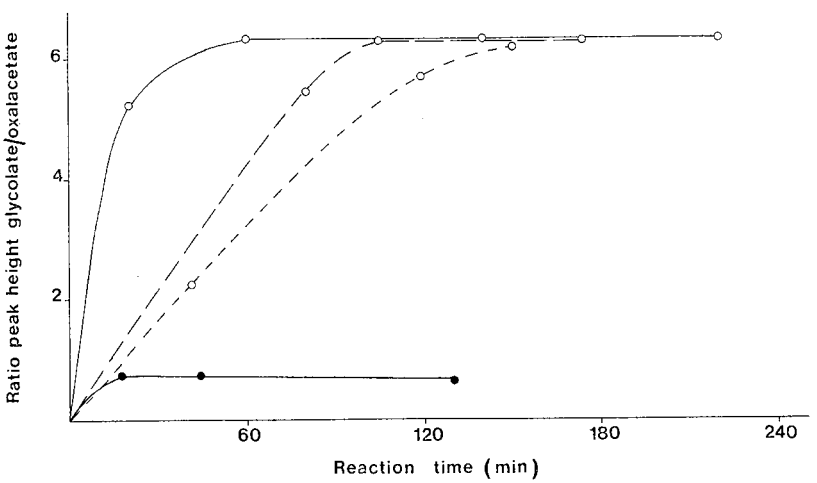

Fig. 1. Urinary glycolate conversion as a function of enzyme activity and glycolate concentration. The reaction was carried out as described in the text. Urine samples containing (i) 3356 μmol/l (○) and (ii) 363 μmol/l (●) of GLY reacted in the presence of 1.25 (———), 0.75 (--- —) and 0.25 (— — —) U of enzyme.

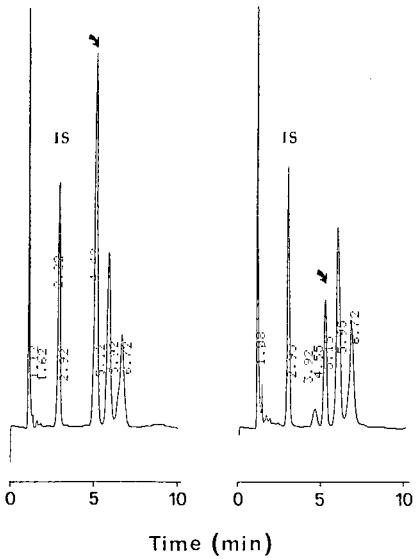

Fig. 2. Typical HPLC traces for the determination of glycolate under the conditions described in the text. Left, glycolate standard, 800 μmol/l in water; right, urine sample. The arrows show the glyoxylate phenylhydrazone peak.

The concentrations of GLY in urine samples were calculated according to the equation

$$\text{glycolate concentration} = \frac{(c_{gly})_{st}}{(h_{gly}/h_{is})_{st} - (h_{bl}/h_{is})_{bl}}\left[(h_{gly}/h_{is})_{sa} - (h_{bl}/h_{is})_{bl}\right]$$

where h_{gly} and h_{is} represent the peak heights of GLY and the internal standard (IS), respectively, in the standard solution (st), in urine samples (sa) and in blanks (bl); $(c_{gly})_{st}$ is the GLY concentration of the 800 μmol/l standard solution.

In each batch of samples, a 200 μmol/l standard and one sample, spiked with 200 μmol/l of GLY, were included as a check on the enzyme activity. The natural GLX contribution to the peak was found to be negligible[2] and was therefore not taken into account.

The calibration graph for the determination of GLY, obtained by plotting the GLY and IS peak-height ratios at various GLY concentrations was linear in the range 10.0–1000 μmol/l, and the minimum detectable concentration was 10.0 μmol/l at a signal-to-noise ratio of 10:1.

Two urine samples containing 166 and 643 μmol/l of GLY were analysed five times, yielding an intra-assay coefficient of variation (C.V.) of 3.8% and 4.6%, respectively, and a day-to-day between-run C.V. of 4.6% and 7.5%, respectively. The accuracy was tested by adding known amounts of GLY, ranging from 200 to 1000 μmol/l, to twenty urine samples. A mean recovery of 96.1 ± 7.5% shows the absence of any appreciable enzymatic inhibition or matrix effect.

The addition to urine samples of 1.0 mmol/l of oxaloacetate, α-ketoglutarate, glutarate, L-lactate, pyruvate, oxalate, mesoxalate, L-citrate, L-glucose, L-ascorbate,

L-tartrate, tartronate, malonate, maleate, malate, succinate and the common physiological L-amino acids did not produce any significant interference in the determination of GLY. The same also holds for the addition of 1.0 mmol/l of β-phenylpyruvic and *p*-hydroxyphenylpyruvic acids.

Chromatograms of reaction mixtures without addition of enzyme show the absence of potentially interfering extraneous peaks. Similar results were obtained on adding PH 1 h after the start of the enzymatic reaction, demonstrating the absence from the end products of the enzymatic conversion of non-specific peaks.

Urinary excretion levels determined on normals, ICaSF and Type I HOx patients are reported in Table I. Mean values and standard deviations are shown. The significance of differences was assessed by means of the Mann–Whitney rank-sum test.

The following considerations support the specificity of the proposed enzyme–HPLC method; first, it makes use of the enzymatic and selective transformation of an α-hydroxy acid to the corresponding α-keto acid. Second, only this class of urine carbonyl compounds show a relevant reactivity toward PH, with the rapid production of the corresponding phenylhydrazones.

In the reaction mixture, in the absence of pH, GLX has been found to disappear rapidly. This could be due to a certain affinity of the anzyme for GLX, but in our hands, in the presence of cysteine, in agreement with previous reports[13], neither oxalate nor formate could be detected among the end-products of the oxidation.

The lack of selectivity of α-keto acid oxidases for a homologous series of substrates has already been reported[13,18]. This could represent a drawback to the analytical use of glycolate oxidase in colorimetric determinations. In our work, the derivatives of the homologous compounds of GLY are easily resolved by HPLC, and this obviates the lack of enzymic specificity.

The low detection limits allow the determination of GLY in both normal and pathological urines. The normal ranges of urinary GLY so far reported are conflicting. Our results are in agreement with those obtained by both isotope dilution[19,20] and colorimetric[12] methods and are slightly higher than those found by an earlier enzymatic method[13].

Preliminary results on GLY excretion confirm sharp increases in patients with Type I HOx. In the present series ICaSF also show slightly higher values than healthy individuals. This could be ascribed to the fact that most of the patients considered here had mild hyperoxaluria, which has been reported to be either intestinal[10] or endogenous[8] in origin.

TABLE I

24-h URINARY GLY LEVELS IN NORMALS, ICaSF AND TYPE I HOx

Parameter	*Normals*	*ICaSF*	*Type I HOx*
n	25	60	6[a]
Mean (μmol/l)	450	629[b]	6167[c]
S.D. (μmol/l)	139.9	354.9	4616–0
Range (μmol/l)	207–732	162–2120	1180–10950

[a] Means from three separate urine collections from two patients.
[b] $p < 0.024$ *vs.* normals.
[c] $p < 0.001$ *vs.* normals.

REFERENCES

1 H. E. Williams, *Kidney Int.*, 13 (1978) 410.
2 M. Petrarulo, S. Pellegrino, O. Bianco, M. Marangella, F. Linari and E. Mentasti, *J. Chromatogr.*, 432 (1988) 37.
3 K. E. Richardson, *Toxicol. Appl. Pharmacol.*, 7 (1965) 507.
4 K. E. Richardson, *Toxicol. Appl. Pharmacol.*, 10 (1967) 40.
5 K. E. Richardson, *Toxicol. Appl. Pharmacol.*, 24 (1973) 530.
6 K. L. Clay and R. C. Murphy, *Toxicol. Appl. Pharmacol.*, 39 (1977) 39.
7 J. Y. Chou and K. E. Richardson, *Toxicol. Appl. Pharmacol.*, 43 (1978) 33.
8 R. L. Gambardella and K. E. Richardson, *Biochim. Biophys. Acta*, 499 (1977) 156.
9 K. E. Richardson and M. P. Farinelli, in L. H. Smith, W. G. Robertson and B. Finlayson (Editors), *Urolithiasis. Clinical and Basic Research*, Plenum Press, New York, 1981, pp. 855–863.
10 M. Marangella, M. Bruno, B. Fruttero and F. Linari, *Clin. Sci.*, 63 (1982) 381.
11 M. Menon, C. J. Mahle, *J. Urol.*, 127 (1982) 148.
12 A. Niederwieser, A. Metasovic and E. P. Leumann, *Clin. Chim. Acta*, 89 (1978) 13.
13 G. P. Kasidas and G. A. Rose, *Clin. Chim. Acta*, 96 (1979) 25.
14 R. A. Chalmers and R. W. E. Watts, *Analyst*, 97 (1972) 958.
15 B. G. Wolthers and M. Hayer, *Clin. Chim. Acta*, 120 (1982) 87.
16 K. Tanaka and D. G. Hine, *J. Chromatogr.*, 239 (1982) 301.
17 M. Y. Tsai, C. Oliphant and M. W. Josephson, *J. Chromatogr.*, 341 (1985) 1.
18 J. C. Robinson, L. Keay, R. Molinari and I. W. Sizer, *J. Biol. Chem.*, 237 (1962) 2001.
19 T. D. R. Hockaday, E. W. Frederick, J. E. Clayton and L. H. Smith, Jr., *J. Lab. Clin. Med.*, 65 (1965) 677.
20 S. Johansson and R. Tabova, *Biochem. Med.*, 11 (1974) 1.

Journal of Chromatography, 465 (1989) 95–99
Elsevier Science Publishers B.V., Amsterdam — Printed in The Netherlands

CHROMSYMP. 1536

HIGH-PERFORMANCE LIQUID CHROMATOGRAPHIC EVALUATION OF PCF 39, A NEW IMMUNOMODULATOR AGENT

A. MARZO*, N. MONTI, M. RIPAMONTI and G. CARDACE
Real srl, Via Milano 7/9, 22079 Villaguardia, Como (Italy)
and
E. ARRIGONI MARTELLI
Sigma Tau S.p.A., Via Pontina km. 30,400, 00040 Pomezia, Rome (Italy)

SUMMARY

An high-performance liquid chromatographic analysis of PCF 39, N^2-[5-(hypoxanthin-9-yl)pentyloxycarbonyl]-L-arginine, with ultraviolet detection, has been devised and validated. The main pharmacokinetic results encountered for rats treated intravenously with PCF 39 at a dose of 100 mg/kg are described.

INTRODUCTION

PCF 39 (Fig. 1) is a new drug which in animal immunopharmacological investigations has been demonstrated to normalize the immune defence of immunodepressed mice and to activate the endogenous production of lynphochines and other non-anticorpal immunologic mediators; experimental evidence suggests a macrophage activation as the mechanism of the PCF 39 activity[1–3]. An analytical method meeting all the requirements for quantitative evaluation of the drug in biological samples was standardized in order to investigate its pharmacokinetics in the rat, mouse and human beings. This paper describes the analytical procedures and the main pharmacokinetic results with the rat.

EXPERIMENTAL

Materials

Solvents and chemicals, all of analytical or HPLC grade, were supplied by Merck (Bracco, Milan, Italy). PCF 39 was supplied by Sigma Tau (Rome, Italy).

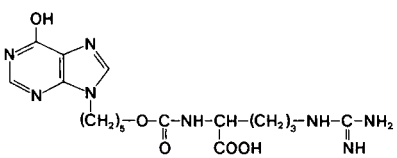

$C_{17}H_{26}N_8O_5$ M.W. = 422.44

Fig. 1. Chemical structure of PCF 39.

0021-9673/89/$03.50

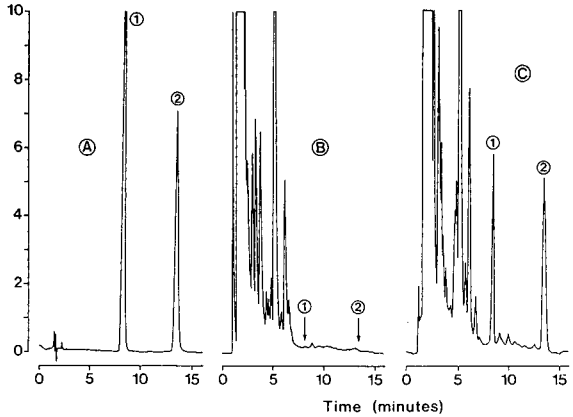

Fig. 2. Chromatograms of PCF 39 (1) and caffeine (2). (A) Authentic standards; (B) blank plasma; (C) plasma of rat treated with the drug. For chromatographic conditions, see Experimental.

A Varian Model 5020 liquid chromatograph and a Varian Model 2050 UV variable detector were used for the analysis. The column was a Supelcosil LC-18 DB, 5 μm, 250 mm × 4.6 mm I.D., supplied by Supelco (Supelchem, Milan, Italy). The statistical computations were performed on a Macintosh Plus personal computer (Apple computer, Reggio Emilia, Italy).

Methods

A 1 ml volume of plasma (or urine or tissue homogenate) was deproteinized with 2 ml methanol. After stirring for 10 min and centrifuging at 2400 *g* for 10 min, an aliquot of the supernatant was separated and evaporated under a nitrogen flow at 40°C. The solution was then reconstituted with 75–150 μl water for high-performance liquid chromatography (HPLC). An appropriate amount of internal standard (caffeine) was added after the extraction to monitor recovery, and before extraction in the routine analysis.

The mobile phase consisted of methanol–0.05 *M* phosphate buffer at pH 7.2 (18:82). The flow-rate was 1.8 ml/min. Absorbance was monitored at 250 nm. Retention times were 8.27 min for PCF 39 and 13.40 min for caffeine. Fig. 2 shows a typical HPLC chromatogram of the two substances.

Sprague-Dawley male rats, weighing 230–270 g, supplied by Charles River (Calco, Italy) were used in all the experiments.

PCF 39 was administered in doses of 25, 50 and 100 mg/kg intravenously. The rats were sacrified by cervical dislocation, and the serial plasma concentrations and tissue distribution in the gastric and intestinal wall, liver, kidneys, lungs, myocardium, lymph nodes, thymus and spleen were evaluated as described above. Similarly, the parent drug was evaluated in urine excreted over 0–3, 3–6, 6–9 and 9–24 h periods following administration. The cumulative biliary excretion of the drug was also investigated, in anesthetized rats through a biliary fistula.

TABLE I

RECOVERY OF PCF 39 FROM RAT PLASMA IN TRIPLICATE TRIALS

Internal standard (I.S.) was added in such a way as to achieve a ratio drug/I.S. of 1 : 1 for each drug level. During routine analysis, I.S. was such as to remain in a ratio drug/I.S. ranging from 1 : 4 to 4 : 1. The linear regression method gave the following correlation: $Y = 0.167 + 0.929\ X$, where $r^2 = 0.9978$.

PCF 39 added (= X) (μg/ml)	*PCF 39 recovered (= Y)*			*Recovery (%)*
	Mean (μg/ml)	*S.D.*	*% C.V.*	
0.5	0.50	0.008	1.54	99.3
1	0.99	0.03	3.07	99.3
2.5	2.42	0.07	2.73	97.0
10	9.85	0.23	2.37	98.5
25	24.91	0.14	0.55	99.6
50	45.46	1.04	2.29	90.9
100	92.27	2.64	2.87	92.3
250	232.87	11.60	4.98	93.1
			Mean	96.2 ± 4.08
			% C.V.	4.24

RESULTS AND DISCUSSION

The hydrophilic nature of PCF 39 did not allow it to be extracted from biological samples by solvent partition. This problem was solved by deproteinization, followed by sample concentration and injection. This procedure enabled high recovery of PCF 39, *i.e.*, 96.2%, and linear in the range of 0.5–250 μg/ml, with a correlation

TABLE II

LINEARITY OF DETECTOR RESPONSE WITH A FIXED DRUG-TO-INTERNAL STANDARD RATIO (1 : 1), ASCERTAINED BY A CONSTANT DETECTOR RESPONSE FACTOR (DRF)

$$\text{DRF} = \frac{\text{I.S. peak area}}{\text{analyte peak area}} \cdot \frac{\text{analyte concentration}}{\text{I.S. concentration}}$$

PCF 39 injected (ng)	*DRF (mean ± S.D.) (n = 4)*
40	0.667 ± 0.0043
100	0.672 ± 0.0017
200	0.677 ± 0.0021
400	0.684 ± 0.0006
1000	0.686 ± 0.0017
2000	0.686 ± 0.0030
4000	0.684 ± 0.0035
Mean	0.679
S.D.	0.0076
% C.V.	1.11

TABLE III

DETECTOR RESPONSE FACTOR AT DIFFERENT PCF 39 TO INTERNAL STANDARD (I.S.) RATIOS WITH AMOUNTS RANGING BETWEEN 250 AND 1000 NG

Linearity was ascertained as in Table II.

Drug / I.S. (ng)		*DRF*
250/1000		0.684
500/1000		0.688
1000/1000		0.689
1000/500		0.688
1000/250		0.681
	Mean	0.686
	S.D.	0.0034
	% C.V.	0.50

coefficient, r^2, of 0.9978 (Table I). The extraction recovery of the caffeine internal standard (I.S.) was similar to that of PCF 39. The linearity was verified in the range 40–4000 ng of PCF 39 and I.S., injected at drug-to-internal standard ratios of 1:1 and 1:4–4:1 respectively (Tables II and III).

The reproducibility tests gave an inter-assay coefficient of variation of 1.11% with a fixed ratio drug/I.S. and 0.50% with a variable ratio drug/I.S. When replication of the same drug concentration was carried out, an intra-assay coefficient of variation (C.V.) of 0.35% was obtained. The C.V. rose to 4.24% when the entire process of extraction was completed (Tables I–III).

The lowest detectable amount of PCF 39 was 1 ng, which is 30 ng/ml in terms of plasma or tissue concentration.

When injected intravenously, PCF 39 was cleared from plasma with a three-phase behaviour from the highest value of 225 μg/ml observed at 3.75 min to the lowest, 52 ng/ml, observed after 6 h(Fig. 3). The three phases showed $t_{1/2}$ values of 2.98, 21.3 and 156.9 min respectively. This may be governed by (a) the physical

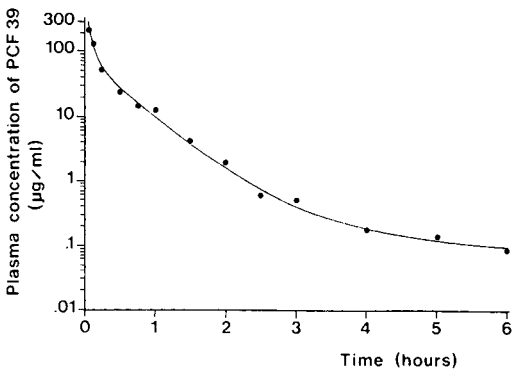

Fig. 3. Plasma concentration *vs.* time curve after i.v. administration of PCF 39 to rats. $C_p t = Ae^{-\alpha t} + Be^{-\beta t} + Ce^{-\gamma t}$, where A = 403 μg/ml, α = 13.9 h^{-1}, B = 68.4 μg/ml, β = 1.9 h^{-1}, C = 0.46 μg/ml and γ = 0.26 h^{-1}.

dilution of the drug, (b) both rapid and slow plasma–tissue equilibration processes, (c) urinary excretion, which occurs mainly in the first 3 h and (d) biotransformation processes.

Cumulative urinary excretion was as high as 55%, and biliary excretion in 5 h rose to 12% on average. Among the tissues investigated, the kidneys, liver, lymph nodes and thymus showed the highest concentrations of the drug [60.6, 94.2, 38.4 and 28.3 μg/g of wet organ respectively after intravenous (i.v.) administration of PCF 39 at a dose of 100 mg/kg].

In conclusion, this method achieved a sufficient degree of validation for pharmacokinetic application. With this method a skillful operator can routinely analyse around 30 samples a day by manual injection and use of an automatic integrator. As only routine instrumentation is required, the method is simple, easy and inexpensive.

REFERENCES

1 P. Cornaglia-Ferraris, R. G. Coffey and J. W. Hodden, *EOS*, 2 (1984) 34.
2 P. Puccetti, F. Campanile, C. Riccardi and P. Cornaglia-Ferraris, *Int. J. Immunopharmacol.*, 7 (1985) 338.
3 P. Cornaglia-Ferraris, L. Cornara and A. Melodia, *Int. J. Immunopharmacol.*, 4 (1986) 463.

Journal of Chromatography, 465 (1989) 101–111
Elsevier Science Publishers B.V., Amsterdam — Printed in The Netherlands

CHROMSYMP. 1537

PROTEIN A, HYDROXYAPATITE AND DIETHYLAMINOETHYL: EVALUATION OF THREE PROCEDURES FOR THE PREPARATIVE PURIFICATION OF MONOCLONAL ANTIBODIES BY HIGH-PERFOMANCE LIQUID CHROMATOGRAPHY

CLAUDIO POIESI*, ANNA TAMANINI, SALVATORE GHIELMI and ALBERTO ALBERTINI
Department of Clinical Chemistry and Propedeutic Biochemistry, University of Brescia, 1-25100 Brescia (Italy)

SUMMARY

Three rapid, reproducible and feasible monoclonal antibody purification procedures by means of high-performance liquid chromatography have been evaluated. The stationary phases employed were high-performance hydroxyapatite, high-performance Protein A and high-performance anion-exchange resin. The purity of the final immunoglobulin preparations was determined by sodium dodecyl sulphate-polyacrylamide gel electrophoresis under reducing conditions and, subsequently, by high-performance gel permeation chromatography. The immunoreactivity of purified monoclonal antibodies was determined by the radioimmunoassay method.

INTRODUCTION

Intraperitoneal injection of hybridoma cells into mice generates ascitic fluid, containing not only monoclonal antibodies (MoAbs), but also some other proteins, such as transferrin, albumin and proteases[1]. Due to their high specificity, MoAbs have found a great number of applications in the field of diagnosis, therapy and basic and applied research. The demand for large amounts of purified MoAbs for *in vitro* and *in vivo* use prompted the development of rapid, reproducible and feasible purification procedures.

Classical open-column chromatography is the most widely employed method for obtaining MoAbs on a large scale by means of anion-exchange (DEAE-cellulose)[2], affinity (Protein A)[3] and gel chromatography (Sephacryl, Sephadex)[4]. Recent improvements in high-performance liquid chromatography (HPLC) technology and the availability of new rigid polymeric resins has allowed the development of more rapid, convenient and efficient procedures for MoAbs purification. However, though several reports regarding the analytical procedure have been published[5–7], little has been done to develop preparative HPLC techniques for purification of MoAbs[16,17].

We have studied the preparative purification of MoAbs by HPLC, in order to verify the applicability of conventional purification techniques to HPLC. In this paper, we compare preparative Protein A, hydroxyapatite and anion-exchange HPLC

0021-9673/89/$03.50

focusing attention on protein recovery, purity of MoAbs and immunoreactivity. The three procedures employed provided highly purified MoAbs and a high protein recovery. The high-performance Protein A chromatography is therefore preferred for purification of immunoglobulin G (IgG). A previous chromatographic procedure to separate different MoAbs from the contaminant proteins is not required. The pH stepwise gradient elution can allow the separation of IgG subclasses[3]. Anion exchange or hydroxyapatite chromatography was employed for IgM purification.

MATERIALS AND METHODS

Materials

All the solvents employed were of HPLC reagent grade (E. Merck, Darmstadt, F.R.G.). Glycine, sodium chloride, disodium hydrogenorthophosphate, sodium dihydrogenphosphate, citric acid, tris(hydroxymethyl)aminomethane hydrochloride (Tris–HCl) and 2-mercaptoethanol were from Farmitalia Carlo Erba (Milan, Italy). Bovine serum albumin (Fraction V, chemical grade) was obtained from Miles Biochemicals and Immunochemicals (Milan, Italy). Polyethylene glycol (PEG) 6000 was from Merck.

The mouse ascitic fluid, containing an IgG1 kappa light-chain antibody (EK3) against human thyrotropin hormone (hTSH) was provided by Professor Ekins (Middlesex Hospital, London, U.K.).

Chromatographic equipment

Preparative purification of MoAbs was performed with an HPLC system (MAPS Preparative System 100; Bio-Rad, Richmond, CA, U.S.A.). The system was supplied with an automated injection mechanism (50-ml injection capacity), a variable-wavelength UV detector and a conductivity monitor for gradient elution. The MAPS Preparative System also featured dual-flow paths for analytical and preparative separation and a fraction collector. For integration and peak area reports, a Model 3392A integrator (Hewlett-Packard, Vancouver, WA, U.S.A.) and a Bio-Rad recorder, respectively, were used.

An Affi-Prep Protein A preparative column (100 mm × 25 mm; 50-ml bed volume), MAPS HPHA preparative guard cartridge (25 mm × 15 mm; 7.5-ml bed volume), MAPS HPHA preparative column (50 mm × 25 mm; 25-ml bed volume) and MAPS HPHA analytical cartridge (30 mm × 4.6 mm; 0.5-ml bed volume) were obtained from Bio-Rad. A Protein Pak DEAE 5PW semipreparative column (150 mm × 21.5 mm; 55-ml bed volume) was from Waters Associates (Milford, MA, U.S.A.). A high-performance gel permeation column (Bio-Sil TSK 250, 300 mm × 7.5 mm; Bio-Rad) together with a Waters 510 pump and an U6K injection system were used for the evaluation of the purity of MoAbs. Detection was performed at 278 nm by employing a Waters 481 UV spectrophotometer. For peak area integration, a Waters 730 data module was used.

Electrophoresis system

The purity of MoAbs was also evaluated by high-performance gel permeation chromatography (HP-GPC) as well as by sodium dodecyl sulphate-polyacrylamide gel electrophoresis (SDS-PAGE) under reducing conditions, according to the method

of Laemmli[8]. SDS-PAGE was performed on the Phast system (Pharmacia, Uppsala, Sweden) which consists of integrated separation and development units. The samples were loaded onto prepacked gels (PhastGel gradient 10-15). Gels were stained with Coomassie Brilliant Blue on a Phast system development unit.

Sample preparation

Prior to purification, ascitic fluid was treated with ammonium sulphate (50% saturation) at 4°C for 1 h. The solution was then centrifuged at 4000 rpm for 20 min; the pellet was resuspended and then dialyzed overnight at 4°C against deionized and distilled water. The sample was dried in a Speed-Vac concentrator (Savant Instrument, Farmingdale, NY, U.S.A.). It was resuspended in the chromatographic starting buffers and passed through a 0.45-μm filter.

Preparative high-performance hydroxyapatite (HPHA) chromatography

The conditions for HPHA chromatography were according to a previous report on the purification of murine MoAbs[9]. In order to optimize the separation method, the sample (100 μl) diluted to 1 ml in 10 m*M* phosphate buffer at pH 6.8 (buffer A) was injected into an HPHA analytical cartridge. A linear gradient was then performed from buffer A to 300 m*M* phosphate buffer at pH 6.8 (buffer B) in 15 min at a flow-rate of 0.4 ml/min.

As shown in Fig. 1a, the MoAb peak was not separated from contaminant proteins. A second chromatographic development was carried out with the same sample (100 μl); the cartridge was conditioned with 10% buffer B. After injection of 100 μl of the sample diluted to 1 ml in buffer A containing 10% of buffer B, the

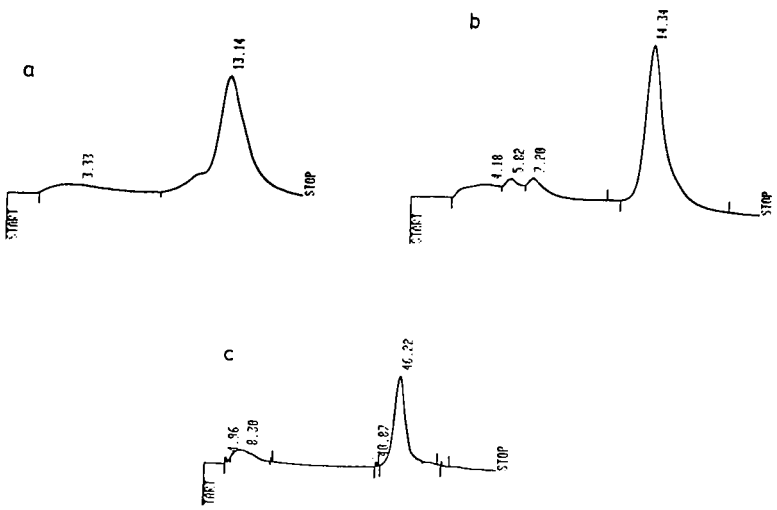

Fig. 1. Development of scale-up methodology for HPHA chromatography. (a) First chromatography on the HPHA cartridge; (b) chromatogram of the second injection into the HPHA cartridge; (c) elution of a 10-ml sample of ammonium sulphate-precipitated mouse ascites from the preparative HPHA column. Peak at 46.22 min is the IgG peak.

elution was performed with a linear gradient from 10 to 100% of buffer B in 15 min at a flow-rate of 0.4 ml/min.

Fig. 1b depicts the chromatographic pattern of the second injection. The MoAb peak was eluted at 14.34 min, while the contaminant proteins (as confirmed by SDS-PAGE) were fully eluted with 15% buffer B. The preparative HPHA column was conditioned with 15% of buffer B at a flow-rate of 4 ml/min. After injection of 10 ml (150 mg total protein) of the sample, isocratic elution with 15% buffer B for 30 min was followed by a linear gradient up to 100% buffer B in 30 min. The preparative elution profile is shown in Fig. 1c.

Preparative high-performance Protein A (HPPA) chromatography

Preparative Protein A chromatography was performed with a high-molarity binding buffer (1.5 *M* glycine, 3 *M* sodium chloride, pH 9.0) which allows efficient binding of all murine IgC subclasses and an elution buffer of low pH and ionic strength (0.1 *M* citrate buffer pH 3.0)[10]. The flow-rate was 4 ml/min. A 10-ml volume (150 mg total protein) of ammonium sulphate-treated ascitic fluid, resuspended in binding buffer, was loaded onto the column. As soon as the baseline of the unretained material returned to zero, the immunoglobulins were eluted with the acidic buffer. Fig. 2 shows the preparative purification of EK3 MoAb.

Protein Pak DEAE 5PW chromatography

The dried ascitic fluid (150 mg) was resuspended in 10 ml 20 m*M* Tris–HCl buffer (pH 8.5), and the sample was applied to the Protein Pak DEAE 5PW semipreparative column, equilibrated in the same buffer. The elution buffer was 50 m*M* Tris–HCl, 0.3 *M* NaCl (pH 7.0) and the flow-rate was 4 ml/min. The elution conditions were: isocratic for 10 min with starting buffer, then a linear gradient to 100% of elution buffer in 60 min. Fig. 3 depicts the anion-exchange chromatographic pattern.

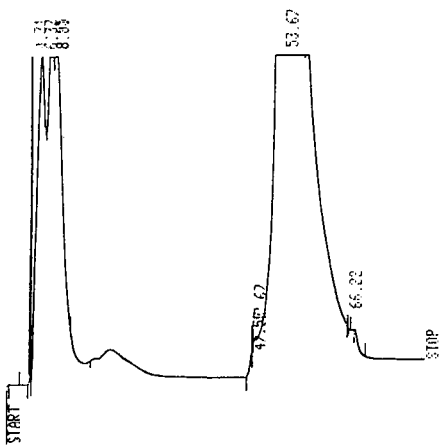

Fig. 2. High-performance Protein A chromatography of ammonium sulphate-precipitated mouse ascitic fluid (10 ml). Peak at 53.67 min is the IgG peak.

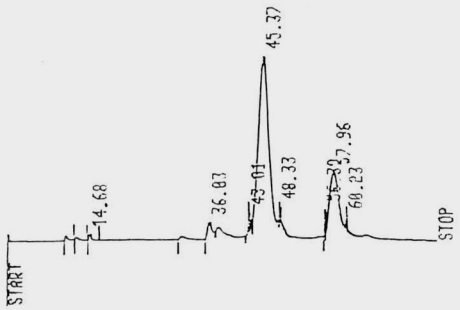

Fig. 3. Anion-exchange chromatography on a Protein Pak DEAE 5PW column of 10 ml of ammonium sulphate-precipitated ascitic fluid; flow-rate, 4 ml/min; elution for 10 min with 20 m*M* Tris–HCl (pH 8.5), then linear gradient from 20 m*M* Tris–HCl (pH 8.5) to 50 m*M* Tris–HCl, 0.3 *M* NaCl (pH 7.0) in 60 min.

Other assay methods

Protein recovery was determined by measuring the amount of proteins in ascitic fluid and in the collected peaks with the Bio-Rad protein assay kit. The immunoglobulin titration was performed with a radioimmunoassay method: 100 μl (30 000 cpm) [^{125}I]hTSH (Eurogenetics, Turin, Italy) were added to 100 μl of crude ascitic fluid or purified MoAb serial dilutions, both at an initial concentration of 1 mg/ml, and incubated overnight at room temperature. The MoAb–antigen complex was separated from unbound MoAb using 2 ml of 20% PEG 6000 (w/v in Veronal buffer, pH 8.6) in the presence of 100 μl of normal human serum. The titre was calculated as the dilution of the MoAb that binds 50% of the tracer. The inverse of this value was defined as the specific anti-hTSH activity.

RESULTS

Collected peaks from the three chromatographic methods were dialyzed against saline phosphate buffer (PBS, pH 7.2) and analyzed by reducing SDS-PAGE in order to determine the immunoglobulin peak. Fig. 4 shows the SDS-PAGE of the preparative HPHA chromatographic peaks. Lane 6, peak at 46.22 min (Fig. 1c), contains only bands corresponding to immunoglobulin heavy and light chains, while lane 5 is the unretained material (albumin and other contaminant proteins). The immunoglobulin peak (100 μl) was then passed through the HP-GPC column to establish the degree of purity. The eluent was PBS and the flow-rate was 1 ml/min. The column was first calibrated with molecular-weight standards (gel filtration calibration kits, low and high molecular weight, Pharmacia) in order to determine the immunoglobulin retention time. The immunoglubulin peak area percent was taken as the percent of purity. The peak area percent of IgG in the preparative HPHA purification was 98% (Fig. 5).

The SDS-PAGE analysis of chromatographic peaks, obtained by HPPA purification, is shown in Fig. 6. Immunoglobulin heavy and light chains (lane 3) were free from contaminants, as confirmed by HP-GPC analysis with a purity of 99% (Fig. 7). Albumin, transferrin and other contaminant proteins in ascitic fluid were found in the unretained material (lane 4).

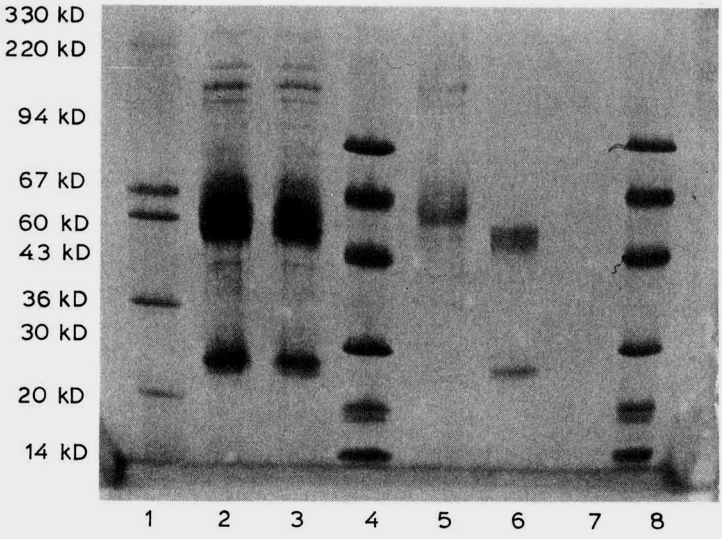

Fig. 4. Reducing SDS-PAGE of the preparative HPHT fractions. Lanes: 1, high-molecular-weight (HMW) standards; 4 and 8, low-molecular-weight (LMW) standards; 2 and 3, crude ascites; 5, peak at 8.3 min; 6, peak at 46.22 min.

In DEAE chromatography the MoAb peak (45.37 min) was well separated from the albumin peak (57.96 min), as confirmed by SDS-PAGE (lanes 3 and 6, and 4 and 7, respectively, Fig. 8). Fig. 9 shows the HP-GPC analysis of the MoAb peak (100 μl); the immunoglubulin area percentage was 99%.

The protein recovery and immunoreactivity was substantially the same in all the three chromatographic methods (Table I), and the purification factor (MoAb fraction/crude ascites anti-hTSH specific activity ratio; crude ascites anti-hTSH specific activity was 80 000) ranged from 4.8 to 4.0.

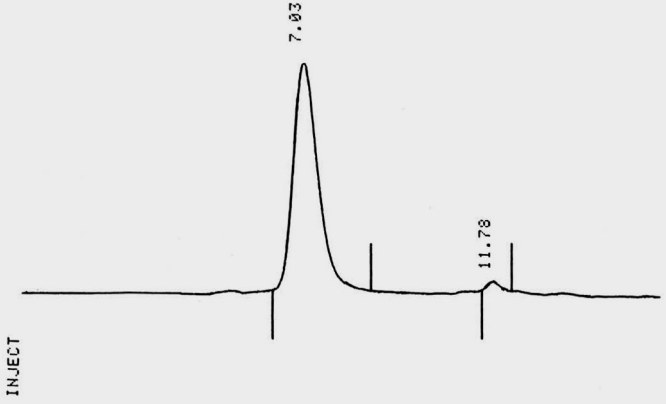

Fig. 5. HP-GPC chromatogram of the peak at 46.22 min containing immunoglobulins. The chromatogram was developed isocratically after injecting 100 μl of purified MoAb into a Bio-Sil TSK 250 column. The mobile phase was PBS. Flow-rate: 1 ml/min. Chart speed: 60 cm/h. Detection: 278 nm.

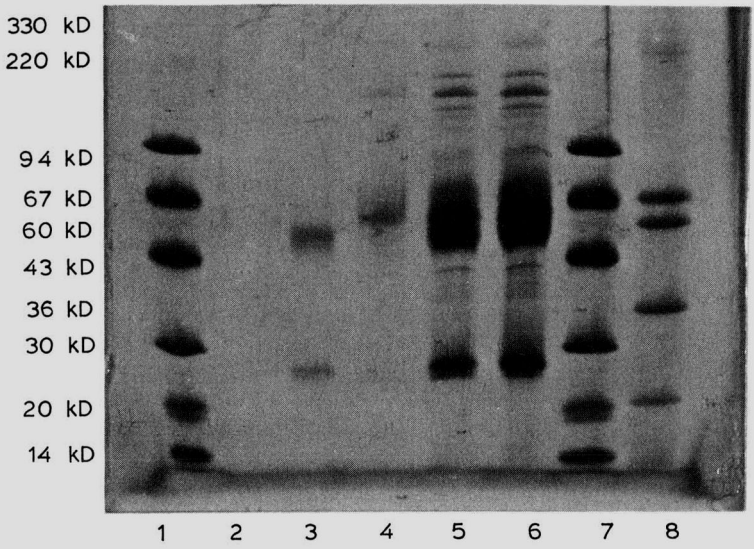

Fig. 6. Reducing SDS-PAGE of the preparative Protein A peaks from Fig. 2. Lanes: 1 and 7 LMW standards; 8, HMW standards; 3, peak at 53.67 min; 4, peak at 56.32 min from Fig. 2; 5 and 6, crude mouse ascites.

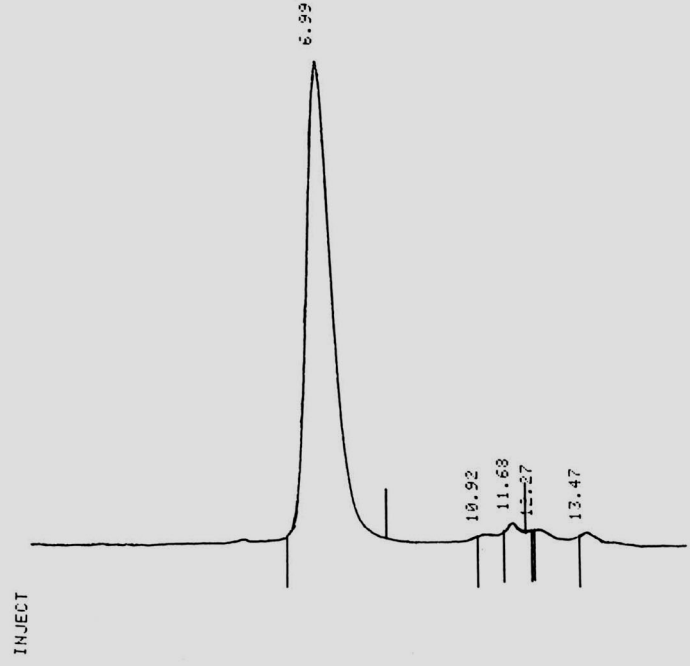

Fig. 7. HP-GPC analysis of the Protein A bound fraction. For chromatographic conditions, see Fig. 5.

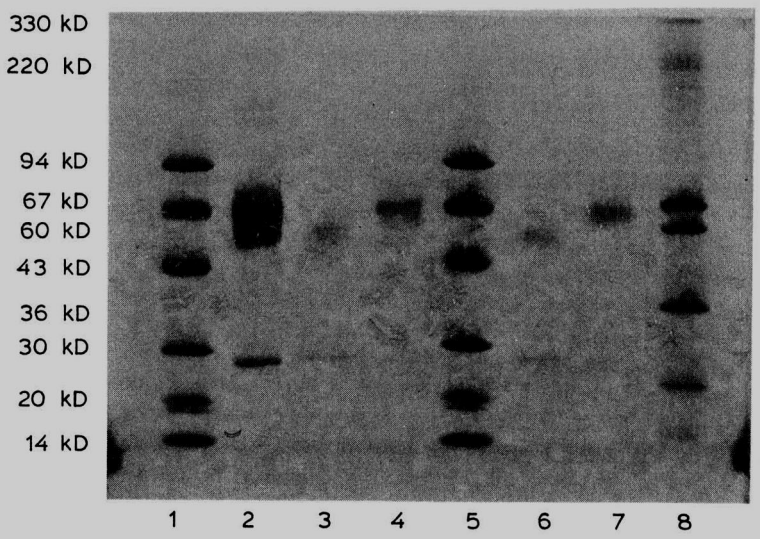

Fig. 8. Reducing SDS-PAGE after anion-exchange chromatography. Lanes: 1 and 5, LMW standards; 8, HMW standards; 2, crude mouse ascites; 3 and 6, peak at 45.37 min from Fig. 3; 4 and 7, peak at 57.96 min from Fig. 3.

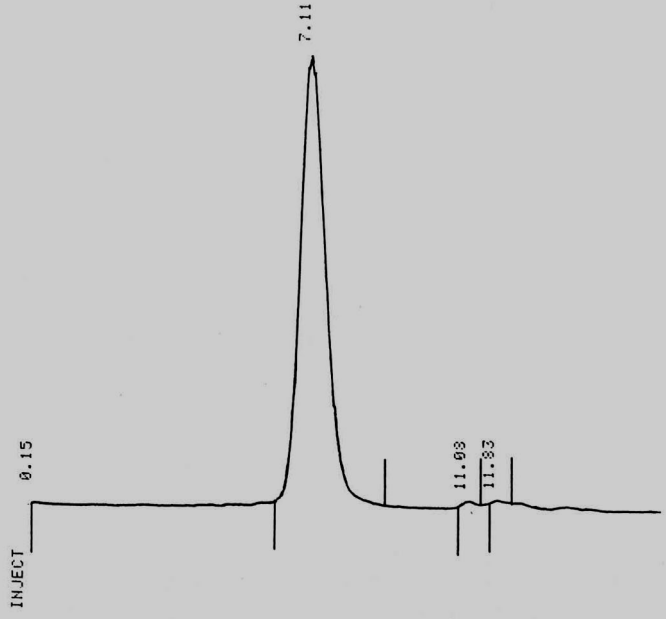

Fig. 9. HP-GPC analysis of the peak at 45.37 min from Fig. 3. For elution conditions, see Fig. 5.

TABLE 1

PURIFICATION AND YIELD OF MoAb EK3 USING HPHA, HPPA AND DEAE PURIFICATION PROCEDURES

Stationary phase	*Specific activity*	*Protein loaded (mg)*	*Protein recovery (%)*	*MoAb recovery (MG)*	*MoAb yield (%)*	*HP-GPC purity (%)*	*Purification factor*
HPHA	318 000	150	85	79.5	53	98.5	4.0
HPPA	385 000	150	90	81.0	54	99.2	4.8
DEAE	335 000	150	90	72.0	48	99.2	4.2

The maximum load capacity of the columns was also determined by charging increasing amounts of purified MoAb, obtained from previous purifications and by measuring the immunoreactivity of the void volume. As much as 250, 350 and 380 mg of MoAb were loaded in HPPA, HPHA and Protein Pak DEAE 5PW preparative columns, respectively, without found any immunoreactivity in the void volume. These quantities represent, for HPPA and HPHA, the actual column capacity, because the whole stationary phases of the columns are employed for the MoAb retention. The antibody was collected from HPHA and HPPA columns after the bulk of contaminant proteins had been eluted in the void volume. In this way the binding capacity of the matrices was employed only for antibody retention.

A further test of the Protein Pak 5PW column was performed by loading increasing amounts of MoAb and albumin in order to ascertain when the two proteins were no longer separated. Different amounts of a 1:1 mixture of pure MoAb and bovine serum albumin (BSA) were injected. The elution protocol was performed as described under Protein Pak DEAE 5PW chromatography. Resolution was effected at 250 mg of the mixture.

DISCUSSION

The advent of MoAb technology has opened up new application areas, such as diagnostics (radioimmunoimaging), therapeutics (radioimmunotherapy) and basic and applied research. In each of these areas, highly purified MoAbs are required. The methods traditionally used for purifying polyclonal antibodies (salt and polyethylene glycol precipitation, classical open-column chromatography) can often be used successfully to purify MoAbs, but these techniques usually require several hours to perform, or provide not highly purified antibodies.

Preparative HPLC chromatography provides an extremely useful alternative to conventional MoAbs purification techniques. Speed, ease and purity as well as quantitative protein recovery and large-scale production are the advantages of HPLC purification.

This paper describes three procedures for preparative purification of an IgG1 MoAb. Hydroxyapatite provides highly purified material thanks to the capacity of its crystal surface able to separate proteins with slight differences in their adsorption groups. Its calcium, phosphate and hydroxide ions adsorb oppositely charged sites of proteins or other large molecules. For this reason, the molecular tertiary structure is

very important in this separation method which does not involve the isoelectric point of proteins but an ionic interaction between molecules and the hydroxyapatite stationary phase[11,12]. Affinity chromatography on Protein A is the most widely employed method for the specific separation of immunoglobulins from contaminant ascitic fluid proteins. Unlike previously published reports of the use of Protein A[13,14] to purify MoAbs, the employment of an high molarity binding buffer at pH 9.0 provides increased capacity to bind the mouse IgG1 subclass. A total capacity of 250 mg of IgG1 was achieved using the preparative Protein A column. Furthermore, the hydrophilic rigid matrix to which Protein A is linked allows high flow-rates (up to 10 ml/min) and substantially reduced separation times. Anion-exchange chromatography has been widely used for many years in the purification of antibodies. The analytical anion-exchange column (Mono Q, Pharmacia) has been succesfully used to purify MoAbs[5]. Large-scale preparation of MoAbs on a semipreparative anion-exchange HPLC column had not been investigated, so far. The experiment performed in our laboratory demonstrates that the separation of MoAb from albumin was still possible up to 250 mg of a 1:1 mixture of the two components.

Table I lists the parameters investigated to compare the purification protocols of HPHA, HPPA and DEAE 5PW chromatography. The protein recovery, MoAb purity and immunoreactivity of the three procedures are very similar. Such purified MoAbs can be employed in all the previously mentioned applications. On the contrary, differences in the applicability of each purification method were found. The HPHA chromatography requires at least two chromatographic developments of the HPHA analytical cartridge to accomplish the MoAb purification. As reported previously[15], IgM can be purified on an HPHA column. The use of extremely mild conditions preserves the MoAb activity. HPPA chromatography is very easy to perform, and gradient elution with buffers at different pH can be employed to separate IgG subclasses. Mouse IgM cannot be quantitatively purified by Protein A chromatography, because of their low affinity for Protein A[14]. An high-molarity and high pH binding buffer not only retains mouse IgG1 more strongly on Protein A, but is also able to buffer the acidic step of MoAb elution. The MoAb bound to the matrix begins to be eluted as the pH is decreased. The first portion of the MoAb fraction contains a residual of binding buffer which maintains neutral pH for the whole MoAb fraction.

DEAE anion-exchange chromatography can be employed to purify both IgG and IgM. Mild elution conditions preserve the MoAb activity. The MoAb fraction obtained by DEAE 5PW chromatography was well separated from contaminant proteins, but, as reported by Burchiel *et al.*[5], it is also possible to find a protein (transferrin) eluted with MoAb. In this case the contaminant protein can be removed by a second purification step, using a gel permeation column able to eliminate the low-molecular-weight contaminant protein.

In our laboratory, preparative purifications of mouse IgG monoclonal antibodies are performed on HPPA columns. Affinity chromatography on Protein A was selected because it does not require further setting up of the method and thus can be employed in routine purification of different MoAbs. Furthermore, by means of the pH stepwise gradient elution, endogeneous mouse immunoglobulins can be partially removed from the MoAb fraction. Mouse IgM or antibodies of other animal species that show low affinity for Protein A are purified on HPHA or DEAE 5PW columns.

REFERENCES

1 G. Kohler and C. Milstein, *Nature (London)*, 495 (1975) 256.
2 J. W. Goding, *J. Immunol. Methods*, 285 (1980) 39.
3 P. L. Ey, S. J. Prowse and C. R. Jenkin, *Immunochemistry*, 429 (1978) 15.
4 A. P. Philips, K. L. Martin and W. H. Harton, *J. Immunol. Methods*, 385 (1984) 74.
5 S. W. Burchiel, J. R. Billman and T. R. Alber, *J. Immunol. Methods*, 33 (1984) 69.
6 H. R. Alonzo, Dorothee Herlyn and Hilary Koprowski, *J. Immunol. Methods*, 102 (1987) 227.
7 H. Juarez-Salinas, G. S. Ott, J. C. Chen, T. L. Brooks and L. H. Stanker, *Methods Enzymol.*, 121 (1986) 615.
8 U. K. Laemmli, *Nature (London)*, 680 (1970) 227.
9 H. Juarez-Salinas, S. C. Engelhorn, W. L. Bigbee, M. A. Lowry and L. H. Stanker, *Bio-techniques*, 164 (1984) 2.
10 *Separation News*, Pharmacia Laboratories, Uppsala, 13.5, 1986.
11 J. N. Gorbunoff and S. N. Timasheff, *Anal. Biochem.*, 136 (1984) 440.
12 T. Kawasaki, S. Takahashi and K. Ikeda, *Eur. J. Biochem.*, 152 (1985) 361.
13 A. Suroglia, D. Pain and N. J. Khan, *Trends Biochem. Sci.*, 7 (1982) 74.
14 R. Lindmark, K.T. Tolling and J. Sjoquist, *J. Immunol. Methods*, 62 (1983) 1.
15 T. L. Brooks, L. H. Stanker, R. von Wedel, J. D. Chen, G. S. Ott, R. Walker and H. Juarez-Salinas, presented at the *4th International Symposium on HPLC of Proteins Peptides and Polynocleotides, Baltimore, MD, December 10–12, 1984.*
16 D. R. Nau, presented at the *12th International Symposium on Column Liquid Chromatography, Washington, DC, June 19-24, 1988.*
17 R. Matson, M. Little, K. Talmadge and C. Siebert, presented at the *12th International Symposium on Liquid Chromatography, Washington, DC, June 19–24, 1988.*

Journal of Chromatography, 465 (1989) 113–119
Elsevier Science Publishers B.V., Amsterdam — Printed in The Netherlands

CHROMSYMP. 1538

FULL AUTOMATION OF CATECHOLAMINE METABOLITE DETERMINATION BY COLUMN SWITCHING AND HIGH-PERFORMANCE LIQUID CHROMATOGRAPHY

G. GROSSI*, A. BARGOSSI, R. BATTISTONI, A. LIPPI and G. SPROVIERI
Laboratorio Centralizzato, Policlinico S. Orsola, via Massarenti 9, 40138 Bologna (Italy)

SUMMARY

The urinary catecholamine metabolites, vanilmandelic acid, homovanillic acid, 3,4-dihydroxyphenylacetic acid and 5-hydroxyindoleacetic acid, were extracted on a silica-bonded strong-anion-exchanger cartridge (SAX) and then injected into an high-performance liquid chromatographic (HPLC) system by column switching. Chromatography was performed on a reversed-phase analytical column with electrochemical detection. Full automation was obtained by coupling two devices: a solid-phase automatic sampler and an intelligent autosampler. For each substance the recovery was >95% and the coefficient of variation was *ca.* 3%; the analysis takes 11 min. Substance instability problems are overcome, because the samples are extracted and injected in rapid succession. The normal values and correlation with manual HPLC were established for a large number of samples.

INTRODUCTION

The major metabolic end products of norepinephrine, epinephrine and dopamine, urinary 4-hydroxy-3-methoxymandelic acid (vanilmandelic acid, VMA) and 4-hydroxy-3-methoxyphenylacetic acid (homovanillic acid, HVA), respectively, are measured as an aid in the diagnosis of patients with pheocromocytoma or neuroblastoma[1]. The ratio VMA/HVA is important for the prognosis after surgical removal of the tumour[2].

Urinary VMA and HVA have been determined by liquid chromatography[3] by separating the compounds under various conditions and assaying them individually with electrochemical detectors. A method for the simultaneous analysis of VMA and HVA has been reported[4], in which urine is injected directly into a reversed-phase column and the effluent is monitored with an electrochemical detector, but the analysis time exceeded 25 min.

In previous work[5] we developed a method for urinary VMA, HVA, 3,4-dihydroxyphenylacetic acid (DOPAC, a metabolite of dopamine) and 5-hydroxyindoleacetic acid (5-HIAA, the major metabolite of serotonine) determination by reversed-phase high-performance liquid chromatography (RP-HPLC) with electrochemical detection (ED), after a solid-phase clean-up. In the clinical laboratory these

0021-9673/89/$03.50

metabolites are usually determined together with urinary and plasma catecholamines. We have also developed a fully automated catecholamine analyzer[6].

Here we present a fully automated analyzer for VMA, HVA, DOPAC and 5-HIAA, which is compatible with the catecholamine analysis. A pump metering four solvents permits all of these analyses to be performed with the same instrumentation and analytical column. It only takes a few minutes for equilibration to change from one analysis to another.

EXPERIMENTAL

Materials

The standards, VMA, HVA, DOPAC and 5-HIAA, were obtained from Sigma (St. Louis, MO, U.S.A.); sodium dodecyl sulphate was from BDH (Poole, U.K.). Extraction cartridges, containing silica-bonded quaternary amine (AASP Cassette SAX), and the packing material for the 150 mm × 4.6 mm saturation column (customer-packed), containing Sepralite reversed-phase C_{18} (40–60 μm) material were from Analytichem Int. (Harbor City, CA, U.S.A.) and the analytical column, octadecyl C_{18}, 50 mm × 4.6 mm, 3 μm, was from Baker (Deventer, The Netherlands) as was the HPLC-grade acetonitrile. All other reagents were of analytical grade. The water employed for buffers and mobile phase preparation was purified with a Milli-Q system (Millipore, Bedford, MA, U.S.A.) and the mobile phase was filtered through a 0.2-μm Durapore membrane (Millipore) and degassed. The HPLC analytical column was protected with an on-line filter (Model 7315; Rheodyne, Cotati, CA, U.S.A.).

The HPLC pump was a Model LC 21C from Brüker (Brema, F.R.G.). The Epson QX 16 computer and Epson FX 85 printer were also from Brüker. The Valco ten-port valve and the solid-phase autosampler, Model AASP, were from Varian (Walnut Creek, CA, U.S.A.) and the sampler preparator, Model 222 as well as the metering pump, Model Dilutor 401, were from Gilson (Villiers-le-Bel, France). The interface between the sample preparator and the AASP autosampler, Model Anachem, was from Gilson and the interface between the Epson computer and the Gilson sample preparator, Event Box I/O, was from Brüker.

The column effluent was monitored with a dual-electrode coulometric electrochemical ESA detector (Model Coulochem 5100 A with a 5021 conditioning cell and a 5011 high-sensitivity cell; Environmental Scienes Assoc., Bedford, MA, U.S.A.). The detector signals were recorded on a Model 56 recorder (Perkin-Elmer, Norwalk, CT, U.S.A.) and were also integrated with the Epson computer.

The optimized HPLC system was assembled by connecting in series solvent reservoirs, HPLC pump, saturation column, ten-port valve, AASP extraction cartridge, ten-port valve, filter, analytical column, conditioning cell, high-sensitivity cell, recorder and data system.

The urine samples were preserved with 0.1 *M* HCl. They can be kept up to 1 week at 4°C and for 3 months at –30°C. To obtain standard solutions, an acidified normal urine was fortified with VMA, HVA, 5-HIAA and DOPAC to give concentrations of 0.00, 6.25, 12.50, 25.00 and 50.00 mg/l. Calibration standards can be stored at –30°C for 3 months.

METHODS

In operation, the AASP solid-phase autosampler is connected with the autosampler (Fig. 1) and the extraction microcolumns (50 mg of sorbent), assembled in a cassette of ten, are substituted for the autosampler vials. The disposable extraction cartridge is pneumatically positioned on-stream with the analytical column.

The autosampler (Fig. 2) consists of a syringe pump (A) and a 5-ml loop (B), which are connected to the needle, which moves in sequence: needle washing step; 0.2 *M* NH_4Cl–NH_4OH buffer, pH 8.5, containing 0.05% of EDTA (7); void tube (4); sample (1); void tube (4); water (W); 0.3 *M* H_3PO_4; methanol–water (1:1) solution (CM); water (BF); buffered sample (4); water (BF); methanol (M); injection port (E). The autosampler dilutes 25 μl of urine in 500 μl of 0.2 *M* NH_4Cl–NH_4OH buffer pH 8.5 containing 0.05% of EDTA. Then it draws in sequence: 900 μl of water; 25 μl of 0.3 *M* H_3PO_4; 500 μl of methanol–water (1:1); 1000 μl of water; 25 μl of buffered sample; 500 μl of water; 500 μl of methanol. It pumps these solutions in reverse order through the cartridge positioned on the AASP. For the elution, the ten-port valve connects the cartridge on-stream with the analytical column for 0.2 min.

The four HPLC eluents were: (A) methanol–acetonitrile–50 m*M* NaH_2PO_4 buffer pH 2.8 (15:8:77), containing 200 mg/l of SDS (for catecholamine elution only); (B) 50 m*M* NaH_2PO_4 buffer pH 2.8, containing 200 mg/l of SDS; (C) acetonitrile–water (1:1), containing 200 mg/l of SDS; (D) methanol containing 200 mg/l of SDS. The gradient elution of the analytical column, at a flow-rate of 1 ml/min was: 100% B for 0.1 min; from 100% B to 90% B–10% C in 1.0 min; from 90% B–10% C to 80% B–20% C in 2.0 min; from 80% B–20% C to 70% B–30% C in 4.0 min; 100% B for 3.9 min.

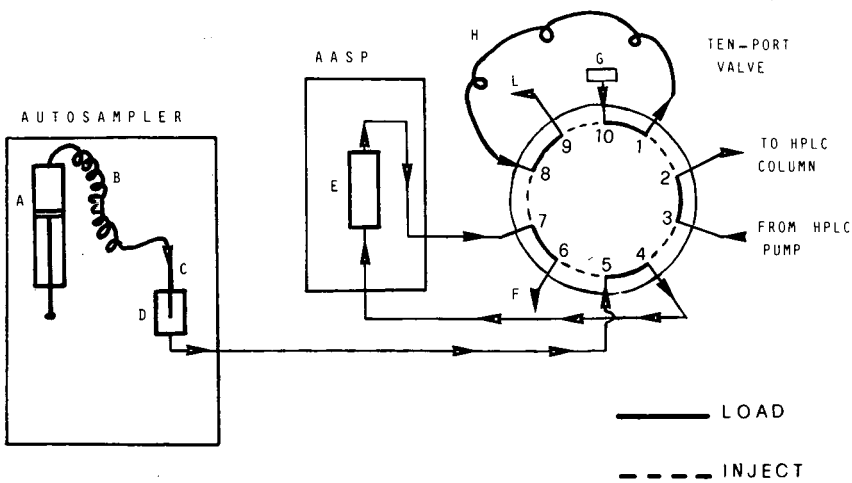

Fig. 1. Sample processing diagram. A = Syringe pump; B = 5-ml loop; C = needle of the autosampler; D = injection port; E = AASP extraction cartridge; F = purge solvent drain; G = septum for manual injection; H = manual injection loop; L = manual injection drain.

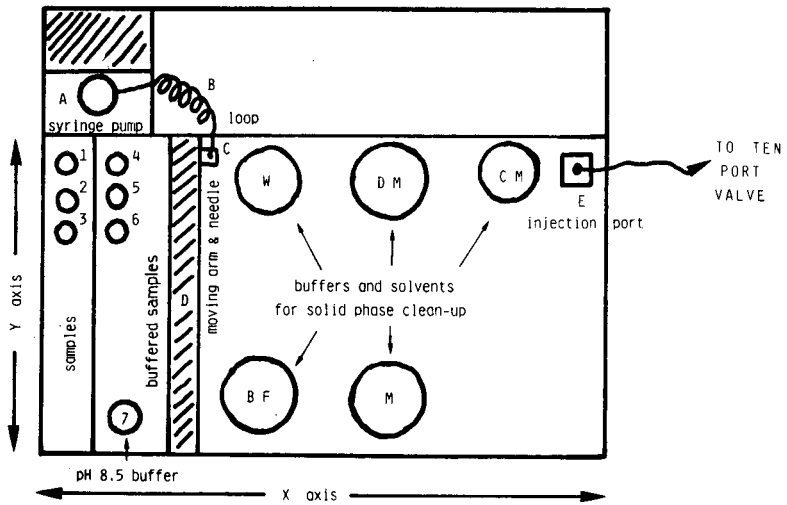

Fig. 2. Autosampler. The arm (D) moves the needle (C) along the axes *X* and *Y* on a tray containing the samples (up to 40) and the buffers necessary for the column switching clean-up. For details, see text.

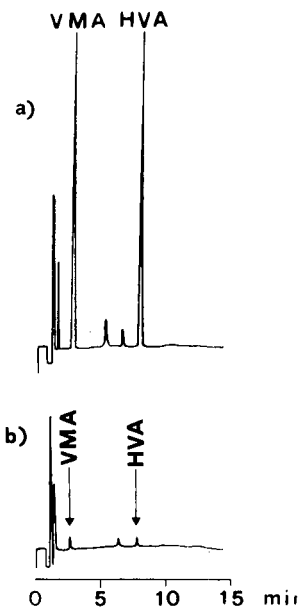

Fig. 3. Chromatogram of urine containing VMA and HVA: (a) 53.0 and 53.1 mg/l, respectively; (b) 2.2 and 1.9 mg/l respectively. Analytical conditions: column, octadecyl C_{18}, 50 mm × 4.6 mm, 3 μm; mobile phase eluent B, 50 mM NaH_2PO_4 buffer pH 2.8, containing 200 mg/l of SDS; eluent C, acetonitrile–water (1:1), containing 200 mg/l of SDS; gradient elution 0.1 min 100% B from 100% B to 90% b–10% C in 1.0 min; from 90% B–10% C to 80% B–20% C in 2.0 min; from 80% B–20% C to 70% B–30% C in 4.0 min; 3.9 min at 100% B; flow-rate 1 ml/min; detector conditioning cell, +0.00 V; det. 1, +0.00 V; det. 2, +0.35 V, gain 1 × 2, response 2.

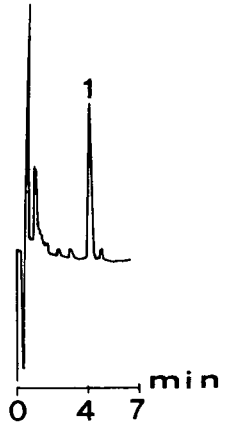

Fig. 4. Chromatogram of an urine containing 13.1 mg/l of 5-HIAA. Peak 1, 5-HIAA. Analytical conditions: column, octadecyl C_{18} 50 mm × 4.6 mm, 3 μm; mobile phase 8% acetonitrile in 50 m*M* NaH_2PO_4 buffer pH 2.8 (8:92), containing 200 mg/l of SDS; isocratic elution; flow-rate, 1 ml/min; detector, conditioning cell, –0.20 V; det. 1, –0.20 V; det. 2, +0.25 V, gain 1 × 2, response 2.

RESULTS AND DISCUSSION

Fig. 3. shows the chromatograms obtained from urine subjected to simultaneous analysis for VMA and HVA. The SDS added to the mobile phase acts by compressing the metabolite peaks and results in higher column efficiency and improved separation from artefacts.

The chromatogram of 5-HIAA is reported in Fig. 4. Isocratic elution is employed because samples for 5-HIAA usually do not have to be analyzed for VMA and HVA also.

Fig. 5 shows the chromatogram obtained for urine DOPAC determination. The retention times for VMA, DOPAC, 5-HIAA and HVA are 2.5, 4.6, 6.5 and 7.5 min, respectively. For the isocratic elution of 5-HIAA the retention time was 4.0 min. The autosampler takes 10 min to prepare a sample and the analysis time is 11 min, limited by the speed of the Gilson 222.

The minimum detectable concentration in urine is 0.1 mg/l for all the metabolites, but the sensitivity can easily be enhanced by changing the detector gain or the amount of urine extracted. The recoveries and the precision of the column-switching method are summarized in Table I. The normal ranges of metabolite concentrations were calculated for urine samples obtained from healthy adults (Table II). For 40 urine samples from healthy adults we studied the correlation between manual and automated analysis (Table III).

5-HIAA is not stable in acidic media and DOPAC is not stable in basic media; therefore manual extraction of 5-HIAA is difficult and ion-exchange manual extraction of DOPAC is impossible (for DOPAC, reversed-phase cartridges are used for manual extraction). For full automation, the sample is kept in these media for only a few seconds; no instability problems have been encountered.

By selecting eluent A as the mobile phase for isocratic elution, changing extraction cartridges to AASP cassette C_{18} and substituting Gilson buffers and solvents, the

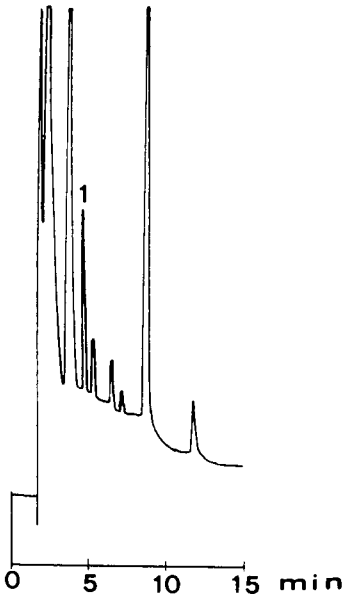

Fig. 5. Chromatogram of an urine containing 26.3 mg/l of DOPAC. Peak 1 = DOPAC. Analytical conditions are the same as in Fig. 3, but: detector, conditioning cell, +0.45 V; det. 1, -0.40 V; det. 2, +0.05 V, gain 1 × 2, response 2.

TABLE I

RECOVERIES AND PRECISION OF THE METHOD

	Fortified urine (mg/l)			*% Recovery*		
	Low	*Medium*	*High*	*Low*	*Medium*	*High*
VMA	3.1	15.1	53.0	95.1 ± 3.7	98.3 ± 2.0	99.4 ± 1.8
HVA	2,9	14.7	53.1	97.4 ± 3.1	99.6 ± 1.9	101.5 ± 1.6
5-HIAA	1.8	27.0	52.0	96.5 ± 3.6	98.2 ± 2.2	101.7 ± 2.1
DOPAC	0.9	13.5	51.0	94.3 ± 4.2	97.3 ± 2.5	99.1 ± 2.3

TABLE II

NORMAL RANGES

Compound	*Range*
Males[a]	
VMA	2.5 ± 1.25 mg/g of urinary creatinine
HVA	2.8 ± 0.95 mg/g of urinary creatinine
5-HIAA	2.8 ± 0.97 mg/day
Females[b]	
VMA	3.3 ± 1.29 mg/g of urinary creatinine
HVA	3.6 ± 1.30 mg/g of urinary creatinine
5-HIAA	2.1 ± 0.53 mg/day

[a] VMA and HVA, 7-h collection, n = 60, age 25–45 years. 5-HIAA, 24-h collection, n = 40, age 20–60 years.

[b] VMA and HVA, 7-h collection, n = 64, age 25–45 years. 5-HIAA, 24-h collection, n = 38, age 20–60 years.

TABLE III

CORRELATION OF RESULTS ON URINARY METABOLITES, ANALYZED BY TWO METHODS

X = Bond Elut extraction, manual injection; Y = column-switching extraction and injection; n = 40.

Compound	*Regression equation*	
VMA	$Y = 0.9925X + 0.1260$	$r = 0.9961$
HVA	$Y = 1.0124X - 0.0612$	$r = 0.9981$
5-HIAA	$Y = 0.9873X + 2.2561$	$r = 0.9972$
DOPAC	$Y = 0.9885X + 1.9223$	$r = 0.9987$

analyzer becomes the same as that used for catecholamines[6] and after 30 min of equilibration it is possible to start urinary or plasma catecholamine analysis (with correct detector settings).

REFERENCES

1 S. E. Gitlow, L. M. Bertani, A. Rausen, D. Grifetz and S. W. Dziedzic, *Cancer (Phila.)*, 25 (1968) 1377.
2 E. H. La Brosse, Com-Nouguéc, J. M. Zucker, E. Comoy, C. Bohuon, J. Lemerle and D. Schweisguth, *Cancer Res.*, 40 (1980) 1995.
3 S. R. Binder and G. Sivorinovsky, *J. Chromatogr.*, 336 (1984) 173.
4 K. Fujiita, K. Maruta, S. Ito and T. Nagatsu, *Clin. Chem.*, 29 (1983) 876.
5 G. Grossi, A. Bargossi, R. Battistoni, A. Lippi and L. Biagetti, in M. F. Burke (Editor), *Int. Conf. Sample Preparation and Isolation Using Bonded Silicas, Cherry Hill, PA, May 6–7, 1986*, Analytichem Int., Harbor City, CA, 1986, pp. 279–297.
6 G. Grossi, A. Bargossi, A. Lippi and R. Battistoni, *Chromatographia*, 24 (1987) 842.

12th International Symposium on Column Liquid Chromatography, Washington, DC (U.S.A.), June 19–24, 1988 (late papers)

END OF SYMPOSIUM PAPERS

PUBLICATION SCHEDULE FOR 1989

Journal of Chromatography and Journal of Chromatography, Biomedical Applications

MONTH	J	F	M	A	M	
Journal of Chromatography	461 462 463/1	463/2 464/1	464/2 465/1 465/2	466 467/1	467/2	The publication schedule for further issues will be published later
Bibliography Section		486/1		486/2		
Biomedical Applications	487/1	487/2	488/1 488/2	489/1 489/2 490/1	490/2	

INFORMATION FOR AUTHORS

(Detailed *Instructions to Authors* were published in Vol. 445, pp. 453–456. A free reprint can be obtained by application to the publisher, Elsevier Science Publishers B.V., P.O. Box 330, 1000 AH Amsterdam, The Netherlands.)

Types of Contributions. The following types of papers are published in the *Journal of Chromatography* and the section on *Biomedical Applications:* Regular research papers (Full-length papers), Notes, Review articles and Letters to the Editor. Notes are usually descriptions of short investigations and reflect the same quality of research as Full-length papers, but should preferably not exceed six printed pages. Letters to the Editor can comment on (parts of) previously published articles, or they can report minor technical improvements of previously published procedures; they should preferably not exceed two printed pages. For review articles, see inside front cover under Submission of Papers.

Submission. Every paper must be accompanied by a letter from the senior author, stating that he is submitting the paper for publication in the *Journal of Chromatography*. Please do not send a letter signed by the director of the institute or the professor unless he is one of the authors.

Manuscripts. Manuscripts should be typed in double spacing on consecutively numbered pages of uniform size. The manuscript should be preceded by a sheet of manuscript paper carrying the title of the paper and the name and full postal address of the person to whom the proofs are to be sent. Authors of papers in French or German are requested to supply an English translation of the title of the paper. As a rule, papers should be divided into sections, headed by a caption (*e.g.*, Summary, Introduction, Experimental, Results, Discussion, etc.). All illustrations, photographs, tables, etc., should be on separate sheets.

Introduction. Every paper must have a concise introduction mentioning what has been done before on the topic described, and stating clearly what is new in the paper now submitted.

Summary. Full-length papers and Review articles should have a summary of 50–100 words which clearly and briefly indicates what is new, different and significant. In the case of French or German articles an additional summary in English, headed by an English translation of the title, should also be provided. (Notes and Letters to the Editor are published without a summary.)

Illustrations. The figures should be submitted in a form suitable for reproduction, drawn in Indian ink on drawing or tracing paper. Each illustration should have a legend, all the *legends* being typed (with double spacing) together on a *separate sheet*. If structures are given in the text, the original drawings should be supplied. Coloured illustrations are reproduced at the author's expense, the cost being determined by the number of pages and by the number of colours needed. The written permission of the author and publisher must be obtained for the use of any figure already published. Its source must be indicated in the legend.

References. References should be numbered in the order in which they are cited in the text, and listed in numerical sequence on a separate sheet at the end of the article. Please check a recent issue for the layout of the reference list. Abbreviations for the titles of journals should follow the system used by *Chemical Abstracts*. Articles not yet published should be given as "in press" (journal should be specified), "submitted for publication" (journal should be specified), "in preparation" or "personal communication".

Dispatch. Before sending the manuscript to the Editor please check that the envelope contains three copies of the paper complete with references, legends and figures. One of the sets of figures must be the originals suitable for direct reproduction. Please also ensure that permission to publish has been obtained from your institute.

Proofs. One set of proofs will be sent to the author to be carefully checked for printer's errors. Corrections must be restricted to instances in which the proof is at variance with the manuscript. "Extra corrections" will be inserted at the author's expense.

Reprints. Fifty reprints of Full-length papers, Notes and Letters to the Editor will be supplied free of charge. Additional reprints can be ordered by the authors. An order form containing price quotations will be sent to the authors together with the proofs of their article.

Advertisements. Advertisement rates are available from the publisher on request. The Editors of the journal accept no responsibility for the contents of the advertisements.

Foxy matches fractions to your chromatogram.

Not to the clock.

Program your collection by absorbance peaks, retention times, timed intervals, counted drops, or pumped volumes. You can even enter fraction size directly in ml if you have a Wiz peristaltic pump. Foxy rejects void volumes, locates and saves desired peaks in separate tubes, controls valves and pumps to make gradients or automate your system, and changes racks and volumes according to peaks or time. For HPLC, collect successive injections without resetting, and overlay repeated injections of the same sample to collect identical peaks in the same tubes. The sloped keyboard, 12-digit display, and logical programming make it all easy to do.

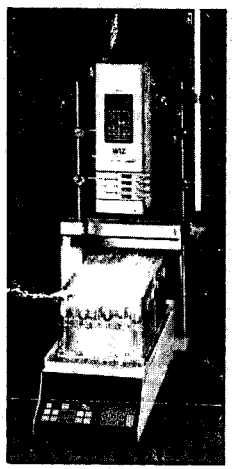

Foxy takes practically any size test tube, plus 28 mm scintillation vials and even 500 ml bottles. It holds up to four columns and 288 tubes on just a narrow slice of your bench.

To learn more, call toll-free **(800)228-4250** U.S.A. except AK, NE. Or write Isco, Inc., P.O. Box 5347, Lincoln, NE 68505.

ISCO

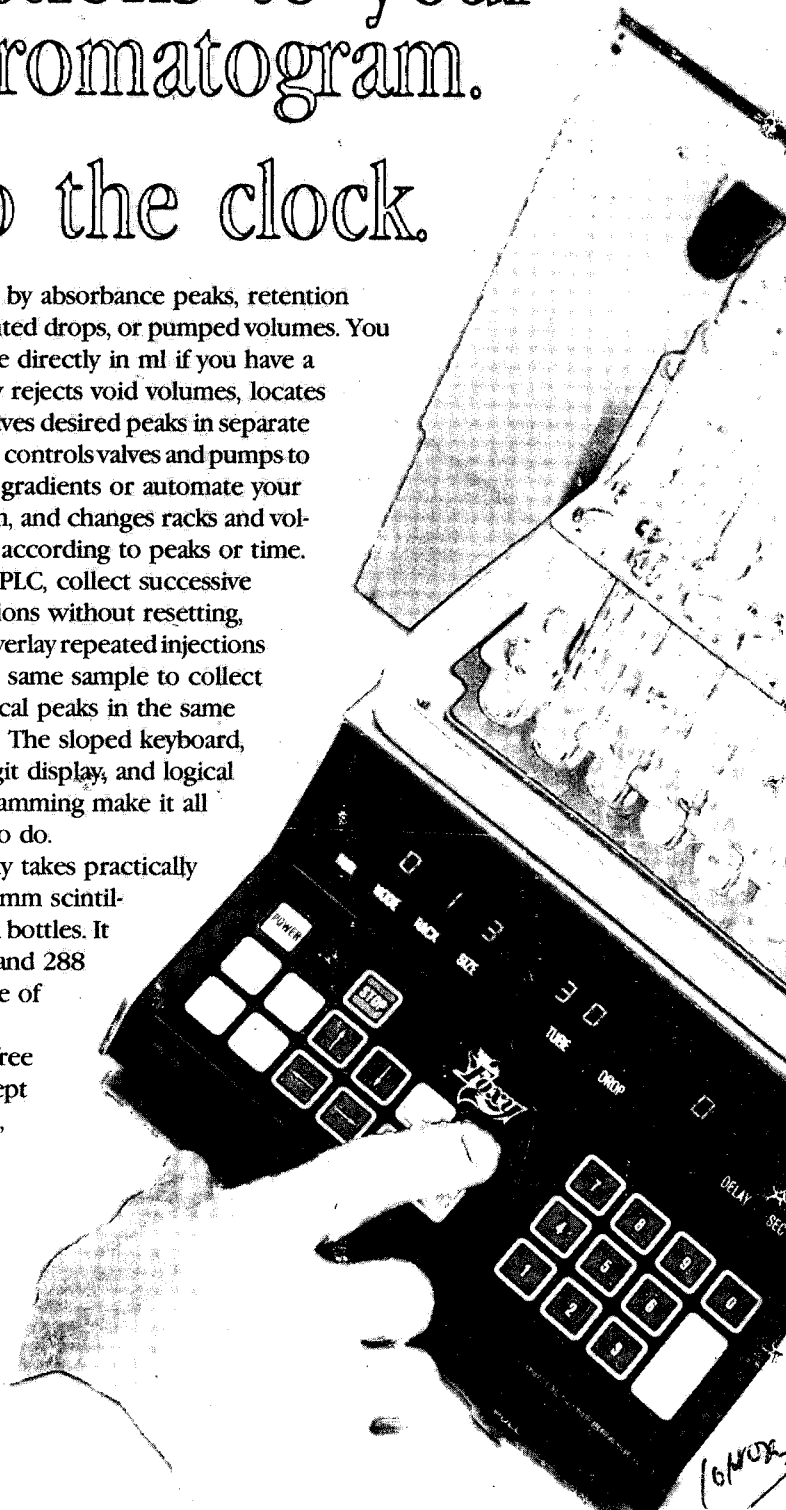

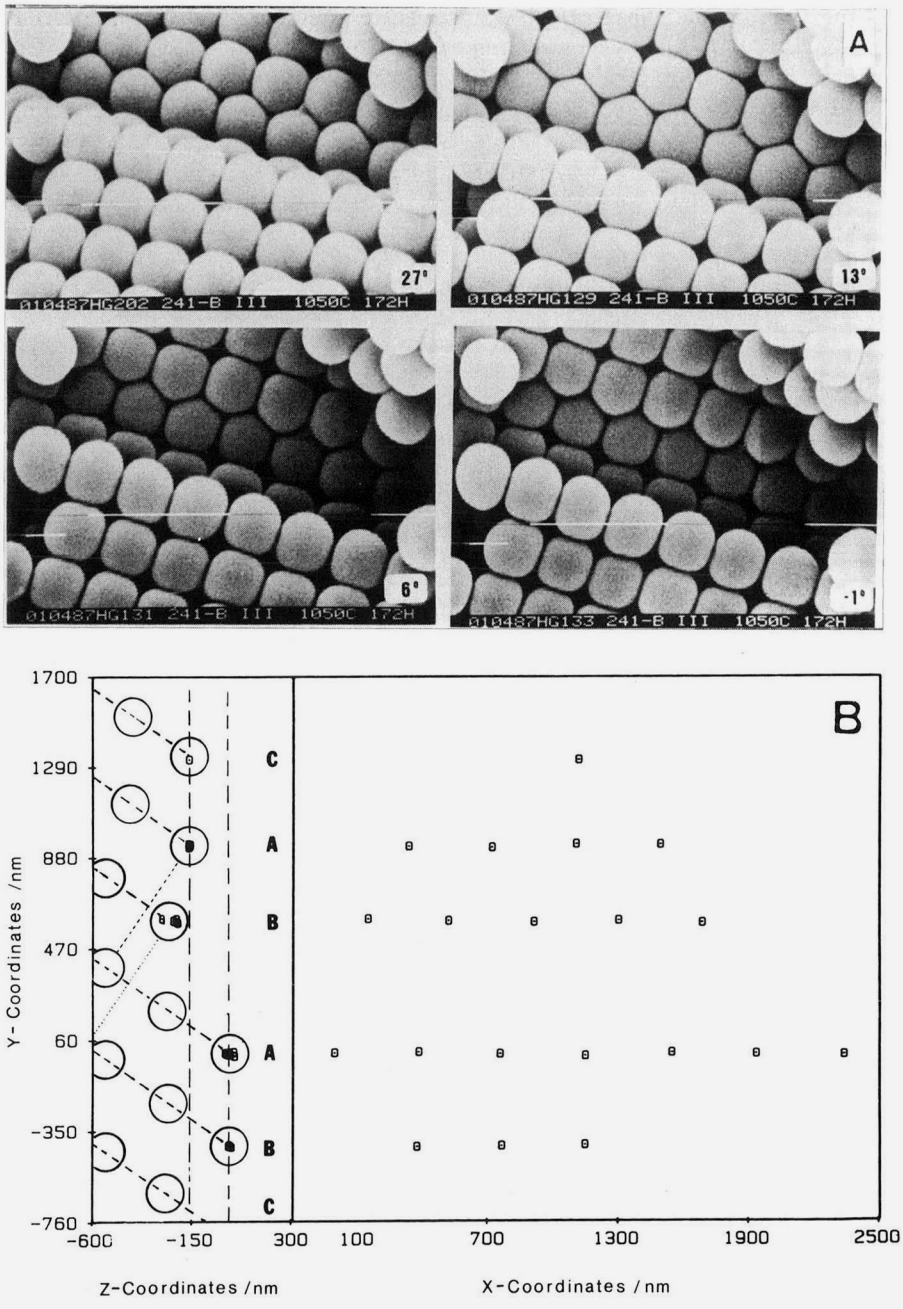

Fig 4. (A) Stereo scanning electron micrograph of aggregates spheres (batch B241/III, $d_p = 431 \pm 9.2$ nm). (B) Assessment of the position of beads in the x,y,z coordinates in the structure.